Development and evaluation of nano-formulations for immediate release oral dosage forms of poorly soluble drugs

Inaugural-Dissertation

to obtain the academic degree

Doctor rerum naturalium (Dr. rer. nat.)

submitted to the Department of Biology, Chemistry, Pharmacy

of Freie Universität Berlin

by

Zun Huang

from Hubei, China

Berlin, 2021

The enclosed doctoral research work was accomplished from November 2017 until November 2021 under the supervision of Prof. Dr. Roland Bodmeier at the College of Pharmacy, Freie Universitat Berlin.

1st Reviewer: Prof. Dr. Roland Bodmeier
2nd Reviewer: Prof. Dr. Philippe Maincent

Date of defence: 17.12.2021

To my family

Acknowledgements

Table of Contents

1. GENERAL INTRODUCTION

1.1. Challenges of poorly soluble drugs

With the application of high-throughput screening technology and combinatorial chemistry technology in drug development, synthetic new drugs have made significant progress in the quality and quantity of research and development (Bleicher et al., 2003). However, up to 40% of newly developed active drug molecules have poor water solubility, resulting in low bioavailability and being unable to enter clinical applications, thus being phased out, which prolongs the cycle of new drug development and increases costs (Chen et al., 2011; Sareen et al., 2012). Clinically, conventional formulations of poorly water-soluble drugs often suffer from poor bioavailability and are highly variable in the human body (Fahr and Liu, 2007). The bioavailability of an orally administered drug depends primarily on its solubility in the gastrointestinal tract and its permeability across cell membranes, which forms the basis for the biopharmaceutical classification system (BCS) (Amidon et al., 1995). Drug molecules are required to be present in a dissolved form in order for them to be transported across biological membranes. Therefore, low aqueous solubility can either delay or limit drug absorption. According to statistics, more than 60 billion US dollars of drugs each year face severe imbalances between efficacy and investment in treatment due to low bioavailability (Du et al., 2015).

1.1.1. Basic concepts of solubility and dissolution

A true solution is a homogeneous mixture of two or more components at the molecular level. In a two-component system, the component present in a larger proportion is commonly referred to as a solvent, and the other is a solute. When the solute is in contact with the solvent, mixing occurs since all molecules tend to be randomized, increasing the system's overall entropy (Franks and Ives, 1966). Solute molecules begin to detach from the surface of the bulk solute and enter the solvent system. The separated solute molecules move freely throughout the solvent to form a homogeneous solution. Some of these solute molecules hit and re-deposit on the bulk solute surface. Once the capability of solvent to carry the solute molecules is saturated, the rate at which the solute molecules leave from bulk is equal to the rate of re-deposition (dynamic equilibrium) (Atkins and Paula, 2014). The concentration of the solute in the solvent that reaches this equilibrium is defined as thermodynamic solubility. The solute's equilibrium solubility mainly depends on its affinities towards the solvent molecules and fellow solute molecules.

The rate at which the equilibrium is achieved is the dissolution rate. Thus, solubility is an equilibrium concept, while dissolution is a kinetic phenomenon. The dissolution rate of a

solute in a solvent is directly proportional to its solubility, as described by the Noyes – Whitney equation (Noyes and Whitney, 1897):

$$\frac{dM}{dt} = \frac{DA}{h} \, (C_s - C_t)$$

(1.1)

The terms of the equation (1.1) are: dM/dt, the rate of increase of the amount of material in solution dissolving from a solid; D, the diffusion coefficient of the dissolved solute (cm^2/sec); A, the surface area of the drug (cm^2); h, the static boundary layer (cm). C_s is the saturation solubility of the drug in solution in the diffusion layer, and C_t is the concentration of the drug in the bulk solution at time (t).

1.1.2. Factors affecting solubility and dissolution

Solubility and dissolution are dependent on many factors, including the structural attributes of the compound (e.g., molecular weight, lipophilicity, pKa); the solvent being used (e.g., pH, composition), and the *in vitro* study conditions (e.g., equilibration time, temperature, separation technique of supernatant from solid) (Florence and Attwood, 2015). The solid forms of the compound can also affect solubility and dissolution, and one compound may exist in many different forms: amorphous, crystalline, polymorphs (Blagden et al., 2007). The relevance of polymorphism and solid-state properties to equation (1.1) lies in that A is determined by particle size. Particle size reduction, if it leads to a change in polymorph, results in a change in C_s. In more general terms, one can use the Noyes – Whitney equation to predict the effect of solvent change or other parameters on the dissolution rate of solid drugs (Dokoumetzidis and Macheras, 2006). These factors are listed in Table 1.1.

Table 1.1. The factors affecting dissolution rate based on Noyes – Whitney equation

Equation parameter	Comments	Effect
D (diffusion coefficient of drug)	Presence of substances that increase the viscosity of the medium	(-)
A (area exposed to solvent)	Micronization or nanonization	(+)
h (thickness of diffusion layer)	Increased agitation in gut or flask	(+)
C_s (solubility in diffusion layer)	Crystal structure, pH change, salt or buffer ingredient	(-) (+)
C_t (concentration in bulk)	Removal of drug by partition or absorption	(+)

Increase (+) and decrease (-) of dissolution rate

1.2. Strategies for solubility and dissolution rate enhancement

Currently, there are various formulation approaches available for compounds that are poorly soluble in water. Those improvement techniques can be categorized into physical modification, chemical modification and other techniques. Physical modification techniques contain particle size reduction like micronization and nanonization (Rasenack and Müller, 2004; Junghanns and Müller, 2008), crystal structure modification like polymorphs (Censi and Di, 2015), cocrystals and amorphous (Babu and Nangia, 2011; Good and Rodriguez-Hornedo, 2009), and drug dispersions in carriers like eutectic mixtures, solid dispersions and solutions (Goldberg et al., 1965; Serajuddin, 1999). Chemical modification techniques contain pH modification (Riis et al., 2007), complexation and salt formation (Serajuddin, 2007; Loftsson, 2017). Other techniques include adding solubilizers, cosolvent, supercritical fluid processes, and so on (Yasuji et al., 2008).

1.2.1. Drug nanocrystals (nanosuspension)

Nanocrystal refers to a new class of pharmaceutical formulation with particle reduction techniques. Nanocrystals are sub-micro particles composed of a small amount of surfactants or polymer materials as stabilizers and nanosized pure drug particles. If the particle size of pure drug particles is less than 1000 nm and dispersed in an aqueous medium, it is also defined as a nanosuspension; if the drug particles exist in a partially crystalline or all crystalline state is defined as a nanocrystalline drug (Rabinow, 2004). Nanocrystal increases the surface area of drug particles by reducing the size, thereby increasing the *in vitro* dissolution and bioavailability of poorly soluble drugs (Liversidge and Cundy, 1995). In addition, nanocrystal could also reduce the effect of individual differences and the impact of dietary conditions on the efficacy of drugs (Park, 2013).

1.2.1.1. Theoretical overview

Nanocrystals can be formed either by building crystals up from the molecular state, as in precipitation; or by breaking larger crystals down, as in milling until the nanosized range is reached. In both cases, a new surface area, ΔA, is formed, which necessitates a free-energy (ΔG) cost, as defined by the equation (Rabinow, 2004):

$$\Delta G = \gamma_{s/l} \cdot \Delta A \tag{1.2}$$

In which $\gamma_{s/l}$ is the interfacial tension between the solid particle surface and the liquid. When the new surface is formed, the interfacial tension also arises. This phenomenon is

explained when water molecules located at a free surface create fewer attractive forces than other water molecules. Due to the increment of free energy, the system prefers to reduce this increase in surface area. In order to counteract the higher free energy and interfacial tension, there are two ways: by either dissolving incipient crystalline nuclei, in case of precipitation and crystal growth, or by agglomerating small particles. This tendency would cause severe thermodynamic instability problems during the nanocrystal formulation. In equation 1.2, the surface area of the nanocrystal is consistently increased to maintain the higher dissolution rate; the only way to reduce the free energy of the system is by reducing the interfacial tension. Therefore, scientists find a way to prevent the tendency of instability by the addition of surface-active agents which lower the interfacial tension. Those surface-active agents could be categorized into two classes: charged or ionic surfactants and non-ionic polymers. According to different classifications, the two main mechanisms of nanosuspension stability is steric hindrance and electrostatic repulsion (Wang et al., 2013). The steric hindrance is achieved by the steric effect formed by the adsorption of the stabilizer on the surface of the nanoparticles. A non-ionic polymeric surfactant is usually used to coat the particle surface with a hydrophobic chain as most of the used APIs are poorly water-soluble with hydrophobic properties. In addition, the structural conformation of adsorbed non-ionic polymer permits its hydrophilic tail to project into the water phase (Ali, 2001). Based on the theory that the gaining of entropy is always favorable, thus during the Brownian motion process of small particles, if two polymeric adsorbed particles collide and compress with each other, the interpenetration of the polymeric chains increases the density of the polymer segments in the surrounding of the particles. Therefore, more water medium prefers to penetrate within the tails to reduce the local osmotic pressure increment between the overlapping side chains of the polymer. Moreover, the entanglement of the polymeric chain will cause loss of entropy and is therefore unfavorable, which is called "entropic repulsion." The aforementioned mechanism will provide an effective repulsive barrier and balance with attractive Van der Waals (VdW) interactions between two neighboring particles (Fig. 1.1). However, the entropic steric interactions are inherently more sensitive to temperature fluctuations. Therefore, temperature cycling which was uncontrollable during the manufacturing process can disrupt a nanosuspension stabilized by non-ionic polymeric stabilizers (Rabinow, 2004). To prevent this, ionic surfactants which could provide electrostatic are used as well. And the mechanism is briefly described below.
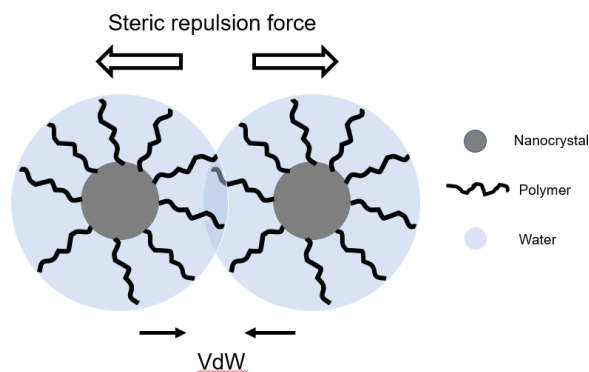
Fig. 1.1. Stabilization of nanocrystals: Force balancing of attractive VdW interactions with repulsive steric interactions.

The electrostatic mechanism is fundament in the Derjaguin-Landau-Verwey-Overbeek (DLVO) theory, which explains the aggregation of aqueous dispersions quantitatively and describes the force between charged surfaces interacting through a liquid medium (Derjaguin and Landau, 1993). It combines the effects of the VdW attraction and the electrostatic repulsion due to the so-called double layer of counter-ions. The total potential energy is the sum of the attraction potential and the repulsion potential. When two particles approach each other, electrostatic repulsion and the VdW attraction potential increase together. While at a specific maximum energy barrier, the repulsion force is greater than the attraction force (Fig. 2). To overcome this energy barrier to aggregate, two particles on a collision course must have sufficient kinetic energy due to their velocity and mass, which is unfavorable to the system. Therefore, a charged stabilizer, such as an ionic surfactant or a charged polymer, can form an electric double layer on the surface of a nanosuspension and generate electrostatic repulsion (Rabinow, 2004). According to the different properties of polar groups after dissociation, ionic surfactants can be further divided into anionic surfactants, cationic surfactants, and zwitterionic surfactants.
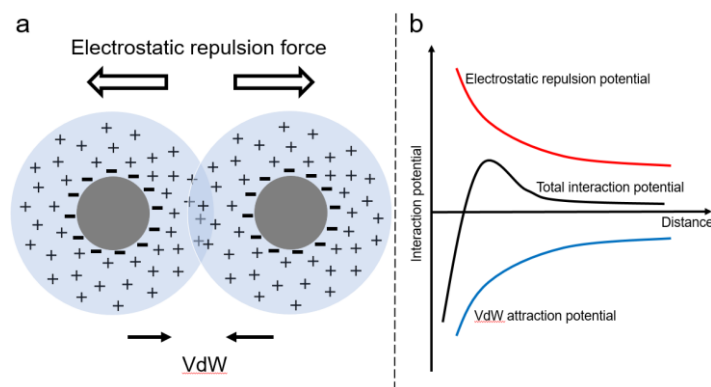
Fig. 1.2. Stabilization of nanocrystals: (a) force balancing of attractive VdW interactions with repulsive electrostatic force (b) illustration of the potential energy as a function of interparticle distance (classical DLVO).

During the process of formulation investigation, multiple surface-active agents could be applied. The non-ionic polymeric stabilizer combined with ionic surfactant stabilizers has been investigated in many studies (Bilgili et al., 2016; Soisuwan et al., 2019). There is a synergy mechanism between the two types of stabilizers because self-repulsion of the charged surfactant molecules is minimized, promoting more excellent coverage and closer packing of both the stabilizers. In addition to the type of stabilizer, concentration of the stabilizer and its ratio to the drug are also critical. Physically stable nanosuspensions are prepared when the weight ratio of drug to stabilizer is typically 20:1 to 2:1 (Merisko-Liversidge and Liversidge, 2011). At present, the research on nanosuspensions' physical stability has formed several commonly accepted theories, thus being summarized: (1) The concentration of the amphiphilic stabilizer in the system should be lower than the critical micelle concentration; otherwise, the drug particles are liable to aggregate (Yang et al., 2018). (2) The main factor determining the stability of nanosuspensions is not the molecular weight and molecular chain structure of the copolymer but the hydrophobicity of the copolymer stabilizer (Lee et al., 2005). (3) The more robust the binding force between the stabilizer and the surface of the nanosuspension, the higher the stability, such as ibuprofen nanosuspension with HPMC as the stabilizer (Verma et al., 2009); the closer the surface energy, the higher the stability, such as Naproxen nanosuspension with PVP as a stabilizer (Kocbek et al., 2006). (4) The stability of the electrostatic repulsive force depends on the absolute value of the zeta potential, and has nothing to do with the positive or negative charge. (5) The absolute value of the nanosuspension zeta potential is relatively stable at 20 ~ 40 mV (Honary and Zahir, 2013).

1.2.1.2. Production techniques for nanocrystals

Generally, nanocrystals can be prepared by two methods: "Bottom-up" and "Top-down" technology (Fig. 1.3). The "Bottom-up" technology principle is to control the precipitation or crystallization of drug particles so that the particles are rapidly formed under specific particle size (Sinha and Müller, 2013). The "Top-down" technology principle is to reduce the large-sized drug particles to smaller particles mechanically (Van Eerdenbrugh et al., 2008). Another combined technology is to combine crystallization with subsequent size reduction steps to obtain more uniform drug nanoparticles (Salazar et al., 2012). Nanocrystal preparation in laboratory research is also termed lab-scale preparation technology. The prepared nanocrystals could be scaled up and reach the same particle size and stability level in common scale preparation afterward. The lab-scale preparation methods accelerate formulation screening and allow estimation of large-scale production parameters, and this simultaneously can save raw materials and reduce R&D costs. For different drugs, the choice of multiple preparation methods requires careful consideration of the physical and chemical properties of the drug, the uniformity, stability, and particle size of the nanocrystals, the feasibility and safety of the instrument, etc. In order to prepare the uniform drug nanocrystals with small particle size and high stability effectively, a solid foundation for the process principle and parameter is required. The principles and applications of those nanocrystal preparation methods are described in detail below.
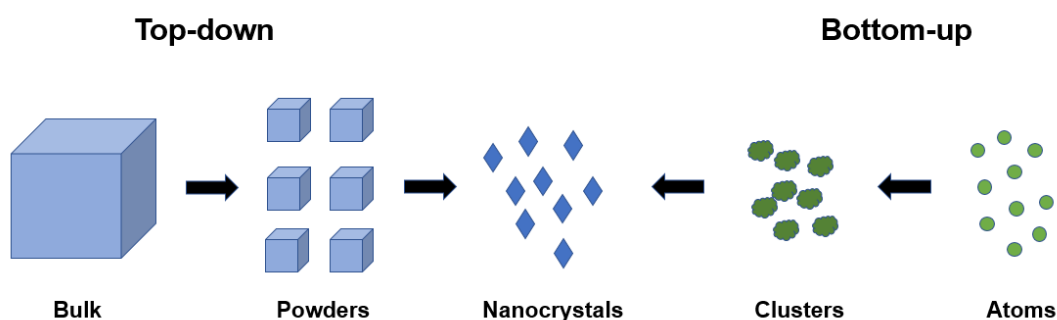
Fig. 1.3. Scheme of top-down and bottom-up technology.

"Bottom-up" technology

"Bottom-up" technology is to dissolve the drug in an organic solvent and control the crystallization conditions while injecting the organic phase into the aqueous phase dispersed with the stabilizer to form nanosized particles with a uniform distribution (Sinha et al., 2013). It is also known as self-assembly technology or controlled precipitation technology. "Bottom-up" technology was mainly divided into two methods: precipitation

method and emulsification method (Chan and Kwok, 2011). The precipitation method is to fully dissolve the drug in an organic phase which is miscible with water, and then disperse this organic phase into drug insoluble or hardly soluble water phase by slow or rapid injection under the action of external forces such as ultrasound or stirring, resulting in drug supersaturation followed with precipitation into small nanocrystals. Controlling temperature, ultrasonic intensity, time of ultrasonic, and drug infusion rate in the process can affect the growth of crystal nuclei to obtain nanocrystals with acceptable properties. The difference between the emulsification method and the precipitation method is that the drug is dissolved in an organic phase which is immiscible with water, an O/W emulsion is formed by adding organic phase into the water, afterward, the organic solvent is volatilized to accelerate the precipitation process of the drug into nanocrystals. "Bottom-up" technology may also generate amorphous drug nanoparticles, which have the characteristics of fast dissolution rate and high saturation solubility (Kumar et al., 2014). In addition to the above two commonly used methods, there are other bottom-up technologies, such as high-gravity-controlled sedimentation technology, impinging liquid jet sedimentation and multi-inlet vortex mixing technology (Xia et al., 2014; Chang et al., 2015).

"Bottom-up" technology has the advantages of feasible operation, short preparation time, and low cost. However, it also has many disadvantages: the toxicity problems of residual organic solvents, which are usually difficult to remove completely (Salazar et al., 2012); drugs (excluding new drugs that are difficult to dissolve in aqueous solution and organic medium at the same time) need to be soluble in at least one organic solvent; during the crystal growth stage, due to rapid crystallization, the needle-like particles tend to grow in one direction, which affects the physical stability of the nanocrystals (Xia et al., 2014); furthermore, the fast crystallization process may also produce various unstable polymorphs, hydrates, solvates or even their mixture, which are not conducive to the physical and chemical stability of nanocrystals (De et al., 2008). Due to those disadvantages discussed above, "Bottom-up" technology can significantly impact the formulation and stability of nanosuspensions and hence their overall performance. Therefore, no pharmaceutical products based on this technology are currently available on the market until now. With the progress of science and technology and the optimization of process conditions, the "Bottom-up" technology will have more excellent application space and development value in the future.

"Top-down" technology

"Top-down" technology relies on mechanical force to reduce millimeters of large crystal particles in the range of micrometers and even nanometer size to produce drug nanocrystals. This technology is mainly divided into two methods: the medium milling method and the high-pressure homogenization method (Fig. 1.4). The most common medium milling method for nanocrystal preparation is wet milling. Wet milling is to disperse drug particles in a solution containing a stabilizer and add them to a milling container containing milling beads (usually 0.1-0.9 mm). The agitator rapidly moves the milling beads, and the drug crystals are ground by force of friction and collision between the moving beads, the inner wall of the milling container and other drug crystals. Those effects cause the drug crystals to be broken and the particle size to be reduced, thereby obtaining nanocrystals. The low-energy media milling process, NanoCrystal® technology, was first developed by Liversidge and his colleagues (Merisko-Liversidge et al., 2003). Many products on the market are produced using this technology. Due to the simple preparation method, it is the most widely used method in laboratory research. The high-pressure homogenization method is to force an aqueous medium suspension of a drug containing a stabilizer to pass through a narrow gap repeatedly (usually about 25 µm) at a very high speed, causing the static pressure to drop below the boiling pressure of water, and when the drug suspension flows out of the gap and reaches normal pressure again, the cavitation effect caused by the bubble burst, the collision between the drug crystal and the steel wall, and the shearing effect of the liquid cause the drug particles to break. The particle size is reduced to form a nanosuspension. Müller and his colleagues developed this high-energy preparation method under the trade name DissoCubes® (Müller, 2002).
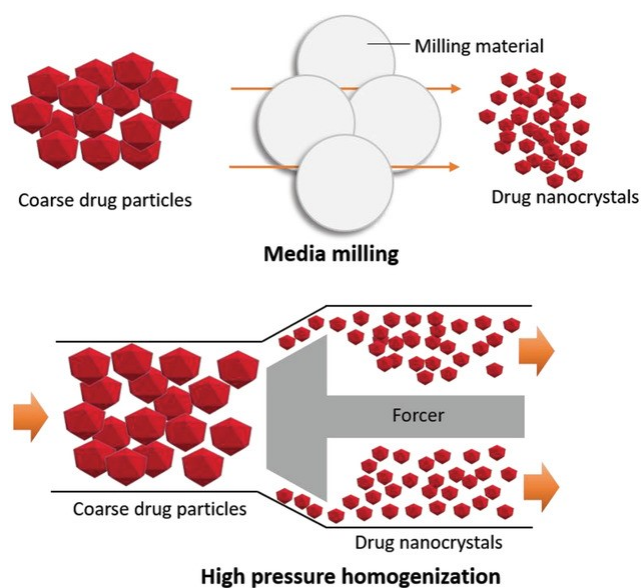
Fig. 1.4. Scheme of media milling and high-pressure homogenization methods (Paredes et al., 2021).

The process of preparing drug nanocrystals using the media milling method is simple, but if drug nanocrystals with small particle size, narrow particle size distribution range and good uniformity are needed, the milling time required is longer; thus, the efficiency is lower with medium milling method. Furthermore, it is susceptible to grow bacteria in the water phase, mainly when producing sterile parenteral products. At the same time, too long milling time will cause the abrasive of beads and contaminate the produced nanocrystals; the separation procedure of the drug nanocrystals with milling beads and the replacement of the milling beads also requires corresponding time and cost. The high-pressure homogenization method has the advantages of a short preparation cycle, small human error, good process reproducibility, easy to scale up production, etc. Compared to the media milling method, the high-pressure homogenization method can allow aseptic production (Pandey et al., 2010). However, the preparation of nanocrystals by this method requires high pressure (1500-2000 bar) and multiple cycles (up to 20 cycles), which also leads to inevitable problems such as high production energy consumption and wear of equipment. Traditional preparation techniques always have more or fewer shortcomings, so new nanocrystal preparation techniques have emerged. If it is challenging to produce drug nanocrystals with excellent properties by using one technology alone, then it is necessary to use different combinations or invent new technologies. It will combine the advantages of different preparation methods, enhance strengths and avoid weaknesses, and facilitate experimental operations.

Combined technology

Due to the limitation of some drugs with intractable properties like extreme hardness or thermal instability, the single choice of "Bottom-up" technology and "Top-down" technology cannot obtain the desired nanocrystals. The selective combination of "Top-down" and "Bottom-up" technology can avoid the disadvantages of a single method and effectively increase the feasibility and safety of subsequent preparations of nanocrystals (Salazar et al., 2012). The combined technique is first to pretreat the drug and physically modify the strongly hydrophobic drug so that the drug particles can be easily dispersed in an aqueous solution containing stabilizers to form a uniform suspension and then subjected to the homogenization or wet milling process. This requires less input of energy (lower pressure and fewer cycles) to produce nanocrystals with smaller particle size and better stability, reducing mechanical wear; in addition, the amount of stabilizer used can also reduce gastrointestinal tissue irritation during administration. The combined technologies mainly include freeze-drying-high-pressure-homogenization (H96), spray-drying-high-pressure homogenization (H42), precipitation-high-pressure homogenization (H69), grinding-high-pressure homogenization (CT) and rotary evaporation-high-pressure homogenization (Müller and Keck, 2008).

Freeze-drying-high-pressure homogenization (H96) and spray-drying-high-pressure homogenization (H42) are applied for drugs with longer grain crystals and higher hardness, which require long milling time while using the media milling method alone. Using the high-pressure homogenization method alone will cause clogging of the instrument, and the nanocrystals obtained by the two methods are difficult to meet the ideal particle size requirements. The freeze-drying-high-pressure homogenization (H96) process is similar to the spray-drying-high-pressure homogenization (H42) process in that the freeze-drying or spray-drying technology is used instead of the recrystallization step of drug synthesis as in the "bottom-up" process, and the drug substance is pretreated. During the pretreatment of drug substances, the imperfect crystallization of the drug would cause the bulk drug to present in a loose and porous form. With physical modification of the drug particles, the pretreated drug would be more suitable for high-pressure homogenization and can be used under the condition of low homogenization pressure and low number of cycles; it can also reduce the abrasion of drugs to high-pressure homogenizers and avoid heavy metal pollution caused by metal erosion caused by high friction (Krause et al., 2000). The main principle of freeze-drying technology is to freeze the water in the liquid medium into ice in an ultra-low temperature environment and then sublimate the ice into water vapor in a low-

temperature vacuum environment. The main principle of spray drying technology is to use a nebulizer to spray a liquid medium containing a drug into small mist droplets and then fall into a hot air stream to obtain a dried sample quickly. The two dried techniques could be used for the pretreatment of the drug substance and can be used to dry nanosuspensions into powders, which ensure the long-term stability of nanocrystals while facilitating their storage, transportation and subsequent formulation.

Precipitation-high-pressure homogenization (H69) technology is a combination of the precipitation technology in the "Bottom-up" technology and the high-pressure homogenization technology in the "Top-down" technology. During the precipitation process, nanocrystals of crystalline particles may be generated when the drug is precipitated, and amorphous nanocrystals may also be produced. Based on these two types of nanoparticles, nanocrystals with further high energy input with smaller polydispersity index and smaller particle size are easily obtained in high-pressure homogenization processes. However, this method still cannot avoid using organic solvents, which would not be suitable for the high-pressure homogenizer, and the explosion of organic solvents may happen during the process. In the meantime, the precipitation and crystallization processes are performed simultaneously, which is challenging to operate.

Grinding-high-pressure homogenization (CT) is the combination of two "Top-down" methods. The principle is using the pretreatment of drugs with media milling instead of precipitation. Short-term milling can reduce the particle size of drug particles to a range of micrometers and then be performed with a high-pressure homogenization process. The milling time during the milling process and the homogenization pressure during high-pressure homogenization play essential roles in determining the final particle size (Liu et al., 2015). The research found that the nanocrystals prepared by the grinding-high-pressure homogenization technology have improved electrolyte stability and better long-term stability than those prepared by the simple media grinding method. However, after the milling process, the drug nanocrystals need to be separated from the milling beads, which will cause some drug loss.

1.2.1.3. Advantages and drawbacks of nanocrystals

Advantages of nanocrystals

The drug particles in the nanosuspension must first be dissolved and converted into molecular forms before they can be used by the human body to exert their efficacy. The dissolution rate of drug particles is an essential factor in determining bioavailability. When the temperature and the dissolution medium remain stable, according to Noyes-Whitney,

the surface area of the particles has a significant effect on the dissolution rate of the drug. After the particles of the nanosuspension are processed by nanotechnology, the particle size is reduced, and the surface area is significantly increased. Therefore, nanosuspensions have a higher saturation solubility, dissolution rate, rapid formation of drug molecules, and greater bioavailability than traditional dosage forms. The increase of saturation solubility is typically interpreted by the Ostwald-Freundlich equation, relating the increase in solubility to the radius (curvature) of a particle (Van Eerdenbrugh et al., 2010):

$$ln\frac{C_{s,r}}{C_{s,\infty}} = \frac{2\gamma V_m}{rRT}$$ (1.3)

With $C_{s,r}$ and $C_{s,\infty}$ the solubilities of a particle of radius r and of a particle of infinitive radius, respectively, γ is the interfacial tension between the solid surface and the surrounding medium, V_m is the molar volume of the compound, R is the universal gas constant and T is the absolute temperature. From the Ostwald-Freundlich equation, when the temperature and solvent remain unchanged, the saturation solubility of the drug has an extensive relationship with the particle size of the particles. When the particle size is reduced, the saturated solubility of the drug will increase accordingly, which is why it has a higher solubility than traditional dosage forms. While substituting the increased saturated solubility into the Noyes-Whitney equation, the enhanced saturation solubility also contributes to a faster dissolution rate. The performance of traditional dosage forms is not ideal in improving the bioavailability of poorly soluble drugs, while nanosuspensions can effectively solve this problem because they can accelerate the dissolution rate of the poorly soluble drugs and have increased solubility, especially for immediate release oral dosage forms.

Nanosuspension consists of drug nanoparticles and stabilizers. Compared with traditional dosage forms and other nanoparticle systems, the drug loading of nanosuspensions has been significantly improved; thus, nanocrystal formulation could effectively reduce the dosage and the risk of adverse reactions, which improved patient compliance. When traditional formulation technology solves the problem of the low solubility of compounds, it is common to add a large amount of cosolvents or surfactants to improve the bioavailability of poorly soluble drugs. In comparison, nanosuspension drugs contain less stabilizers and other functional additives and can be prepared without adding organic solvents. Nanosized particles have a small particle size, making it challenging to block capillaries during transmembrane transport, effectively overcomes the drawbacks brought by the high-dose use of traditional drugs, and improves the safety of drugs (Rabinow, 2004).

Nanosuspension drugs significantly increase the surface area of the particles by reducing the particle size; thus, nanosized particles have strong adhesion to the biofilm during the *in vivo* transport and delivery process. For example, in the treatment experiment of rat toxoplasma, the atovaquone nanosuspension is absorbed by the gastrointestinal tract after oral administration (Borhade et al., 2014). The strong adhesion of the nanosuspension to the gastrointestinal tract mucosa reduces the probability of being cleared and prolonged residence time in the gastrointestinal tract. Compared with the same dose of ordinary atovaquone dosage form, atovaquone nanosuspension has a better therapeutic effect, reducing the infection rate from 40% to 15%. Compared with traditional dosage forms, nanosuspensions have better biofilm adhesion and are not easily removed in oral or nasal medications. The drug can be quickly absorbed into the blood circulation system through the mucosa of the site, which has the advantages of the rapid effect, avoiding the first-pass effect of the liver, prolonged drug absorption time, and greatly improved the corresponding bioavailability (Rabinow, 2004). By adding certain compounds to the nanosuspension, such as chitosan, carbomer and polyethylene glycol, etc., the surface properties of the drug particles can be changed to further enhance the adhesion (Sosnik et al., 2014; Nagarwal et al., 2009). After surface modification, nanosuspensions can meet the requirements of increasing mucosal adhesion during oral administration and achieve specific targeting in intravenous administration after selective surfactant/polymer modification (Ranjita, 2013).

Drawbacks of nanocrystals

Drug nanocrystals are usually stored in form of suspensions, spray-dried or lyophilized powders. If stored as a suspension in a liquid environment, drug nanocrystals with large particle sizes or unevenly distributed will easily aggregate or agglomerate. Microbial contamination is also an issue that needs to be considered during storage. While nanocrystals were stored as a spray-dried or lyophilized powder, although the powder has better stability and is easier to transport, the re-dispersibility and whether their properties have changed is another concern. Furthermore, those nanosized powders cannot be directly utilized for oral dosage drug products due to their poor powder properties.

Nanocrystals are superior in dissolution based on their large surface area compared with micro or macro drug particles. However, a large surface area would increase Gibb's free energy, and the system tends to agglomerate or aggregate to minimize the total energy. Nanocrystals were prepared with properties of normal particle size distribution. The concentration gradient between the large particles and the small particles in the nano range

is extensive; smaller particles have higher saturation solubility and dissolution rate and gradually become smaller, while supersaturation occurs on the surface of large particles, dissolved small particles will subsequently precipitate on the large particles, thus causing the crystal growth and sedimentation (Lindfors et al., 2006). On the other hand, the crystal form of the drug may change during nanocrystals preparation and downstream process. This change of crystal form is mainly categorized as amorphization and polymorphism (Sharma et al., 2009). During the preparation process, take wet milling as an example; in order to reduce the particle size, high energy was consistently applied. High energy may cause amorphous on the particle's surface or directly change the crystal lattice of drugs. The amorphous or polymorphous states are likely to reconvert to the most thermodynamically stable crystalline form upon storage. Different solid states remarkably affect drug solubility and uniformity; thus, safety issues after administration arise.

Another notable drawback of nanocrystal formulation has been realized by more and more researchers in latest years. Van Eerdenbrugh and his colleagues evaluated the effect of particle size on saturation solubility of nanocrystals based on the Ostwald-Freundlich equation and different analytical methods (Van Eerdenbrugh et al., 2010). They found that a critical selection of analytical methods plays a vital role in valid solubility results. The solubility increases due to nanosizing are small, with measured increases of only less than 15%. Considering the low intrinsic solubility of poorly soluble drugs, this 15% enhancement is so trivial that the rapid dissolution kinetics should be regarded as the main characteristics upon evaluating the value of nanocrystals for oral drug product development. This fundamentally fails to solve the problem that some drugs need to increase their water solubility to increase their *in vivo* bioavailability. Sarnes et al. evaluated the bioavailability of itraconazole nanocrystal formulation and the market product *in vivo* (Sarnes et al., 2014). They found it difficult to predict the *in vivo* behavior based on the *in vitro* analysis; more specifically, the superior *in vitro* dissolution enhancement of nanocrystal formulation was not realized in *in vivo* drug absorption. Through those researches, nanocrystal formulation may not be suitable for those poorly soluble drugs with the solubility-limited issue during oral absorption.

1.2.2. Drug cocrystals

Solid-state chemistry involves the synthesis, structure and properties of solid materials. It focuses on the intermolecular interaction between the solid component, designed with new features and improvements based on the material properties. The solid material can be

either a single component or a multi-component, further divided into several categories, such as host-guest compounds, intramolecular salt, hydrate, solvates and cocrystals. When the active pharmaceutical ingredient is deficient in physicochemical properties, the compound forms as a salt or a complex is the preferred way to improve physical and chemical properties. However, this method requires at least one active pharmaceutical ingredient to be ionized. Because of this, non-ionic drugs cannot improve their properties through salt formation or complex formation. Moreover, less physiologically acceptable non-toxic acids or bases also significantly limit the application of this method. The physicochemical properties of the active pharmaceutical ingredient and the selected crystal form will primarily affect the drug's therapeutic effect. Therefore, how to choose the most effective crystalline form of the active drug is the most critical step in drug development and design. Research on the solid state of active pharmaceutical ingredients has become a pivotal aspect of new drug development in recent years.

The introduction of co-crystallization technology with excellent development potential into the pharmaceutical industry and the use of cocrystals as a new method that can effectively improve the physicochemical properties of active pharmaceutical ingredients has attracted widespread attention from researchers (Schultheiss and Newman, 2009). Co-crystallization technology can improve the physical and chemical properties of ionic or non-ionic active pharmaceutical ingredients. Furthermore, it helps us shorten the research and development cycle considerably with lower labor costs and obtain independent intellectual property rights for pharmaceutical products.

1.2.2.1.   Theoretical overview

Cocrystals have been known to humankind long ago, and quinone hydroquinone cocrystals were reported as early as 1844 and 1893 (Wöhler, 1844; Ling and Baker, 1893). However, little research has been done on cocrystals. The term "cocrystal" was first used to describe composite crystal molecules of pyrimidine and purine (Schimidt and Snipes, 1967). Various definitions of a cocrystal have appeared in the literature. However, a simple working definition can be taken as "a stoichiometric multi-component system connected by non-covalent interactions where all the components present are solid under ambient conditions" (Aakeröy and Salmon, 2005). A pharmaceutical cocrystal is composed of an active pharmaceutical ingredient (API) and an appropriate co-former.

In essence, cocrystal is a supermolecular self-assembly system (supermolecular synthon), resulting from the balance between thermodynamics, kinetics, and molecular recognition. During molecular self-assembly, intermolecular interactions and spatial effects affect the

formation of supramolecular networks, which directly affect the composition of crystals. In the cocrystal system, the interactions between different molecules are mainly divided into hydrogen bonds, halogen bonds, π stacking, and van der Waals forces.

Hydrogen bonds

The bond energy of hydrogen bonds is generally between 2-170 kJ/mol, much smaller than the bond energy of covalent bonds but is much larger than other non-covalent bonds (Desiraju, 2011). The hydrogen bond in cocrystal has saturation and directionality, which is the most vital force to form the cocrystals. At present, the hydrogen bonds existing in drug cocrystals are mainly O-H$\cdots$X (X=O, N), C-H$\cdots$X (X=O, N, π) and N-H$\cdots$N (Fig. 1.5). The statistical study of the cocrystal structure in Cambridge Structural Database (CSD) found that hydrogen bonding mainly occurred between specific cocrystal components: carboxylic acid-carboxylic acid, carboxylic acid-pyridine, carboxylic acid-amide, alcohol-pyridine and alcohol-amine (Wouters, 2011). For example, carbamazepine, a broad-spectrum antiepileptic drug, uses carbonyl groups in the molecule and imide groups in the saccharin molecule to form O$\cdots$H-N hydrogen bonds (Schultheiss and Newman, 2009). The -N= of methylpurine drugs, theophylline, forms hydrogen bonds as N$\cdots$H-O between oxalic acid, malonic acid, maleic acid, glutaric acid and a series of carboxylic acids constitute corresponding cocrystals.
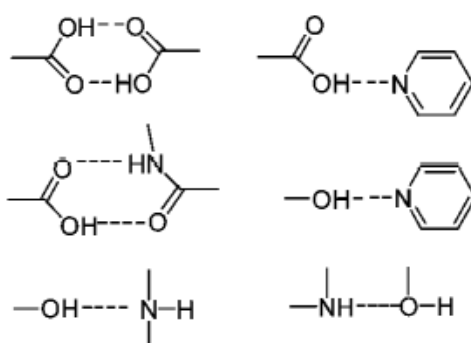
Fig. 1.5. Hydrogen bonding synthons.

Halogen bonds

Halogen bonds are non-covalent bonds formed between hetero atoms (N, O, S) containing lone pairs electrons and Lewis acid halogen atoms (Cl, Br, I). Halogen bonding is one of the fundamental forces for the molecular assembly of many halogen-containing organic compound crystals. A halogen atom is an electron-withdrawing group in a halogen bond,

and a hetero atom is an electron-donating group. For example, thiomorpholine forms with tetrafluoro-1,4-diiodobenzene and tetrafluoro-1,2-diiodobenzene through N···I, S···I between N, S and I on the thiomorpholine molecule. Bonding forms linear and zigzag halogen bond chains, thus forming a cocrystal (Cincic et al., 2008).

π stacking

π stacking plays an important role in small molecule crystallization, drug receptor recognition, drug receptor linkage, DNA spiral structure, and protein folding. There are two forms of π stacking, parallel superposition and parallel shift geometry. In addition, due to the mutual stabilization of C-H···π from the edge to the surface, the benzene ring often appears in a crossed T-shaped geometry. π stacking is a non-covalent bond with a certain elasticity, which can produce a variety of molecular level structures and guide molecules to form supramolecular aggregates with a topological structure. Thalladi et al. found that phenazine and 5,10-dihydrophenazine could form cocrystals with different proportions depending on the π stacking effect between the two (Thalladi et al., 2000).

Van der Waals force

Van der Waals force is a weak intermolecular force generated by neutral electrostatic interactions between neutral atoms. It has no directionality and saturation, and its range of action is only between a few hundred picometers. Caffeine and 2-hydroxybenzoic acid (2-HBA) are stacked in parallel end-to-end under the weak action of Van der Waals force, and then form a two-dimensional sheet structure under the influence of C-H···O hydrogen bonding and adjacent sheet structures are connected by Van der Waals force (Bucar et al., 2009).

In addition, some studies also found that there is often not only a single intermolecular force between the cocrystal components but a balance of multiple forces to achieve a stable lattice. Although there have been many researches and reports about the cocrystal structure and intermolecular forces, many problems in this field are worthy to research and exploration.

1.2.2.2. Physicochemical properties

The physical and chemical properties of cocrystals are of great importance to the development of APIs. The most important application value of cocrystals in pharmacy is that they can change the drug's physical and chemical properties without changing its

covalent structure. Compared with polymorphs, due to the introduced different components, cocrystals may cause more remarkable changes in the properties of drugs. Because of the different types of coformers, the properties of drugs can be adjusted to varying degrees. The overall motivation for investigating pharmaceutical cocrystals as an alternative approach during drug development is adjusting the physicochemical properties to improve a dosage form's overall stability and efficacy (Blagden et al., 2008). Physicochemical properties, such as crystallinity, melting point, solubility, dissolution, and stability have been studied extensively by researchers. Some critical physicochemical properties of pharmaceutical cocrystals are summarized as follows.

Melting point

The melting point is the temperature at which the solid and liquid phases reach equilibrium. It is a fundamental physical property and needs to be considered during solid dosage form development. There is a complex correlation between melting point and other physical properties like solubility, stability and processability. Drug cocrystals introduce another component into the drug crystal lattice, the melting points of APIs can be altered through forming cocrystals. Schultheiss et al. has investigated more than 50 cocrystalline samples, and found that 50% of the melting points of cocrystals were in between of the APIs and coformers and about 40% were lower than that of the APIs and coformers (Schultheiss and Newman, 2009). TRPV1 receptor antagonist AMG517 was investigated with 10 coformers to form cocrystals. The melting point of all the cocrystals was in between the APIs and coformers. 78% of the cocrystals' melting point variation is caused by the change of the melting point of coformers. These data indicated that the melting point of the cocrystals could be controlled by selecting different coformers.

Solubility and dissolution rate

During the development of solid dosage forms, solubility is another one of the most important quality attributes of APIs. The dissolution factors of solid drugs mainly depend on the intermolecular forces in the lattice and solute-solvent forces in the medium (Alhalaweh et al., 2012). The total free energy of the solution can be expressed as:

$$\Delta G_{solution} = \Delta G_{lattice} + \Delta G_{solvation} \qquad (2.1)$$

$\Delta G_{lattice}$ and $\Delta G_{solvation}$ are the lattice energy and the solvation energy during dissolution,

respectively. The formation of the cocrystals changes the original molecular arrangement and lattice packing of the drug; thus, during the solvation, the interaction between the drug and the solvent changes. The lattice energy of the drugs would be decreased after cocrystal formation, and it would be much easier for the cocrystals to dissolve. In addition, after the cocrystal is dissolved, it may affect drug-solvent interactions or change solution properties to improve drug solubility. Another explanation of the solubility enhancement of cocrystals is that during the dissolution, the coformers may dissolve faster than the APIs, which disrupts the arrangement of the lattice and could be seen as an amorphous form. In this case, the solubility of the APIs would be increased.

The dissolution rate increment is not only because of the solubility enhancement but also caused by the changed shape of the cocrystals. For example, the shape of adefovir is acicular. After the formation of adefovir-saccharin cocrystal, the shape of the cocrystal is a flake. Compared with an acicular shape, the flake shape has a larger surface area and has better wettability (Gao et al., 2011).

Stability

Drug stability is an essential factor in developing new drugs. Different types of stability (such as hygroscopicity, thermal stability, chemical stability, solution stability, etc.) need to be evaluated based on APIs' different molecular structures and characteristics. Generally, relevant chemical and physical stability data are obtained under accelerated stability conditions to determine the shelf life. By choosing a suitable coformer to form a cocrystal with the API can change the stability of the drug.

Hygroscopicity refers to the ability of a drug to absorb moisture in the air. This property is related to the chemical composition and structure of the drug. Most active pharmaceutical ingredients are susceptible to hydrate formation under high humidity conditions. However, when a hydrogen bond is formed between the active drug component and the coformers, the group that can form a hydrogen bond with water molecules in its structure is occupied, thereby hindering the interaction between the drug and water and reducing the hygroscopicity of the drug. For example, caffeine has two crystalline forms, α and β, and a hydrate. The stable crystalline form β can be converted to metastable crystalline form α at high temperatures. Interchanges can occur under the circumstances when caffeine forms drug cocrystals with coformers such as oxalic acid, malonic acid, maleic acid, and glutaric acid. Under 20 °C and relative humidity of 0%, 43%, 75%, and 98%, the 2:1 caffeine-oxalic acid cocrystal is the most stable form (Trask and Jones, 2005).

Thermal stability is another common parameter used to investigate the chemical and physical stability of drugs. Thermal stability tests can provide valuable information for drugs' chemical and physical stability. The drug cocrystal formed by paracetamol and 4,4'-bipyridine has good thermal stability and showed the same melting endothermic properties with monoclinic paracetamol (Oswald et al., 2002). Examining the transformation of crystals at high temperatures can help solve problems that may arise in the production and storage afterward, and provide theoretical guidance for the drying process.

Chemical stability refers to the ability of a substance to maintain its original physical and chemical properties under the influence of chemical factors. The chemical stability of drug refers to the drug content and color change due to chemical degradation reactions such as hydrolysis and oxidation. In addition, it also includes drugs and drugs, drugs and solvents, additives, impurities, containers and chemical reactions that occur between substances (air, light, moisture, etc.), resulting in the decomposition and deterioration of drugs. For example, the double bond on the carbamazepine heterocycle is prone to photodegradation reactions to produce dimers or oxidation products. When carbamazepine forms a cocrystal, its crystal packing structure and molecular arrangement change, thereby inhibiting the photodegradation reaction. Although there are few reports on the chemical stability of cocrystals, these evaluations have important implications for the development. The excellent chemical stability of drug cocrystals provides a new way to inhibit drug degradation from crystal engineering.

Bioavailability

In pharmacology, bioavailability is a measurement of the extent to which a drug reaches the systemic circulation (Shargel and Yu, 1999). The ultimate goal for cocrystal investigation is to improve the bioavailability of an API. Animal bioavailability is an important parameter to consider when preparing new forms of a compound. There are limited numbers of animal bioavailability studies on cocrystals. One research on the poorly soluble drug AMG517 cocrystal found that its bioavailability in a 10% Pluronic F108 suspension was higher than AMG517 (Bak et al., 2008). Further research showed that the cocrystal formed by AMG517 and the preservative sorbic acid in suspension have higher water solubility. The pharmacokinetics of AMG517 and its cocrystal were administered separately. The results showed that the C_{max} of the 10 mg/kg cocrystal dose was the same as that of the 500 mg/kg dose, and the AUC could reach half of the latter; the C_{max} and AUC of the 500 mg/kg cocrystal were respectively 8 times and 9 times of 500 mg/kg drug. Another

pharmacokinetic study demonstrated an improved bioavailability of indomethacin–saccharin cocrystal over the pure API indomethacin (Jung et al., 2010).

Mechanical properties

Different crystal forms will cause differences in drug density, mechanical processing properties, particle fluidity and miscibility, etc. These properties will affect the choice of the preparation process. Sun et al. investigated the tableting properties of caffeine, methyl gallate and caffeine-methyl gallate cocrystals (Sun et al., 2008). After the cocrystals were prepared, the cocrystal existed as a lamellar crystal and the force between the adjacent layers was mainly consist of weak Van der Waals force. Under shear force, the energy barrier required for relative sliding between adjacent layers is low. Therefore, the plasticity was significantly improved compared with the two drugs. Thus, cocrystals can avoid the phenomenon of sticking and punching when tableting a single API.

1.2.2.3. Manufacturing process of cocrystals

Drug cocrystals provide opportunities to improve the properties of drugs but also increase the scope of solid drug screening. Therefore, drug cocrystals need systematic and effective preparation methods. Up to date, different methods have been reported for the preparation of cocrystals by researchers (Fig. 1.6). Generally, traditional methods include solution crystallization methods, grinding methods. Some newly emerging methods used to form cocrystals are fusion, spray drying, and supercritical fluid techniques.
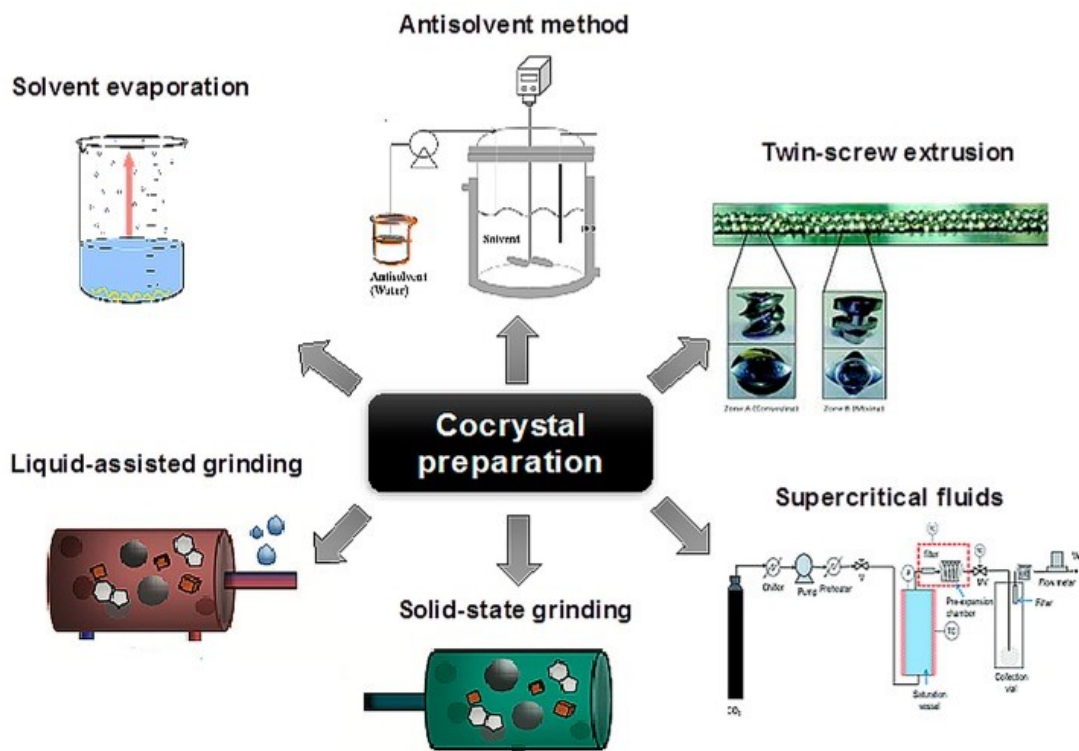
Fig. 1.6. Schematic presentation of methods applied in cocrystal formation (Karagianni et al., 2018).

Solution crystallization methods

Researchers have investigated different types of solution crystallization methods. Solution-based methods include solvent evaporation method, reaction crystallization and slurry conversion methods, etc. The principle of solution crystallization methods refers to dissolving API and coformers in solvent, and then use specific methods (such as solvent evaporation, cooling or antisolvent addition, etc.) to make the solution in the supersaturated state (Nolan et al., 2016; Nishimaru et al., 2016). In a solution containing multiple components, if both molecular structures contain groups that can form cocrystal bonds, and the interaction of these two molecules in the solvent is more substantial than other intermolecular forces (intermolecular or interaction with solvent molecules), the cocrystals would be highly possible to precipitate from the supersaturated solution. While applying the solution crystallization method, the two components should preferably have similar solubility in the solvent. Otherwise, the less soluble component may crystallize separately. For the combination where it is difficult to obtain a cocrystal in a single solvent, a mixed solvent can be selected to eliminate the difference in solubility of the components in the solvent and prevent the formation of solvates. The disadvantage of the solution crystallization method is that many crystallization solvents and crystallization conditions

need to be tested, and the single component crystallization may occur, which makes it difficult to separate and purify the cocrystal.

Grinding methods

Solid grinding can be traced back to thousands of years ago. People use a mortar similar to today's mortar to crush herbs. It is the earliest precursor of mechanochemistry. Solid grinding first appeared in scientific research in the study of quinone hydroquinone in 1844 (Wöhler, 1844). The grinding method in cocrystal preparation has been popular since 1980s, and it is a common method to transform between different solid forms. Grinding methods are generally classified into neat grinding and liquid-assisted grinding.

Neat grinding is to mix the cocrystal components in a particular proportion and then use a mortar or a ball mill to grind the components. During the grinding process, the ability to react between solid components depends on the structural complementarity and mobility of the two molecules. Jayasankar et al. prepared the cocrystals of carbamazepine and saccharin by neat grinding at room temperature and low temperature, and determined the structure of the obtained cocrystals by X-ray powder diffraction (Jayasankar et al., 2006). The study found that the yield of cocrystal grinding at room temperature is higher than that at low temperature; raising the temperature help improve the reactivity of the molecules during grinding.

The difference between liquid-assisted grinding and neat grinding is that it adds a small amount of solvent during the hybrid system to prepare a drug cocrystal. The mixture of cis 1,3,5-tricarboxylic acid cyclohexane and 4,4'-bipyridine did not form a cocrystal during neat grinding, but formed a cocrystal by adding small amount of methanol (Shan et al., 2002). Trask et al. studied on the cocrystals of caffeine and glutaric acid, and the cocrystals obtained by n-hexane, cyclohexane, or heptane solution-assisted grinding were columnar crystals (Trask et al., 2004). The bulk cocrystals were obtained by grinding with polar solvents such as chloroform, dichloromethane, acetonitrile, or water. Therefore, compared with neat grinding, liquid-assisted grinding has a broader range of applications, higher cocrystal yield, higher crystallinity, and can control the formation of polymorphs. In addition, liquid-assisted grinding avoids excessive use of solvents, which is somehow a green process.

Fusion methods

The cocrystal prepared by the fusion methods can generally be divided into differential scanning calorimetry (DSC), thermal microscopy, and hot-melt extrusion.

The differential scanning calorimetry method uses a differential scanning calorimeter (DSC) to prepare cocrystals. The components of the cocrystal are mixed in a specific measurement ratio and placed in a crucible. When temperature was raised, the mixed solid reached a molten state to obtain a cocrystal. Whether the cocrystal was formed can be determined by changing the substance's melting point. Compared with the traditional solution method, this method avoided the solvent selection process, dramatically shortened the cocrystal screening time, and was efficient and straightforward. Lu et al. used differential scanning calorimetry to measure four active pharmaceutical ingredients (caffeine, carbamazepine, sulfamethoxine, theophylline) and five coformer molecules (glutaric acid, nicotinamide, saccharin, salicylic acid and urea) (Lu et al., 2008). Sixteen cocrystals were screened out from those combinations, and nine of the cocrystals were new cocrystals that have not been reported.

The thermal microscopy method is also known as the Kofler method appeared at the end of the nineteenth century (Stahly, 2009). A small amount of two different crystalline substances was placed on a microscope slide. As the temperature increases, a part of the substance melts and a part remains solid, forming a strip-shaped contact area between the two substances. Observed by a polarizing microscope, if no crystals are formed at the interface, it indicates that a eutectic is formed between the two; otherwise, a cocrystal is formed. Thermal microscopy could be chosen while systems where the solubility of drugs and coformers differ significantly and it is not easy to obtain cocrystals by solvent crystallization. However, when the melting point of the drug and the coformers are close, screening with this method is more complicated.

In the hot-melt extrusion technique, the cocrystals are prepared by heating the drug and coformers with intense mixing, which improves the surface contacts without solvent. The hot-melt extrusion method can provide more efficient mixing and material contact, which is beneficial to the formation of cocrystals and is conducible for expanding industrial production. Ibuprofen-nicotinamide cocrystal and AMG517-sorbic acid cocrystal were prepared by this method (Dhumal et al., 2010; Medina et al., 2010). The limitation of this method is that both coformer and API should be miscible in molten form and is not suitable for thermolabile drugs.

Spray drying technique

The spray drying method can produce homogeneous powder particles with narrow size distribution and a fine pore structure, which is suitable for producing capsule or sugar-coated drugs to control drug release. The spray drying method mixes a highly dispersed liquid (suspension or emulsion) with a sufficient volume of hot air to produce small droplets. Then the liquid is instantly evaporated to form solid particles. In the spray drying method, the drug is entirely or partially dissolved in the solution, increasing the possibility of phase transition. The solvent in the droplet evaporates instantly, providing a way for rapid metastable or amorphous crystallization. The spray drying method reduces thermodynamics in the cocrystal production process and is suitable for industrial amplification (Alhalaweh and Velaga, 2010).

Supercritical fluid technique

Supercritical processes are widely used in pharmaceuticals and related fields, such as health products, petroleum, chromatography, and pigment production. The supercritical fluid method can be used with or without solvents, hence cause no harm to the environment. The supercritical process has attracted more and more attention. The supercritical fluid method is divided into two basic types: the solvent method and the solvent-out method. In a solvent method, the supercritical fluid plays a role as a solvent medium, generating intermolecular forces to promote cocrystal formation. The ability of a supercritical fluid to dissolve a substance is related to its density, which changes with pressure and temperature. After dissolving solid matter in supercritical carbon dioxide, the solubility decreases as the system pressure decreases, resulting in the supersaturation and precipitation of cocrystals. The supercritical solvent-out method uses the mutual solubility of supercritical fluids and organic solvents. Under certain pressure, supercritical carbon dioxide is mixed with an organic solvent in which drugs and coformer molecules are dissolved. The solute's solubility in the mixed solution is reduced, so the cocrystal is precipitated. Padrela et al. used these two supercritical fluid technologies to successfully prepare cocrystals of indomethacin and saccharin (Padrela et al., 2009). Compared with the traditional crystallization method, the advantages of the supercritical fluid are the synchronous processes of the cocrystal and particle formation, and the process is safe and environmentally friendly. It is suitable for structurally unstable substances or heat-sensitive substances.

1.2.2.4. Advantages and drawbacks of cocrystals

Advantages of cocrystals

The biopharmaceutics classification system (BCS) classifies the oral absorption of drugs based on their solubility and permeability, of which BCS Class II drugs account for all commercial and 40% of the total number of developed drugs, their oral absorption is restricted mainly by solubility. Salt formation of compounds is a common method to change the solubility of active pharmaceutical ingredients and improve physical and chemical properties. More than half of the drugs on the market are in the form of salts. However, the ions that can be used for salt formation are less. The drug cocrystal has the following advantages. First, cocrystals are solids and have high stability. Second, the component of a drug cocrystal can be a neutral molecule to encompass all active pharmaceutical ingredients, including acids, bases, and non-ionized molecules. Third, many potential and non-toxic coordination molecules like food additives, preservatives, pharmaceutical excipients, vitamins, minerals, amino acids, and other active pharmaceutical ingredients can form drug cocrystals (Almarsson and Zaworotko, 2004).

In recent years, the application of drug cocrystals in modifying the physical and chemical properties of active pharmaceutical ingredients has received widespread attention. For thermally unstable drugs, the formation of cocrystals can increase the melting point of the drug and effectively avoid its degradation during heating in specific formulation processes (such as hot-melt extrusion). After the hydrogen bond is formed between the active drug component and the coformers, thereby hindering the interaction between the drug and water and reducing the hygroscopicity. Cocrystals could improve the stability during preparation and storage. Furthermore, cocrystals could alter APIs' solubility and dissolution profiles, thus promote the absorption of drugs in the human body.

Drawbacks of cocrystals

Although drug cocrystals improve the solubility, the dissolved API can crystalize separately during the dissolution process, which is called solution mediate phase transition (Greco and Bogner, 2012). After the cocrystal contact with the medium, the cocrystal structural unit is dissolved in the medium in the form of an API-coformer conjugate. This conjugate can be separated into free API molecules and coformer molecules. There is a binding separation equilibrium between API molecules and coformer molecules. When the total API concentration is supersaturated, API solids will precipitate out of the solution, damaging the advantages of cocrystals in improving drug solubility. Furthermore, there is little research on how to suppress this cocrystal solution mediate phase transition.

Studies on multiple groups of drug cocrystals have shown that the dissolution peak of drug dissolution often appears in a short time (< 30 min); ideally, it can maintain a high concentration for a long time (4-6 h) (Wei et al., 2018). The enhancement of solubility profiles by drug cocrystals is similar to the supersaturation of amorphous drugs. The "spring-parachute" theory used to explain the dissolution process of amorphous drugs can be used to explain the disadvantages of cocrystals. First, the cocrystal dissolves into amorphous or nanomolecular clusters. Then, the metastable state with a high dissolution rate is transformed into a crystal form with low solubility. API would become highly supersaturated in the microenvironment on the surface of the drug cocrystal particles and immediately crystallize as the single-component API polymorph thus cover the surface of drug cocrystal particles. The API released from cocrystal is diffusion rate limited within the unstirred water layer on the surface of the particles. Although the bulk solution is always in a state of sink conditions for a single drug particle, this surface-mediated conversion of cocrystal to the component of API polymorph prevents the rapid cocrystal dissolution rate from significantly increased drug solution concentrations.

1.2.3. Drug amorphization

Solid is formed by the accumulation of molecules/atoms. Due to different stacking patterns, the solid matter has a crystalline state (also known as a crystal) and an amorphous state (also known as an amorphous state). The intermolecular packing in crystalline materials is ordered, symmetrical and periodic, while the molecular packing in amorphous materials is disordered. Compared with the crystalline form, the amorphous form lacks a long-range ordered structure. However, the two have similar molecular environments and non-covalent interactions (hydrogen bonding, hydrophobic interaction, and polarization interaction). Due to the different internal stacking structures, the amorphous form of a drug has some physical and chemical properties (such as thermal behavior, dissolution, compressibility, etc.) that are different from its crystalline state and has received significant attention from drug formulators (Baghel et al., 2016).

1.2.3.1. Theoretical overview

If a crystalline solid is heated beyond its melting temperature and cooled back to its original temperature with insufficient time for nucleation, the liquid will lose all long-range orders and become amorphous at temperatures below its melting point. Initially, the supercooled liquid adjusted itself to the changing environment (temperature), giving off excess enthalpy, entropy, and volume, following the equilibrium line extended from the liquid state. The

amorphous material in this temperature range is called a rubber or a supercooled liquid. However, due to the increased viscosity and decreased molecular mobility at a specific lower temperature, the amorphous material will not continue to follow the equilibrium line extended from the liquid state. The amorphous phase in this temperature range is called a glass.

The amorphous form is in a state of high energy disorder, which is directly reflected in the properties of the drug. Amorphous materials have higher Gibbs free energy than their crystalline counterparts, thus have higher apparent solubility and faster dissolution rates, leading to higher bioavailability. Due to the amorphous substance's large free energy per unit surface, the particle is easily hydrated in the suspension after the solid disintegrates, and the deflocculation effect of the thicker hydration film is better than the crystalline substance (Florence and Attwood, 2015). Amorphous drugs can dissolve quickly, making them more concentrated in the gastrointestinal fluid and more accessible to be absorbed. In terms of pharmacokinetic parameters, C_{max} is higher. In addition, if the amorphous drug does not undergo a crystalline transformation in the small intestine, or the rate of crystalline transformation is slow, the drug concentration can be higher than that achieved by the steady-state crystalline.

However, the physical instability of amorphous APIs is a complex problem and the major limitation impedes the broader application of amorphous products in common practice. The amorphous state is thermodynamically unstable, and it is easy to change to lower energy and a more stable crystalline state spontaneously. The transformation will occur in the process of amorphous drug production and during its storage or dissolution. Once the drug changes from amorphous to crystalline, its high solubility advantage will be lost. The rapid crystallization of amorphous drugs is disadvantageous for controlling the stability of amorphous drug formulations. Strategies such as inhibiting the kinetic energy of drug molecules in an amorphous drug system and reducing the free diffusion rate of surface molecules can provide ideas for improving the stability of amorphous drug formulations. In general, many pharmaceutical polymer materials can also be effective crystallization inhibitors to improve the stability of amorphous drugs (Patel and Anderson, 2014). However, the selection and use of polymer inhibitors need to be based on a thorough understanding of the physical and chemical properties and crystallization mechanisms of different amorphous drugs to design rational and effective amorphous drug formulations.

1.2.4. Integration of solubility enhancement techniques

The number of poorly soluble active pharmaceutical ingredients has increased as most innovative drugs in the development pipeline belong to the BCS class II and IV. Since their low solubility and dissolution rate limit bioavailability after oral administration, different solubilization methods (inclusion complexes, salts, solid dispersions/solutions, cocrystals, particle size reduction, etc.) were applied to overcome those limitations (Kumar et al., 2011). However, a single solubilization technique always has its drawbacks (introduced in the above section) which the solubility enhancement would be tailored to a certain level. Thus, the solubility and dissolution rate advantage might be lost. It is, therefore, necessary to find ways to overcome the drawbacks and even further improve the solubility and dissolution rate. De et al. reported itraconazole–adipic acid nano-cocrystal suspension with a particle diameter of 549 nm, and the dissolution and oral absorption of the nano-cocrystal were equal to or greater than those of amorphous formulations (De et al., 2014). Kumar et al. studied the formulation of nano-amorphous spray-dried itraconazole powders and showed the superior oral bioavailability of nano-amorphous systems compared to macro-amorphous powders (Kumar et al., 2014). A binary system called co-amorphous consists of cocrystal and amorphous was investigated (Laitinen et al., 2017). The study demonstrated that co-amorphous binary mixtures of small molecules were a potential strategy to improve drugs' dissolution behavior and to stabilize the amorphous state. Integrating different solubilization techniques might be a promising way to learn from others' advantages to offset one's drawbacks. Furthermore, by overcoming their respective shortcomings, the potential of solubilization could be more stimulated.

1.2.4.1. Integration of nanocrystal and cocrystal

Nanocrystal could significantly increase the dissolution rate of poorly soluble drugs with increased surface area. However, since most drug nanocrystals are in the range of 100 – 1000nm, according to the Ostwald Ripening equation, the solubility of drug nanocrystals in this range could only be improved less than 15%. Considering the low solubility of the drug itself, the enhancement through nanotechnology is negligible.

Cocrystals are multi-component solids, where the crystal contains two or more molecular components. The decrease of the solvation barrier significantly increases the solubility of the whole cocrystal system. However, problems also exist in the cocrystal system. During the dissolution process, the surface of the cocrystal would transform into the original crystal structure, thus covering the surface and tailoring the dissolution of the system.

When the cocrystals are integrated with nanocrystals, i.e., nano-cocrystals, it could be

supposed to maintain a superior dissolution rate. Meanwhile, due to the superior dissolution rate, the surface-mediated transformation could be avoided in the cocrystal system. Recently, there have been only a few publications and patents investigating the integration of cocrystal and nanocrystal. De et al. investigated the bioavailability of itraconazole using nanosized cocrystals prepared with wet milling method in combination with adipic acid and Tween80 (De et al., 2014). The results showed that nanosized cocrystal formulation yields equally or faster releases and larger AUC compared with the market product. However, the ratio of API and coformer in the nanosized cocrystal formulation seemed hard to control, which is not suitable for further investigation and application. Meanwhile, the mechanism of how nanosized cocrystal increases the bioavailability and the physicochemical properties like saturation solubility of the formulation is not thoroughly investigated. Karashima et al. reported a novel solubilization technique consisting of nano-cocrystal by integrating cocrystal and nanocrystal to maximize the solubilization effect (Karashima et al., 2016). They performed monodisperse carbamazepine-saccharin, indomethacin-saccharin and furosemide-caffeine nano-cocrystal formulations with particle sizes of less than 300 nm by wet milling method. The optimized nano-cocrystal formulations were physically stable for at least one month and the dissolution profiles were significantly improved compared with single solubilization methods. In their study, the saturation solubility and the mechanism of improved dissolution are not clarified. Meanwhile, the dissolution profile of indomethacin cocrystal formulation is not shown. Huang et al. reported a nano-cocrystal formulation of phenazopyridine and phthalimide with mean diameters of 20 nm by sonochemical anti-solvent precipitation method (Huang et al., 2017). Release and oral bioavailability studies indicated that the nano-cocrystal showed a superior release rate and oral absorption than the hydrochloride salt and the original cocrystal. However, the stabilizer, SDS, which they used in the formulation, was too much and exceeded the critical micelle concentration.

1.2.4.2. *Integration of nanocrystal and amorphous*

An increase in the exposed surface area (or surface area-to-volume ratio) by particle size reduction causes an increase in the dissolution rate and thus the oral bioavailability. In addition, according to the Kelvin equation, the drug's saturation solubility depends on the drug particle size. However, nanosized crystalline powders may not be a practical approach for solubility-limited drugs (i.e., solubility is rate-limiting for oral bioavailability). In the case of amorphous formulations, the solubility of the drug is increased over the crystalline form due to its high-energy state (higher Gibbs' free energy). However, amorphous formulations

are unstable and will convert to the stable crystalline form over pharmaceutically relevant timescales. Recently, nanosized amorphous formulations, namely "nano-amorphous," have been utilized to enhance the dissolution rates and solubilities of poorly soluble drugs. Theoretically, combining nanotechnology and amorphization approaches may offer absolute or synergistic effects in terms of solubility and dissolution rates. The advantage of amorphous versus crystalline nanoparticles is the considerably higher kinetic solubility of amorphous nanoparticles, which can be as much as 10 to 1600-fold.

A wide range of case studies is reported which describe the advantages of amorphous nanoparticles compared to amorphous solid dispersion and nanocrystalline formulations concerning dissolution and the enhancement of oral bioavailability of poorly soluble drugs. Zu et al. worked on preparing and characterizing amorphous amphotericin B nanoparticles for oral administration using liquid antisolvent precipitation, followed by freeze-drying (Zu et al., 2014). The particle size of amorphous nanoparticles is around 200 nm and during *in vitro* dissolution testing, the amorphous amphotericin nanoparticles resulted in a 2.1X supersaturation level compared to the raw crystalline amphotericin. Jog et al. prepared amorphous ABT-102 nanoparticles (ABT-102 is a selective TRPV1 antagonist used in pain management) via sono-precipitation using 2 different stabilizers (Soluplus and PVP K25) (Jog et al., 2016). This study showed that amorphous nanoparticles prepared using sonoprecipitation followed by spray drying have an enhanced dissolution rate and may enhance bioavailability compared to macrocrystalline drugs. Kumar et al. formulated nano amorphous spray-dried powders to enhance oral bioavailability of itraconazole. *In vitro* dissolution testing and *in vivo* studies showed the superior performance (i.e., higher and faster supersaturation solubility) of the nano amorphous formulations compared to melt-quench amorphous and crystalline itraconazole formulations (Kumar et al., 2014). The nano amorphous formulation resulted in a 2.5-fold and 18-fold increase in bioavailability compared to the macro amorphous (melt quench) and macrocrystalline formulations. Guo et al. investigated a novel method to prepare amorphous nanoparticles of hydrophobic drugs using the nano porous membrane extrusion method (Guo et al., 2018). Three poorly soluble model drugs, silymarin, ß-carotene, and butylated hydroxyltoluene, were investigated. The dissolution velocity of butylated hydroxyltoluene nanoparticles was faster than the untreated powder at pH 7.4 PBS buffer; however, at pH 5.5, the dissolution velocity for both forms was almost the same.

1.3. Downstream process of nanosuspensions transformation to a final oral dosage form product

The downstream processing of nanocrystals mainly refers to processing suspensions containing nanoparticles into dosage forms that can be directly used in various administration routes. Nanocrystals can be applied to many downstream processing methods. In addition to the processing into oral tablets and capsules and intravenous injection dosage forms, the current experimental research also includes other administration routes such as eye, pulmonary and transdermal delivery. Due to nanocrystal's improved dissolution rate and saturated solubility, oral tablets and capsules accelerate the absorption of poorly soluble drugs in the human body and enhance bioavailability. Downstream processed nanocrystal intravenous injections have high drug loading and avoid using non-aqueous solvents, thus reducing the volume of medication, toxicity, and the occurrence of adverse reactions. After processing nanocrystal into ophthalmic agents, the specific corneal adhesion property of nanocrystals can reduce drug loss and reduce the patient's eye tension compared with ordinary eye drops, thus improving patient compliance (Romero et al., 2016). Nanocrystals with small particle sizes can target alveolar macrophages when inhaled and administered to the lungs, reduce the deposition of drugs in the respiratory tract, increase the absorption of drugs in the respiratory tract, etc. (Mangal et al., 2017). Preparation of poorly soluble drugs into nanocrystals and further downstream processing to prepare products of different dosage forms can effectively improve the pharmacokinetic characteristics of the drugs, complete drug delivery, and make up for the defects of ordinary dosage forms. An overview of partial products in the current market or clinic trail based on nanosuspension downstream processing technologies has been presented in Table 2. From the perspective of marketed and clinical research products, downstream processing technology to prepare nanocrystals into oral dosage form products accounts for a large proportion. Therefore, this dissertation will discuss the downstream process of nanocrystals into oral solid dosage forms.

Table 1.2. Overview of partial drug nanocrystals in downstream process (Chin et al., 2014)

Trade name	Drug	Therapeutic use	Administration use	Status
Emend	Aprepitant	Antiemetic	Oral	Listed
Rapamune	Sirolimus	Immunosuppressant	Oral	Listed
Tricor	Fenofibrate	Hypercholesterolemia	Oral	Listed
Megace ES	Megestrol acetate	Antianorexic	Oral	Listed
-	Insulin	Diabetes	Oral	Phase I clinical
-	Cytokine inhibitor	Crohn's disease	Oral	Phase II clinical
-	Budesonide	Asthma	Pulmonary	Phase I clinical
Xeplion	Paliperdidone palmitate	Schizophrenia	Intramuscular	Listed
-	Paclitaxel	Anticancer	Intravenous	Phase III clinical

In terms of clinical application and market sales of oral formulations, solid dosage forms are generally easier to be accepted by patients due to their long-term stability, controllable drug release and absorption, and dose convenience. However, most of the drug nanocrystal formulations used in *in vivo* experiments are aqueous nanosuspension in many studies. The majority of literatures focuses on the preparation and characterization of stable nanosuspension formulations. In contrast, research on the downstream process of nanosuspensions is scarce.

The most widely used dosage forms in oral formulations include tablets, capsules, granules and pellets. There are currently two leading technologies used for the downstream processing of oral dosage forms of nanocrystals: the first technology is to transform the nanosuspension into powder form through drying processes such as freeze-drying and spray drying, and the obtained powder is mixed with other excipients and further processed into a solid dosage form through a molding process (such as direct compression, capsule filling) afterward; the second technique combines the drying process and subsequent

processing described in the first technique in one step. For example, an aqueous nanosuspension is used as a granulation liquid in the granulation process or as a layered dispersion in a fluidized bed process. In the downstream processing of nanocrystals into oral solid dosage forms, the main problem that needs to be solved is how to retain the advantages of small nanocrystal particles' large surface area, and rapid dissolution in the final solid formulations. Nanocrystals tend to form irreversible aggregates during drying or processing, which dramatically affects the *in vivo* release. The drying process need to be optimized to obtain the ideal nanocrystal powder, and various subsequent downstream processes may also affect the final product's performance. For example, when using nanocrystalline powder for direct compression, drug nanoparticles with high surface area provide many contact points for binding. Therefore, the compression force in the tablet production of drug nanocrystals might lead to irreversible aggregation.

1.3.1.   Literature review

Tuomela et al. transformed APIs into nanocrystal suspensions and further developed them into direct compression and granulated tableting masses (Tuomela et al., 2015). They reported that the amount of the nanocrystal powder in the solid formulation was critical. Approximately 40% of freeze-dried nanocrystal powder provided the most advantageous final formulations regarding dissolution enhancement.

Lee et al. studied the physical properties of drug nano and microparticles after processing into solid dosage forms (Lee, 2003). A small amount of hydroxypropyl cellulose was used as a stabilizer. Investigation on fracture surfaces and micro indents showed microcracking (fragmentation) was more extensive in microparticulate compacts. The boundary between primary particles remained even after disintegration in water in nanoparticulate compacts. In the meantime, strength and hardness were found to be slightly higher in nanoparticulate compacts. This phenomenon indicated that it was easier to reach enough hardness with less compression force while using nanoparticles to form tablets.

In another tablet formulation of nanoparticles case, Basa et al. demonstrated that tablet formulation incorporating ketoconazole nanoparticles showed a significantly faster drug dissolution rate in a discriminating dissolution medium compared with commercially available tablet formulation (Basa et al., 2008). They also stressed that the type of disintegrant in the tablet formulation of nanoparticles is critical and may influence the final dissolution profile. Parmentier et al. systematically investigated the influence of the type of coating polymer, bead material and bead size, and coating thickness on the properties of

dried itraconazole nanosuspension-layered beads (Parmentier et al., 2017). The optimized nanosuspension was coated with two different polymers onto two different bead materials and sizes. Bead laying was proved as a suitable method for nanosuspension solidification and further dosage form application. Tan et al. solidified itraconazole nanocrystals through spray coating onto beads, followed by blending with excipients, then tablet compression (Tan et al., 2017). They demonstrated that the compaction of nanosuspension-layered beads is a suitable process for processing an itraconazole nanosuspension into a solid dosage form without compromising drug release.

Nekkanti et al. dried a candesartan nanosuspension with mannitol and compressed the dried powder with 1% colloidal silicon dioxide, 1% magnesium stearate, and 10% sodium starch glycolate, corn starch, or crospovidone (Nekkanti et al., 2009). Although they demonstrated that the disintegration time varied more than two-fold between the fastest disintegrating formulation with crospovidone (10 min) and the slowest with corn starch (>20 min), the disintegration time of formulation with crospovidone is faster than sodium starch glycolate. The findings might be an interesting point worth investigating. Based on common tablet formulation studies, sodium starch glycolate works better than crospovidone as a disintegrant. Here gives a conjecture: compared with ordinary tablets, tablets containing nanocrystalline drugs with more contact points will form a tighter internal structure after compression, thus making it more difficult for water to enter. In addition, nanocrystal will compete with the disintegrant during water absorption due to its high hygroscopicity. Therefore, crospovidone can provide greater disintegration power than sodium starch glycolate when less water is available for absorption during tablet disintegration.

Liu et al. developed a controlled delivery osmotic pump capsule containing carvedilol nanosuspension drying powder, mannitol and plasdone S-630 (Liu et al., 2014). Carvedilol nanosuspension was prepared by precipitation–ultrasonication technique and was further lyophilized. Due to the combined advantages of nanosuspension and osmotic pump system, the bioavailability of carvedilol was significantly improved *in vivo* and the plasma concentrations were more stable than that of the marketed tablets. Nanocrystals can be used not only in immediate-release formulations but also in sustained and controlled release formulations. Under the premise of retaining the advantages of rapid release of nanocrystals, by controlling the downstream processing technology to mediate the dosage form to achieve sustained and controlled release. It was a promising strategy in improving the oral bioavailability, minimizing the frequency of drug administration, and lowering the average peak plasma concentration of poorly soluble drugs.

1.4. Research objectives

The main aim of this work was to explore the combination of nanocrystal techniques with cocrystal and investigate their synergic effect to improve the solubility and dissolution rate of poorly soluble drugs. Further investigation of the supersaturation solubility of nano-cocrystal, precipitation inhibition and formulation optimization were performed. A further objective was to investigate the different downstream processes of nano-cocrystals into oral dosage forms. The specific goals included as follows:

a) To compare different lab-scale preparation methods of nanocrystal formulations;

b) To prepare and characterize nano-cocrystal formulations;

c) To optimize nano-cocrystal formulations and investigate the mechanism;

d) To investigate the downstream process of nano-cocrystals into solid oral dosage forms.

2. MATERIALS AND METHODS

2.1. Materials

Drugs: Itraconazole (BASF AG, Ludwigshafen, Germany), Sporanox® 100 mg capsules (Janssen GmbH, Neuss, Germany), indomethacin (Fluka Chemie AG, Buchs, Switzerland)

Stabilizers: Poloxamer 188, poloxamer 407, Tween 80, D-α-tocopheryl polyethylene glycol 1000 succinate (TPGS) (BASF SE, Ludwigshafen, Germany), sodium dodecyl sulfate (SDS) (Carl Roth GmbH & Co., Karlsruhe, Germany)

Polymers: hydroxypropyl methylcellulose E5/E50 (HPMC E5/E50), hydroxypropylmethylcellulose acetate succinate (HPMCAS) (Colorcon Ltd., Dartford Kent, UK), hydroxypropyl cellulose (HPC-SSL) (Nisso Chemical Europe, Düsseldorf, Germany), polyvinyl pyrrolidone (PVP K30), polyvinyl pyrrolidone vinyl acetate copolymer (PVPVA64) (BASF SE, Ludwigshafen, Germany)

Solvents: Methanol, ethanol, chloroform, tetrahydrofuran, ethyl acetate, dimethyl sulfoxide (DMSO) (Carl Roth GmbH & Co., Karlsruhe, Germany), ultrapurified water purified by a Milli-Q-apparatus (Millipore GmbH, Darmstadt, Germany)

Other chemicals: Fumaric acid, succinic acid, saccharin, nicotinamide (Merck KGaA, Darmstadt, Germany), lactose (Granulac® 200, Meggle AG, Wasserburg, Germany), microcrystalline cellulose (Avicel® PH102, FMC BioPolymers, Philadelphia, USA)), sugar beads (Suglets® 25-30 mesh, 600–710 µm diameter, NP Pharm S.A., Bazainville, France), MCC beads (Celphere® CP-507 grade, 500-710 µm diameter, Asahi Kasei Chemicals Corporation, Tokyo, Japan), hydrochloride (HCl), sodium hydroxide (NaOH), sodium chloride (NaCl) (Sigma Aldrich Chemie GmbH, Steinheim, Germany)

2.2. Preparation and optimization of nanocrystal formulations with different lab scale wet milling methods

2.2.1. Preparation of nanocrystal

1% itraconazole was pretreated with adding to 0.5% poloxamer 407 solutions (all w/w) and homogenized with an Ultra Turrax T-25 (IKA®-Werke GmbH & Co. KG, Staufen, Germany). The yttria-stabilized zirconium oxide beads (Hosokawa Alpine, Germany) possessed various sizes (diameters of 0.1, 0.2, and 0.3 mm). The pretreated suspension was milled with different lab-scale methods described in detail below.

2.2.1.1. Miniaturized milling

The drug suspension was milled in a super reduced scale with a miniaturized milling method (Romero et al., 2016). The milling chamber consisted of a 2 mL glass vial and three cylindrical stirring bars, which disposed vertically one over the other. The ratio of beads (beads size 0.1 mm) to suspension was 3:1 (w/w). After pouring the 0.5 mL pretreated suspension into the vials, the glass vial was fixed on a petri dish containing ice to keep a low product temperature during milling. The suspensions were stirred at 1000 rpm on a magnetic stirring plate. Samples were taken after defined intervals up to 48 h.

2.2.1.2. Beaker milling

The drug suspension was milled on a moderate lab scale with the beaker milling method. 10 mL of pretreated drug suspension was poured into a 50 mL beaker containing beads and a suitable magnetic stirrer. The ratio of beads (0.3 mm) to suspension was kept as 3:1 (w/w). The beaker was fixed on a large petri dish containing ice to keep a low product temperature during milling. The suspensions were stirred at 1000 rpm on a magnetic stirring plate. Samples were taken after defined intervals up to 48 h.

2.2.1.3. Agitator mill

The drug suspension was milled on a larger lab scale with the agitator mill method. 60 mL of pretreated drug suspension was milled at 3200 rpm with a Dyno®-mill KDL-A (Willy A. Bachofen AG, Muttenz, Switzerland) in the discontinuous batch mode. The ratio of beads (0.3 mm) to suspension was kept as 3:1 (w/w). The water was connected to the outer container in order to cool down the system to below 15 °C during operation. Samples were taken after defined intervals up to 3 h.

2.2.1.4. Dual centrifugation

Dual centrifugation is a new lab-scale method related to wet bead milling. It differs from normal centrifugation by an additional rotation of the samples during the centrifugal process. In addition, up to 40 vials (2 mL) can be processed in one run with efficient cooling during the process. DC was performed using a ZentriMix 380 R (Andreas Hettich GmbH und Co KG, Tuttlingen, Germany). 1 mL of pretreated drug suspension and milling beads (0.3 mm) at ratio of 1:3 (w/w) were added into 2 mL small disposable vials. The milling speed was set at 1000 rpm, and the cooling device was set to 0 °C. Samples were taken after defined intervals up to 3 h.

Itraconazole nanosuspension were further optimized regarding to types of stabilizers or polymers (0.5% w/w), filling volume, beads size and ratio, milling speed and time. The optimized nanosuspensions were exposed to freeze under -80 °C and afterwards freeze-dried (Alfa® 2–4 LD Plus freeze-dryer, Martin Christ Gefriertrocknungsanlagen GmbH, Osterode am Harz, Germany). The lyophilization process was performed at -48 °C and 0.055 mbar.

2.2.2. Preparation of physical mixture

Physical mixture (PM) was prepared by shaking the powder mixture of itraconazole and poloxamer 407 (2:1, w/w) together for 1 min in a glass vial or by mixing them gently with a pestle in a mortar.

2.2.3. Characterization of nanocrystal formulations

2.2.3.1. Photon Correlation Spectroscopy (PCS)

The mean particle size (z-average) and the polydispersity index (PDI) of the nanosuspension after dilution and lyophilized nanocrystal powders after redispersion with drug saturated stabilizer solutions were measured by photon correlation spectroscopy (PCS) using a Zetasizer® Nano ZS (Malvern Instruments Ltd., Malvern, UK, n = 3).

2.2.3.2. Light microscopy

Microscopic observations were performed using a polarized light microscope (Axioscope, Carl Zeiss Jena GmbH, Jena, Germany).

2.2.3.3. *Differential scanning calorimetry (DSC)*

Thermal analysis was conducted using a DSC (DSC 6000, PerkinElmer LAS GmbH, Rodgau, Germany), and data were analyzed by Pyris software (PerkinElmer LAS GmbH, Rodgau, Germany). 5 ± 1 mg of raw drug powder, physical mixture, freeze-dried nanocrystal powder were accurately weighed in 50 µL aluminum pans with pierced lids. The samples were heated from 20 to 200 °C with a heating rate of 10 °C/min and afterward cooled to room temperature with a cooling rate of 20 °C/min. The test was performed under a continuously purged dry nitrogen atmosphere (flow rate 40 mL/min).

2.2.3.4. *X-ray powder diffraction (XRPD)*

The XRPD measurements were performed using Cu Kα radiation (λ = 0.154 nm) on a Bruker D8 Advance diffractometer (Bruker AXS GmbH, Karlsruhe, Germany) in the 2θ range from 10° to 50° with a step size of 0.01°.

2.2.4. **Stability studies of optimized nanocrystal formulation**

Nanosuspensions were stored in glass bottles at 4, 25 and 40 °C for a period of up to 1 month. The stability was assessed in average particle size and PDI (at 0, 7 days, 14 days and 1 month).

2.2.5. *In vitro* **dissolution tests**

Drug powder, physical mixture, nanocrystal lyophilized powder, and commercial product Sporanox® without hard gelatin capsules (corresponding to 100 mg of itraconazole) were investigated using the USP rotating paddle method (VK 7010, Vankel Technology Group, Cary, USA) in dissolution medium at 37 °C with 100 rpm stirring speed. The dissolution medium under sink condition was 900 mL 0.1N HCl with 0.7% SDS. And the non-sink condition was 500 mL 0.1N HCl. Samples were taken at given time points and filtered through a 0.1 µm filter. The amount of dissolved drug was measured by UV-spectrophotometrically at 259 nm.

2.3. Combination of cocrystal and nanocrystal techniques to improve the solubility and dissolution rate of poorly soluble drugs

2.3.1. Preparation of macro-cocrystals

Itraconazole (ITZ) cocrystal preparation was described previously (Shevchenko et al., 2013). Briefly, 3.53 g of pure ITZ in 20 mL chloroform and 0.29 g of fumaric acid (FUM) or 0.30 g of succinic acid (SUC) in 20 mL tetrahydrofuran were mixed in a bottle. The prepared mixture was heated to 60 °C until the dissolution of all solids and then the bottles were sealed with a pierced parafilm to allow a slow evaporation. Once observing visible crystals, parafilm was removed to accelerate the evaporation. Finally, the solids were dried in a vacuum oven at 50 °C for 24 h until mass balance.

Indomethacin (IND) cocrystals were prepared by solvent evaporation as previously reported (Basavoju et al., 2008). Briefly, 3.58 g of γ-form IND was mixed with 1.83 g of saccharin (SAC) or 1.22 g of nicotinamide (NCT) in 100 mL ethyl acetate. The prepared solutions were heated to 50 °C with continuous stirring until the dissolution of all solids, then the solvent was allowed to evaporate in fume hood at room temperature. Finally, the solids were dried in a vacuum oven at 40 °C for 24 h until mass balance.

2.3.2. Preparation of physical mixtures

Physical mixtures of ITZ and IND raw drug powder with their coformers were prepared by shaking the powder mixture together for 1 min in a glass vial or by mixing them gently with a pestle in a mortar.

2.3.3. Preparation of nanocrystals, micro-cocrystals and nano-cocrystals

Nanosuspensions of 5% (w/v) ITZ, IND and their macro-cocrystals were prepared by wet milling with yttria stabilized zirconium oxide beads with diameters of 0.3 mm using a ZentriMix 380 R (Andreas Hettich GmbH und Co. KG, Tuttlingen, Germany). The drug powders were added into 1% (w/v) poloxamer 407 solution and homogenized at 2000 rpm for 30 s with an Ultra Turrax T-25 (IKA®-Werke GmbH & Co. KG, Staufen, Germany); subsequently 5 mL of this suspension and milling beads in a ratio of 1:3 (w/w) were transferred into a 10 mL HDPE vial (iphas Pharma-Verpackung GmbH, Würselen, Germany) and milled at the speed of 750 rpm for 4 h. The cooling device was set to 0 °C which results in sample temperatures of approx. 15 °C after preparation. For comparison, ITZ micro-cocrystals were obtained with the same concentrations of drug and stabilizers

as for the nanosuspensions; however, the milling time was shortened from 4 h to 0.5 h. Directly after preparation, the suspensions were separated from beads by filtration through a sieve with a pore size of ~20 μm and frozen at -80 °C and afterwards lyophilized (Alfa[®] 2-4 LD Plus freeze-dryer, Martin Christ Gefriertrocknungsanlagen GmbH, Osterode am Harz, Germany). The lyophilization process was performed at -48 °C and 0.055 mbar.

2.3.4. Characterization of nanocrystals, cocrystals and nano-cocrystals

2.3.4.1. Particle size analysis

The particle size of ITZ, IND raw powder, macro- and micro-cocrystals was measured by laser diffraction (Mastersizer[®] 2000, Malvern Instruments Ltd., Malvern, UK, n = 5). The particle size of the nanocrystals and nano-cocrystals after redispersion of the lyophilized powders in the drug saturated stabilizer solutions was measured by photon correlation spectroscopy (PCS) using a Zetasizer[®] Nano ZS (Malvern Instruments Ltd., Malvern, UK, n = 3).

2.3.4.2. Light microscopy

Microscopic observations were performed using a polarized light microscope (Axioscope, Carl Zeiss Jena GmbH, Jena, Germany).

2.3.4.3. Differential scanning calorimetry (DSC)

Thermal analysis was conducted using a DSC (DSC 6000, PerkinElmer LAS GmbH, Rodgau, Germany) and data were analysed by Pyris software (PerkinElmer LAS GmbH, Rodgau, Germany). 5 ± 1 mg of raw drug powder, physical mixture, macro-cocrystal, nanocrystal and nano-cocrystal freeze dried powder were accurately weighed in 50 μL aluminium pans with pierced lids. The samples were heated from 20 to 200 °C with a heating rate of 10 °C/min, and afterwards cooled to room temperature with a cooling rate of 20 °C/min. The test was performed under a continuously purged dry nitrogen atmosphere (flow rate 40 mL/min).

2.3.4.4. X-ray powder diffraction (XRPD)

The XRPD measurements were performed using Cu Kα radiation (λ = 0.154 nm) on a Bruker D8 Advance diffractometer (Bruker AXS GmbH, Karlsruhe, Germany) in the 2θ range from 10° to 80° with a step size of 0.01°.

2.3.5. *In situ* solubility studies

The solubility experiments were performed by *in situ* measurements with Sirius® inform (Sirius Analytical Instruments Ltd., Forest Row, UK). The cell path length of the probe tip was changed from 10 mm to 1 mm in order to prevent any particle scattering effect and to achieve suitable absorbance range (0.1-0.9). The absorbance was recorded by *in situ* UV-VIS spectroscopy from 200 to 700 nm with an interval of 60 s. During data analysis and evaluation, a broader time interval was considered to obtain a better visualization in some cases. Prior to solubility test, the calculation of the amount of drug dissolved in the media was made by the software (Sirius® inForm Refine) and took into account the molar extinction coefficient (MEC), which was determined through the UV-metric MEC/pKa-assay of Sirius® inForm. A Tyndall-Rayleigh scattering correction was applied to the recorded spectra (Sirius® inForm Refine) to exclude the scattering of undissolved particles and to obtain the absorbance of only dissolved drug. ITZ and IND raw powder, nanocrystals, macro-, micro- and nano-cocrystals powder were investigated under same excess conditions in dissolution media at 37 °C with 300 rpm paddle stirring rate to prevent floating of the powder. Specifically, in case of ITZ, corresponding to 10 mg of drug (40 times excess) all formulations were tested in 50 mL of 0.1N HCl; and in case of IND, corresponding to 8 mg of drug (20 times excess) all formulations were investigated in 40 mL of water. In order to determine the maximum achievable solubility of nano-cocrystals, the solubility study was also performed under different excess (non-sink) conditions, with drug loadings 5-100 times higher than the drug equilibrium solubility.

2.3.6. Stability studies of nano-cocrystal suspensions and powders

The stability studies of suspension and powder forms of nano-cocrystals were carried out at 4, 25 and 40 °C for 90 days wherein samples were analyzed at intervals of initial, 30 and 90 days. The particle size and PDI were measured by the same analytical method described in Section 2.3.4.1. The maximum solubility during dissolution were performed according to methods described in Section 2.3.5.

2.4. Itraconazole-succinic acid nano-cocrystals: Kinetic solubility improvement and influence of polymers on controlled supersaturation

2.4.1. Preparation and characterization of nano-cocrystal formulations

Itraconazole-succinic acid (ITZ-SUC) nano-cocrystals were prepared and characterized according to the previous chapter 2.3. Briefly, nanosuspensions of 5 % (w/v) ITZ-SUC cocrystals with 1 % (w/v) poloxamer 407 were prepared by wet milling using dual centrifugation (ZentriMix 380 R, Andreas Hettich GmbH und Co. KG, Tuttlingen, Germany). The nanosuspensions were dried by lyophilization (Alfa® 2-4 LD Plus freeze-dryer, Martin Christ Gefriertrocknungsanlagen GmbH, Osterode am Harz, Germany) at -48 °C and 0.055 mbar. The particle size was determined after redispersion in ITZ saturated water using photon correlation spectroscopy (PCS, Zetasizer® Nano ZS, Malvern Instruments Ltd., Malvern, UK).

2.4.2. Preparation of ITZ-SUC seed cocrystal suspensions

5 % (w/v) ITZ-SUC cocrystal powder was dispersed in 10 mL 1 % (w/v) poloxamer 407 solution. The suspension was homogenized for about 2 min with an Ultra Turrax T-25 and then milled for 1-4 h at 750 rpm with 0.3 mm yttria stabilized zirconium oxide beads using dual centrifugation. Samples were vacuum-filtered (0.45 μm/ 5.0 μm cellulose nitrate membrane filters, Schleicher & Schuell GmbH, Dassel, Germany) and different sized cocrystals on the top of the filters were redispersed homogeneously in a saturated water solution of itraconazole to avoid further change of particle size and stored at 4 °C in a glass bottle until further use. The concentration of the seed suspensions was determined by UV spectrophometer at 259 ± 1 nm (Agilent 8453, Agilent Technologies GmbH, Waldbronn, Germany).

2.4.3. Solubility measurements with various pre-dissolved PPIs

An excess amount of either itraconazole crystals, ITZ-SUC cocrystals or their physical mixture was added to 0.1N HCl (pH 1.0) in the absence or presence of 0.1 mg/mL pre-dissolved various PPI (HPMC E5, HPMC E50, HPMCAS, HPC, PVPK30 and PVPVA64). The samples were incubated at 37 °C for 48 h in a horizontal shaker (GFL® 3033, GFL Gesellschaft fur Labortechnik, Burgwedel, Germany). Saturated solutions were filtered (0.22 μm membrane filter) and drug concentrations were determined by UV spectrophometer at 259 ± 1 nm (n=3).

2.4.4. Screening of precipitation inhibitors by solvent shift method

10 mL DMSO stock solution of itraconazole (10 mg/mL) was added to 500 mL 0.1N HCl in the absence or presence of dissolved PPIs at a final concentration of 0.1 mg/mL in a USP II apparatus at 100 rpm and 37 °C (n=3). The initial drug concentration was 200 µg/mL and the DMSO concentration in the medium did not exceed 2 % (v/v) which had no significant influence on drug solubility (Yamashita et al. 2011). 5 mL samples were taken at 5, 10, 30, 60, 120, 240 min, filtered through 0.22 µm membrane filters, then rapidly diluted with methanol to avoid drug precipitation and analyzed for dissolved by UV spectrophometer at 259 ± 1 nm.

2.4.5. Contact angle measurements

Compacts (diameter: 13 mm, weight: 300 mg) were prepared by direct compression using a hydraulic press (P/N 25.011, Specac, Orpington, UK) at a compression force of 5 tons and holding time of 5 min. The contact angle measurements were performed with a contact angle goniometer equipped with a micro-syringe attachment (G1, Krüss GmbH, Hamburg, Germany) by the sessile drop method at room temperature (n = 5). A droplet of 10 µL 0.1 N HCl in the absence or presence of various precipitation inhibitors (0.1 mg/mL) is deposited on the compressed tablets using a microsyringe which is fixed 0.5 cm above compact surface. The contact angle was measured 10 seconds after drop formation.

2.4.6. *In situ* nano-cocrystal powder dissolution studies

Powder dissolution experiments were performed to determine the influence of various types of PPIs on dissolution of ITZ-SUC nano-cocrystals by *in situ* UV measurements with Sirius inForm (Sirius Analytical Instruments Ltd., Forest Row, UK). 50 mL of 0.1N HCl (pH 1.0) without and with various precipitation inhibitors at different concentrations (0.01/0.025/0.1 mg/mL) were used as dissolution medium (n=3). Excess amounts (corresponding to 15 mg ITZ) of ITZ-SUC nano-cocrystal formulations were added to the dissolution medium equilibrated at 37 °C; the paddle stirring rate was set to 300 rpm to prevent floating of the powder. The absorbance was recorded every 60 s by *in situ* UV/VIS spectroscopy from 200 to 700 nm. 1 mm of cell path length was selected to prevent any particle scattering effect and to achieve suitable absorbance ranges. A Tyndall-Rayleigh scattering correction was applied to the recorded spectra to exclude scattering of undissolved particles.

To obtain insight on the mechanism of how nano-cocrystals obtained maximum

supersaturation and provide strategies to maximize the area under the concentration−time curve in order to optimize bioavailability, and also to highlight the true "solubility advantage" of nano-cocrystals, the dissolution experiments were conducted under non-sink conditions by manually adding ITZ-SUC nano-cocrystal powder (corresponding to 20 mg of ITZ), in divided quantities at predetermined time intervals to generate different supersaturation rates (Han and Lee, 2017). Powder addition rates of 1, 2, 4 and 20 mg/min were examined with and without 0.1 mg/mL HPMC E5 in 50 mL 0.1N HCl. Four different doses were tested for nano-cocrystals by adding a total of 10, 15, 20 and 30 mg of formulations to determine the maximum potential of nano-cocrystals supersaturation solubility with and without HPMC E5 in immediate release drug delivery system. Additionally, a comparison of dissolution of micronized with nanosized cocrystal powder with and without HPMC E5 was performed.

2.5. Incorporation of itraconazole nano-cocrystal into granulated or bead-layered solid dosage forms

2.5.1. Preparation of nanocrystal and nano-cocrystal suspensions

Itraconazole (ITZ) nanocrystal and itraconazole-succinic acid (ITZ-SUC) nano-cocrystals were prepared according to previous chapter 2.3. Briefly, nanosuspensions of 10% (w/v) ITZ or ITZ-SUC (corresponding to drug) and 2% (w/v) poloxamer 407 were prepared by wet milling with 0.25-0.35 mm yttria-stabilized zirconium oxide beads (SiLibeads®, Sigmund Lindner GmbH, Warmensteinach, Germany) using a ZentriMix 380 R (Andreas Hettich GmbH und Co KG, Tuttlingen, Germany).

A granulation or layering dispersion was prepared by the addition of HPMC E5 (2% w/w) to the prepared ITZ nanosuspension (ITZ NS) or ITZ-SUC nano-cocrystal suspension (ITZ-SUC NS), and the dispersion was mixed with stirring at 100 rpm for 2 h.

2.5.2. Downstream processing of nano-cocrystal suspensions

2.5.2.1. Wet granulation

50 g of either microcrystalline cellulose (MCC) or lactose was well mixed for 5 min in a mixer torque rheometer (Caleva Ltd., Dorset, UK). The ITZ-SUC NS/HPMC granulation dispersion was added to MCC and lactose to obtain a suitable wet mass that can be wet granulated and achieved 10% w/w and 2% w/w drug loading, respectively. The wet mass was forced through a 1 mm sieve and oven-dried overnight at 40 °C. The dried granules

were passed through an 800 µm mesh sieve resulting in WG-MCC and WG-Lac granules, respectively. The actual drug loading achieved was analyzed by the UV method described in the succeeding sections.

2.5.2.2. Spray granulation

Spray granulation of the nanosuspension was performed using Mini-Glatt (Glatt GmbH, Binzen, Germany) fluid bed drier. The chamber was pre-heated by the non-processed air before the granulation process. 75 g of either MCC or lactose was charged into the fluid bed direr. The ITZ-SUC NS/HPMC granulation dispersion was sprayed onto the substrate to achieve 10% and 20% w/w drug loading resulting in SG-MCC and SG-Lac granules. Granulation was carried out using the following process parameters (determined based on preliminary screening experiments, data not shown) in the top-spray mode with 0.3 mm nozzle: inlet air temperature of 60 °C (for lactose) or 65 °C (for MCC), atomizing air pressure of 1.2 bars (for lactose) or 0.9 bars (for MCC) and a suspension feed rate of 4.0 g/min (for lactose) or 2.5 g/min (for MCC). A product temperature in the range of 37-42 °C was maintained throughout the process. The actual drug loading achieved was analyzed by the UV method described in the succeeding sections.

2.5.2.3. Bead layering

Nanosuspension was coated onto beads by Mini-Glatt fluid bed drier. The chamber was pre-heated by the non-processed air before the granulation process. 75 g of either microcrystalline cellulose or sugar beads were charged into the fluid bed direr. The ITZ-SUC NS/HPMC layering dispersion was coated onto substrate to achieve 10% and 20% w/w drug loading resulting in BL-MCC and BL-Sugar beads. Bead layering was carried out using the following process parameters (determined based on preliminary screening experiments, data not shown) in the bottom-spray mode with 0.3 mm nozzle: inlet air temperature of 65 °C, atomizing air pressure of 0.9 bars, and a nanosuspension feed rate of 1.0 g/min. A product temperature in the range of 37-42 °C was maintained throughout the process. The actual drug loading achieved was analyzed by the UV method described in the succeeding sections.

2.5.3. Characterization of suspension and different solid dosage forms

2.5.3.1. Particle size analysis

The particle size of the original nanosuspension, nanosuspension with HPMC E5 and redispersed nanoparticles from prepared granules or beads were assessed by photon correlation spectroscopy (PCS) using a Zetasizer® Nano ZS (Malvern Instruments Ltd., Malvern, UK, n = 3). The suspension was directly diluted with saturated itraconazole solution and measured. For prepared solid dosage forms, granules or beads were dispersed in saturated itraconazole solution and stirred at a speed of 300 rpm for 5 min. Samples were taken and filtered through 0.8 µm membrane and diluted for measurement.

2.5.3.2. Optical microscopy

Optical microscopic images of granules or beads were captured using a polarized light microscope (Axioscope, Carl Zeiss Jena GmbH, Jena, Germany). The physical state of granules or beads and the redispersion of nano-cocrystal from different solid dosage forms after contact with a drop of water were analyzed.

2.5.3.3. Drug content

20 mg of different solid dosage formulations were dispersed in 100 mL methanol solution. The samples were sonicated for 30 min and placed in a shaker overnight. The solution was filtered through a 0.22 µm membrane filter, and a UV spectrometer determined the drug content at 259 nm (Agilent 8453, Agilent Technologies GmbH, Waldbronn, Germany, n=3).

2.5.3.4. Loss on drying

The moisture content (expressed as loss on drying, LOD) of different solid dosage formulations was determined using an HR73 Halogen Moisture Analyzer (Mettler-Toledo Inc., Columbus, OH, USA). About 1 g of sample was spread uniformly in the sample holder and heated to 105 °C, and the loss of water upon drying was monitored till a stable value was reached (n=3).

2.5.3.5. Differential scanning calorimetry (DSC)

Thermal analysis was conducted using a DSC (DSC 6000, PerkinElmer LAS GmbH, Rodgau, Germany), and data were analyzed by Pyris software (PerkinElmer LAS GmbH, Rodgau, Germany). 10 ± 1 mg of different solid dosage formulations were accurately weighed in 50 µL aluminum pans with pierced lids. The samples were heated from 20 to

200 °C with a heating rate of 10 °C/min and afterward cooled to room temperature with a cooling rate of 20 °C/min. The test was performed under a continuously purged dry nitrogen atmosphere (flow rate 40 mL/min).

2.5.3.6. *X-ray powder diffraction (XRPD)*

The XRPD measurements were performed using Cu Kα radiation (λ = 0.154 nm) on a PANalytical Empyrean diffractometer in the 2θ range from 7° to 40° with a step size of 0.01°.

2.5.4. Dissolution study

The dissolution studies were performed by *in situ* measurements with Sirius® inform (Sirius Analytical Instruments Ltd., Forest Row, UK) at 37 °C in 50 mL of 0.1N HCl. Different solid dosage formulations (corresponding to 20 mg drug) were added to the dissolution medium under non-sink conditions. Also, the dissolution profiles of Sporanox® without hard gelatin capsules were studied using the same method and conditions. *In situ* UV-VIS spectroscopy recorded the absorbance from 200 to 700 nm with an interval of 60 s. A Tyndall-Rayleigh scattering correction was applied to the recorded spectra (Sirius® inForm Refine) to exclude the scattering of undissolved drug particles or excipient and to obtain the absorbance of dissolved drug only.

2.5.5. Accelerated stability studies

Stability studies of granules and beads prepared by spray granulation and bead layering methods, packed in double polyethylene-lined aluminum pouches or placed in open bottles (blistered or non-blistered), were carried out at 40 °C/75% RH. Dissolution profiles of stability samples were carried out as the method discussed in section 2.5. Samples were analyzed after 0, 1, and 3 months of storage.

3. RESULTS AND DISCUSSION

3.1. Preparation and optimization of nanocrystal formulations with different lab-scale wet milling methods

3.1.1. Introduction

Nanocrystal refers to a new class of pharmaceutical formulation developed using nano preparation technology. Nanocrystals are sub-micron particles composed of a small amount of surfactants or polymer materials as stabilizers and nano-sized pure drug particles (Rabinow, 2004). In nanocrystal systems, the particle size of nanocrystal drugs is usually 200 ~ 500 nm. Nanocrystals increase the surface area of drug particles by reducing the size of drug particles, thereby increasing the *in vitro* dissolution and bioavailability of poorly soluble drugs. In addition, nanocrystals could reduce the effects of individual differences and dietary conditions on the efficacy of drugs (Gao et al., 2013; Junghanns and Müller, 2008).

Generally, nanocrystals can be prepared by "Bottom-up" technology and "Top-down" technology (Keck and Müller, 2011). The principle of the "Bottom-up" technology is to control the precipitation or crystallization of drug molecules so that nanoparticles are rapidly formed; the principle of the "Top-down" technology is to mechanically reduce the particles of the large-sized drug to smaller (Sinha et al., 2013; Van Eerdenbrugh et al., 2008). Various publications and patents had investigated nanocrystals for their potent applications in drug delivery systems in the past decades. The majority of those investigations prepared nanocrystals by particle size reduction techniques (Colombo et al., 2017b; Rao et al., 2008; Wahlstrom et al., 2007). In all of the particle size reduction techniques, one approach is milling an aqueous suspension containing poorly soluble drug and polymer(s) or surfactant(s) with beads, thus is often named as wet beads milling method (Malamatari et al., 2018). During the wet bead milling method, milling beads are rapidly moved by the agitator. The drug crystals are milled by force of friction and collision between the moving milling beads, the inner wall of the milling chamber, and other drug crystals. The milling beads are made of a hard, dense material, such as yttrium-stabilized zirconium oxide, stainless steel, glass, alumina, etc. The beads' size can vary from < 0.1 to 20 mm. The wet bead milling method is a water-based approach in which no organic solvent was needed. It could be prepared from small to large scale, suitable for formulation screening and critical process parameter determination. In addition, the products prepared by wet bead milling often exhibited less batch variations (Romero et al., 2016; Srivalli and Mishra, 2016; Zuo et al., 2020). Throughout several FDA approved products on the market, most of the

products were produced by wet bead milling method (e.g., Emend®, Rapamune®, TriCor®, and Megace ES®) (Marcato and Durán, 2008; Weissig et al., 2014).

Before producing the nanocrystal formulations from laboratory scale to industrially feasible scale, the transferability of the laboratory manufacture process to a large scale is worth investigating. Meanwhile, during the preformulating process, some drugs' extraction or synthesis yield is small and expensive. Lab-scale preparation facilitated the study of nanocrystals of such drugs under laboratory conditions and saved time and money invested in the early stage. The equipment used to produce nanocrystals with the wet bead milling method in the lab varied in the chamber volume capacity and the stirrer geometry (Hagedorn et al., 2019; Siewert et al., 2018). Although various wet bead milling methods have been applied to laboratory-scale nanocrystal preparation, many differences existed. Some methods exhibit lower milling efficiency; thus, longer milling time and faster milling speed were required to induce more energy in the system (Bilgili et al., 2006). With more energy induced under critical milling conditions, too much heat generated during the milling process may cause degradation or phase transformation to heat-sensitive drugs. Crystal defects due to the disordering of the crystal surface and the generation of localized amorphous regions were also possible. Furthermore, it would increase the risk of wear of instrument components and lead to sample contamination (Colombo et al., 2017a; Juhnke et al., 2012; Lai et al., 2009; Mah et al., 2014). Some methods' batch mode was restricted; thus, a limited number of formulations could be screened. Although different wet bead milling methods have been widely used to prepare nanocrystals in many publications, only a few publications investigated and compared those different methods (Hagedorn et al., 2019).

Therefore, the objective of this study was to select a simple and efficient laboratory-scale method to produce nanocrystal formulations. Itraconazole was selected as the model drug due to its widespread nanocrystal preparation and poorly soluble properties (Badawi et al., 2011; Sarnes et al., 2014; Sun et al., 2011). Miniaturized bead milling, dual centrifugation, beaker milling, and Dyno mill were applied to prepare nanocrystals based on their different milling mechanism and batch volume. The current work evaluated and compared the process efficiency of those methods based on formulation screening ability and process attributes. The evaluated most desirable production method was further applied to formulation and parameter optimization. Finally, the solid-state characterization, dissolution behavior, and long-term stability of the formulations were also evaluated.

3.1.2. Comparison of different lab-scale methods

3.1.2.1. Miniaturized bead milling

The processing time was determined by measuring the time necessary to obtain the aimful particle size (target: 250 nm). The particle size gradually reduced as a function of time during the first 2 h (Fig. 3.1). The targeted particle size diameter was reached after 48 h (220 nm with a PDI of 0.22). However, there existed high variability among the different batches.

Fig. 3.1. Particle size and PDI of itraconazole nanosuspension as a function of milling time with the miniaturized method. (Milling time 48 h; 1000 rpm; beads size: 0.05 mm).

In the miniaturized bead milling method, the particle size achieved by bead milling was related to the size of the milling beads used. The smaller the size of the milling beads, the finer the nanocrystal produced because of increased collision frequency between drug particles and beads. However, too small beads might not be suitable for milling because they cannot generate sufficient energy for particle breakage when they impact drug particles due to their low weight. Below a specific particle size limit, the suspension becomes more viscous due to the particular organization of the excessively small beads (Romero et al., 2016). In the miniaturized bead milling set-up, there was a high risk that small milling beads stuck between the stirring bars and chamber wall, which would significantly damper the efficiency of the milling process, and this also explains why less uniformity existed among different batches. This phenomenon always happened during the experiment intermittently, and supervision was needed occasionally. Generally, the

miniaturized method used only 0.5 mL suspension for one batch, which might be suitable for some expensive APIs; the set-up was easily assembled and cost-effective. However, considering that poor uniformity between batches, low milling efficiency, and constant monitoring requirement, it might not be the ideal method for formulation screening or estimation of large-scale production parameters in the lab.

3.1.2.2. Beaker milling

Compared with the miniaturized bead milling method, the batch volume of the beaker milling method increased from 0.5 mL to 20-50 mL (larger scale to 100 mL is also possible). The set-up was also cost-effective and straightforward, consisting of a magnetic stirrer and a beaker or flask. The particle size was reduced as a function of time during the milling process (Fig. 3.2). The targeted particle size diameter was reached after 8 h (245 nm with a PDI of 0.24).
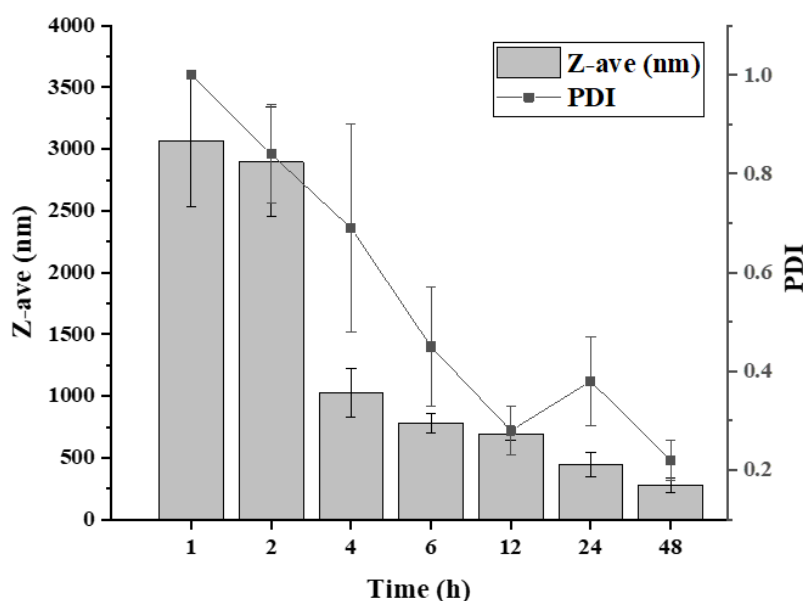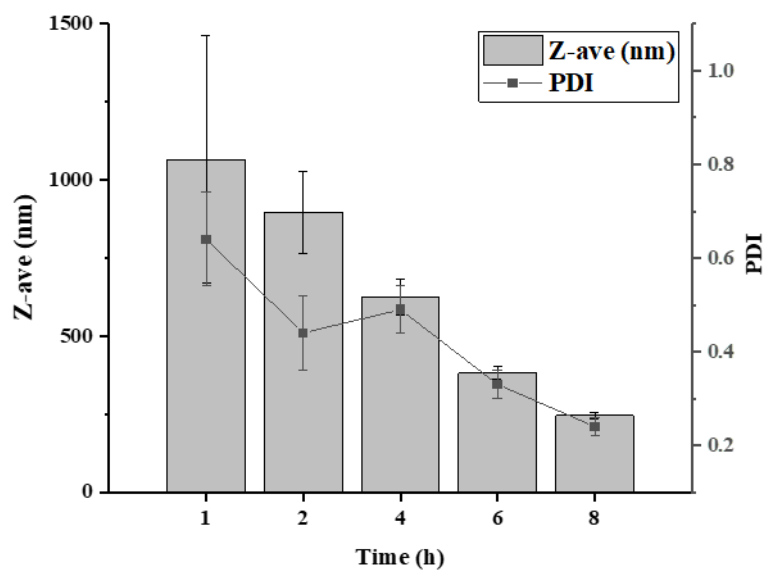

Fig. 3.2. Particle size and PDI of itraconazole nanosuspension as a function of milling time using the beaker milling method. (Milling time 8 h; 1000 rpm; beads size: 0.3 mm).

The efficiency of the process in the beaker milling method was much higher than in the miniaturized method. Furthermore, a minimal batch-to-batch variation was observed in the quality of the dispersion. However, the powerful milling beads caused an apparent wearing of the magnetic stirring bar and the beaker wall after several milling processes. One side of the magnetic stirring bar has been eroded flat, and the glass of the beaker wall was worn like frosted. In order to increase the efficiency of the milling process, the longer milling time

can be compensated to some extent by increasing rotation speed. However, the maximum rotating speed was around 1000 rpm. If the maximum rotating speed was exceeded, the chance of particles colliding becomes less due to excessive centrifugal force; thus, the grinding efficiency became even lower. Therefore, although the efficiency of the beaker milling method was higher than the miniaturized method, there was no space for further improvement, and the probability of sample contamination was problematic.

3.1.2.3. Agitator mill

Dynomill® is one type of closed stirred media mill and is developed through the industry field. The batch mode of the Dynomill® was usually used at a lab-scale (from 60 mL to 1 L) to develop and manufacture small batches for preclinical evaluation. In the horizontal grinding chamber, the agitator discs are mounted symmetrically on the agitator shaft. The system transferred the kinetic energy required for the milling operation to the milling beads. The time for achieving the targeted particle size with the agitator method was 3 h (Fig. 3.3). The particle size was finally reduced to 255 nm with a PDI of 0.21.
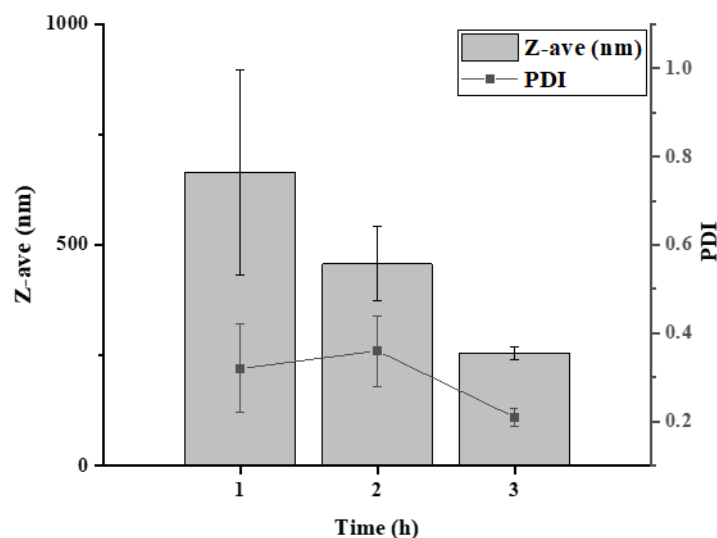
Fig. 3.3. Particle size and PDI of itraconazole nanosuspension as a function of milling time using agitator mill method. (Milling time 3 h; 3000 rpm; beads size: 0.3 mm).

Agitator mill was considered high-speed, closed-type stirred media mills, operating at a circumferential stirrer speed of 8-20 m/s. Compared with other methods described above, the set-up of the Dynomill® stirrer and chamber was more complicated. When the beads were small, they have a high chance of accumulating in undesired milling machine sites, thus leading to a higher risk of damage to the mechanical parts. After every batch

preparation, a whole cleaning process was needed, while the disassembling of the mechanical part was difficult, and some tiny components were easily lost during the cleaning process. Furthermore, although the chamber volume capacity of Dynomill® ranges from 50 mL to 1 L, the chamber volume capacity of each model machine was fixed.

3.1.2.4. Dual centrifugation

The dual centrifugation method is a novel nanocrystal preparation method related to wet bead milling. It was first introduced to prepare nanocrystal in 2017 (Hagedorn et al., 2017). The particle size of itraconazole reached 214 nm with PDI 0.2 after 1.5 h (Fig. 3.4). The dual centrifugation method resulted in nanocrystals with similar or even smaller particle sizes.
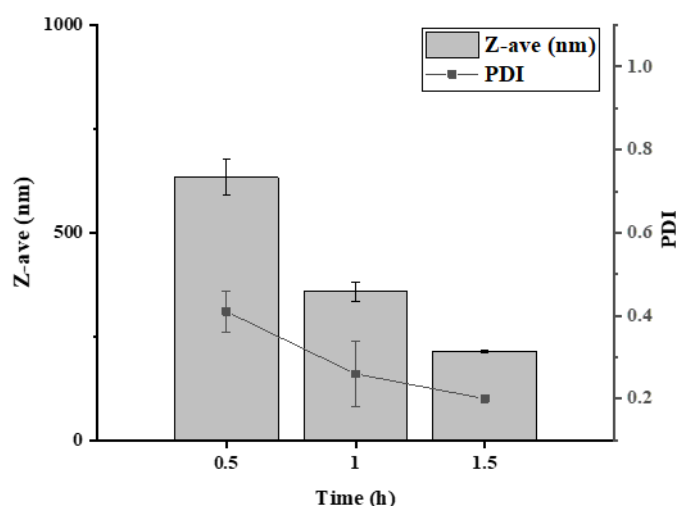
Fig. 3.4. Particle size and PDI of itraconazole nanocrystal as a function of milling time using the dual centrifugation method. (Milling time 1.5 h; 1000 rpm; beads size: 0.3 mm).

The dual centrifugation combined an additional rotation of the samples during the centrifugal process. Thus, the forces introduced in the system were continuously varying from different directions. This resulting powerful movement of the samples and beads inside the vials finally resulted in a highly promoted milling efficiency. The most important advantage of the dual centrifugation method was that up to 40 vials (2 mL) can be processed in one run, which resulted in minimal batch-to-batch variation and high efficiency for formulation screening. Furthermore, the device allowed efficient cooling of the samples during the milling process, which allowed continuous milling without cooling breaks. After formulation screening, the adaptors of the device could be changed, and the volume

capacity of the vials could be increased to 15 mL, providing the potential to investigate further formulation scale-up with controlled critical process parameters and time-saving. Hence, the dual centrifugation method was selected and applied for further nanocrystal formulation optimization.

3.1.3. Preparation of itraconazole nanosuspension with dual centrifugation method

3.1.3.1. Effect of stabilizer type

The choice of a suitable stabilizer was crucial to the preparation of nanosuspensions. The stabilizer must inhibit the growth of nanocrystals and prevent the agglomeration between nanocrystals (Van Eerdenbrugh et al., 2009). In order to overcome agglomeration between nanoparticles, sufficient repulsive force was necessary. There were two main methods to provide repulsion between nanoparticles: steric hindrance and charge repulsion. The steric hindrance effect can be achieved by the adsorption of polymer (like HPC, HPMC, PVP) or stabilizer (like poloxamer) materials on the surface of nanoparticles. When two particles were close to each other, the high osmotic pressure generated by the polymer adsorbed on the surface of the particles promoted the separation of the particles. When charged polymers or surfactants were adsorbed on the surface of the particles, the same charge repelled each other to prevent agglomeration and realized the charge stabilization effect (Soisuwan et al., 2019). The polymers must have a long enough chain length to provide a steric hindrance layer, but the molecular weight should not be too large to affect the dissolution of the drug (Chen et al., 2009; Sharma and Garg, 2010). The nonionic surfactant or anionic surfactant molecules can also be used as stabilizers, such as Tween80 (Tw80) or sodium dodecyl sulfate (SDS). Small molecule surfactants can stabilize nanocrystals, but they can also easily promote the Ostwald ripening effect and affect long-term stability (Van Eerdenbrugh et al., 2009).

When Tw80, TPGS, poloxamer, and SDS were used as stabilizers, the average particle size of itraconazole nanocrystals ranged from 200 to 550 nm (Fig. 3.5). Compared with Tw80 and P407, the particle size distribution value of TPGS and P188 was higher, indicating that they cannot provide sufficient repulsive force between particles to form uniformly distributed nanocrystals during the preparation process. When polymer material like PVPK30 with a larger molecular weight was used as a stabilizer, it was more challenging to obtain smaller particles than a stabilizer like HPC with a smaller molecular weight. The appearance of the suspension with PVP was similar to that of the suspension

prepared without any stabilizer. Large particles in the suspension were visible to the naked eye, and the drug particles aggregated and precipitated to the bottom of the glass bottle after 5 minutes. When HPMC or HPC was used as a stabilizer, a relatively uniform suspension with an average particle size above 500 nm was obtained. One reason was that the higher viscosity of the polymer solution led to lower milling efficiency. Another reason was that those absorbed polymers could not cover the particle surface completely; only when the particle size grew to a certain level it can absorb enough polymer materials on the surface to achieve stability. To cover various types of stabilizers, Tw80, P407, HPC, and SDS were chosen for further investigation.
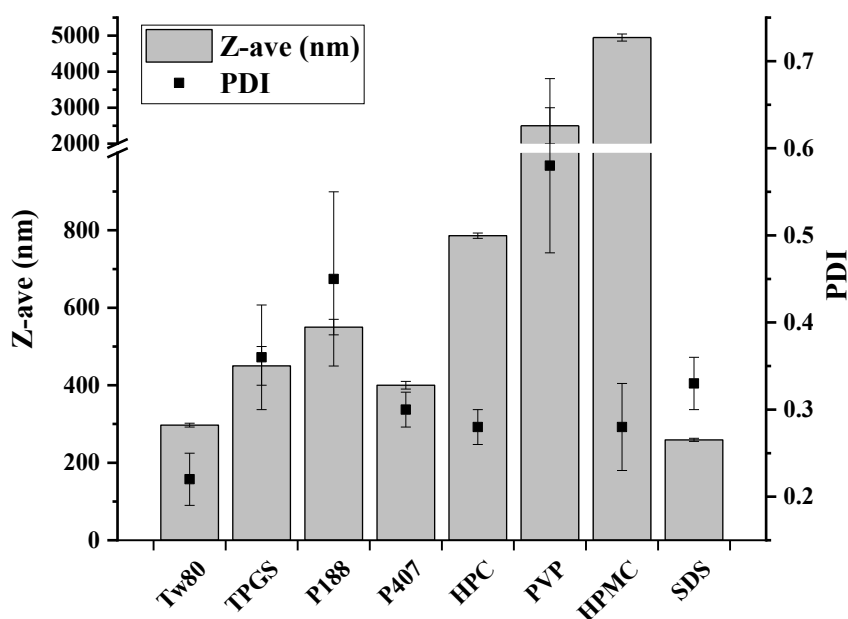
Fig. 3.5. Particle size and PDI of itraconazole nanosuspension as a function of stabilizer type. (Milling time 1 h; 1000 rpm; beads size: 0.3 mm).

3.1.3.2. Effect of filling volume on particle size reduction efficiency

Theoretically, during wet milling with dual centrifugation, the high impact force of the milling beads depended on the strong centrifugal acceleration. The double centrifugal action caused the tube-shaped vials placed in the double-rotor rotating disk to be moved by horizontal and vertical forces. The force of centrifugal movement changed in horizontal and vertical directions led milling beads to accumulate acceleration to increase kinetic energy. The milling beads were accelerated as a whole to impact the top and bottom of the vials simultaneously, including sample material, which meant almost all milling beads were involved in the wet milling process (Hagedorn et al., 2017). The milling efficiency can be greatly improved, and the processing time can be significantly shortened. In addition, the

risks of temperature increment and solid-state phase transformation of APIs caused by the longer milling time were reduced. However, the process attributes of the dual centrifugation method still need to be investigated, and the milling efficiency can be further improved.

In theory, the acceleration of milling beads in the air was higher than that in the water. Therefore, the ratio of the volume occupied by the sample solution and milling beads in the vial to the remaining air volume will affect the milling efficiency. Considering the possibility of subsequent parameter adjustments and followed sample extraction, 30-100% of the filling volume was investigated. As the filling volume increased from 30% to 70%, the nanocrystal particle size increased, consistent with the hypothesis above (Table 3.1). Take P407 as an example, the particle size increased from 240 nm with 30% filling to 390 nm with 70% filling. The less the air volume, the smaller the acceleration velocity of the beads, thus the milling efficiency was also lower. However, when the air volume was reduced from 20% to 0%, there was no clear trend could be observed. More milling beads added to decrease air volume could provide more milling surface area to offset the decrease in acceleration caused by too small air volume. In order to obtain the highest milling efficiency, 30% of the filling volume was applied in further process investigation.

Table 3.1. Mean particle sizes and PDI of itraconazole nanosuspension milled by DC as a function of different filling volume

Filling volume %	Tw80		P407		HPC		SDS	
	Size (nm)	PDI	Size (nm)	PDI	Size (nm)	PDI	Size (nm)	PDI
30%	296 ± 4	0.20 ± 0.02	239 ± 4	0.21 ± 0.02	498 ± 3	0.15 ± 0.03	191 ± 2	0.21 ± 0.02
40%	300 ± 4	0.20 ± 0.03	272 ± 4	0.25 ± 0.02	542 ± 2	0.22 ± 0.02	226 ± 1	0.19 ± 0.01
50%	333 ± 2	0.23 ± 0.02	304 ± 2	0.27 ± 0.02	556 ± 3	0.20 ± 0.03	255 ± 3	0.18 ± 0.04
60%	366 ± 3	0.20 ± 0.02	372 ± 1	0.29 ± 0.02	534 ± 1	0.19 ± 0.03	242 ± 4	0.20 ± 0.01
70%	368 ± 9	0.18 ± 0.05	389 ± 9	0.32 ± 0.05	555 ± 5	0.19 ± 0.06	241 ± 4	0.19 ± 0.03
80%	358 ± 5	0.19 ± 0.03	415 ± 5	0.34 ± 0.03	586 ± 4	0.20 ± 0.04	236 ± 4	0.20 ± 0.02
90%	349 ± 11	0.17 ± 0.06	384 ± 11	0.35 ± 0.06	562 ± 9	0.21 ± 0.05	237 ± 1	0.18 ± 0.03
100%	341 ± 10	0.20 ± 0.02	451 ± 10	0.35 ± 0.03	689 ± 10	0.35 ± 0.02	241 ± 5	0.20 ± 0.02

3.1.3.3. Effect of milling beads size

One of the critical factors that determine the efficiency of nano milling was the size of the milling beads. Smaller beads moved faster than large beads, and consequently, their capacity to compact the surface or break the crystals was stronger. However, nanocrystal with detectable particle size and PDI was unavailable to obtain with milling beads of 0.1 mm in all stabilizer groups (Table 3.2). While the particle size achieved with milling beads of 0.3 mm was in a range of 250-600 nm for all stabilizer groups. The particle size became larger with increasing milling beads from 0.3 mm to 0.5 mm and 0.9 mm. Since the quality of the milling beads during preparation remains constant, adding smaller milling beads meant adding a larger number of beads, resulting in more contact surfaces. However, too small milling beads would result in a viscous gelling effect during preparation. When the system's viscosity was increased, the cloud milling efficiency of dual centrifugation was significantly reduced. In addition, hydrophobic drugs would adsorb on the surface of small milling beads, thus impacting the milling efficiency and resulting in problematic separation afterwards. Therefore, milling beads size of 0.3 mm was generally preferred in this study. Romero et al. put forward a rule that a 1000-fold smaller crystal size was obtained than the size of the beads used (i.e., 0.4 mm beads can lead to crystals around 400 nm) (Romero et al., 2016). However, this rule did not apply in our experiments. The particle size of nanocrystals depended not only on the size of the milling beads but also on the ratio of the milling beads to the drug, the milling speed and time, etc. These factors will be investigated and discussed in later parts.

Table 3.2. Mean particle sizes and PDI of itraconazole nanosuspension milled by dual centrifugation as a function of different beads size

Stabilizer type	Particle size (nm) and PDI			
	0.1 mm	0.3 mm	0.5 m	0.9 mm
Tw80	-	313 ± 7 0.19 ± 0.01	935 ± 24 0.38 ± 0.04	-
P407	-	298 ± 4 0.20 ± 0.02	400 ± 15 0.35 ± 0.03	810 ± 23 0.44 ± 0.05
HPC	-	594 ± 10 0.30 ± 0.04	772 ± 20 0.22 ± 0.05	1143 ± 31 0.33 ± 0.03
SDS	-	256 ± 3 0.25 ± 0.03	-	-

3.1.3.4. Effect of ratio of beads to suspensions

The weight ratio of milling beads to sample suspension was also one of the important factors affecting the milling efficiency. When the ratio of milling beads relative to the sample suspension is increased, smaller particle sizes and more uniform particle size distribution under the same milling conditions were obtained (Fig. 3.6). The only exception was when SDS was used as a single stabilizer; the ratio of 3:1 led to larger particle size and PDI. When the particle size was reduced to a specific range, as the milling process continued, the continuous application of external force led particles to overcome the repulsive force of the stabilizer and re-aggregate. Practically, the ratio of milling beads to suspension cannot be increased infinitely. The yield of P407 group nanosuspension with 1:1 beads to suspension ratio was 87%, while 2:1 and 3:1 was 82% and 75%, respectively. More milling beads would provide a rougher surface for nanocrystal adsorption and more challenging in separation. Therefore, the balance between milling efficiency and yield should be carefully considered in the actual operation process and parameter selection. In this study, a 3:1 ratio of beads to suspension was maintained constant in further investigation. Furthermore, SDS was not applied for further investigation based on its narrow adjustment window and a higher risk of Ostwald ripening (Bilgili et al., 2016).
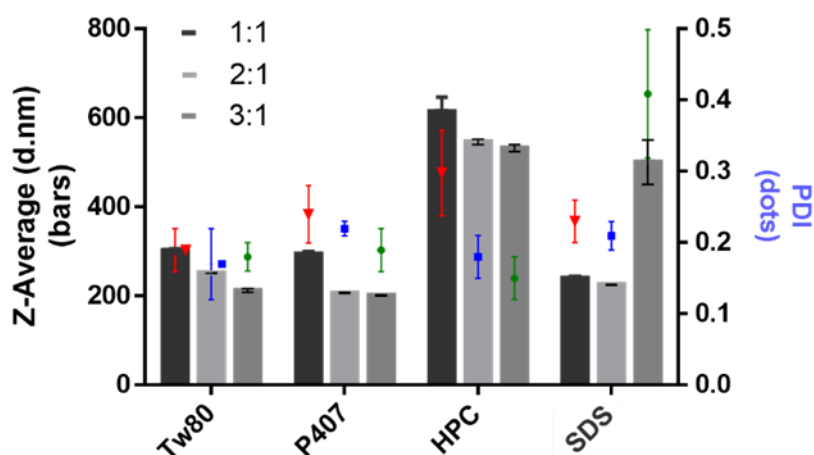

Fig. 3.6. Particle size and PDI of itraconazole nanosuspension as a function of beads to suspension ratio. (Milling time 1 h; 1000 rpm; beads size: 0.3 mm).

3.1.3.5. Effect of milling time and speed

Milling speed and time can also affect nano milling efficiency. Generally, higher milling speed meant shorter milling time, and from another perspective, higher milling efficiency

with higher milling speed can also be compensated by longer milling time. Higher milling efficiency was the primary goal of nanocrystal preparation, and it was reasonable to shorten the milling time by increasing the milling speed. However, too much energy introduced with high milling speed would increase the system's temperature, which may cause particle aggregation, phase transformation, and even damage to the instrument. Other concerns of nano milling with too high speed include possible generation of beads residues due to erosion; thus, contamination problems should be considered. Therefore, finding the balanced relationship between milling speed and time was essential.

The average particle size and distribution of nanocrystals when using different stabilizers (Tw80, P407, and HPC) at three milling speeds (1000, 1500, and 2000 rpm) and five milling times (30, 60, 90, 120, 150 min) has been investigated to determine the optimal preparation parameters (Fig. 3.7). When using Tw80 as a stabilizer, the milling efficiency (defined by smaller average particle size and distribution) that can be achieved at different milling speeds under the same milling time was ranked as 1500 rpm > 1000 rpm > 2000 rpm. The average particle size and distribution continuously decreased with the same milling speed as the milling time increased. Milling at a speed of 1500 rpm for 90 minutes was sufficient to obtain nanocrystals with a mean particle size of 200 nm and PDI of 0.2, while it required 150 minutes milling at a speed of 1000 and for longer than 150 minutes at a speed of 2000 rpm. The same trend in which average particle sizes and particle size distribution continuously decreased as the effect of milling time was also observed for P407. However, the milling efficiency achieved at different milling speeds within 60 min was ranked as 2000 rpm > 1500 rpm > 1000 rpm and ranked as 1500 rpm > 2000 rpm > 1000 rpm from 60 min to 150 min. Average particle size less than 750 nm could only be obtained when applying 1500 rpm milling speed for HPC as a stabilizer. Two opposite processes interacted in the milling vessel: the fragmentation of large particles into smaller particles and particle growth through interparticle collisions (Annapragada and Adjei, 1996). The occurrence of these two opposite phenomena was dependent on the process parameters like milling speed and time. After a certain time point, the particle size has achieved a constant level. Continuing the milling did not further decrease the particle size (e.g., Tw80 and P407); but may even lead to a gradual increase of particle size (e.g., HPC). The process temperature was also measured after milling for 90 min with different milling speeds. The milling speed of 2000 rpm presented a temperature of around 25 °C, 1500 rpm and 1000 rpm showed process temperatures of 14 °C and 10 °C, respectively. Combining all results, milling for 90 minutes under 1500 rpm was selected as the optimal milling parameter.
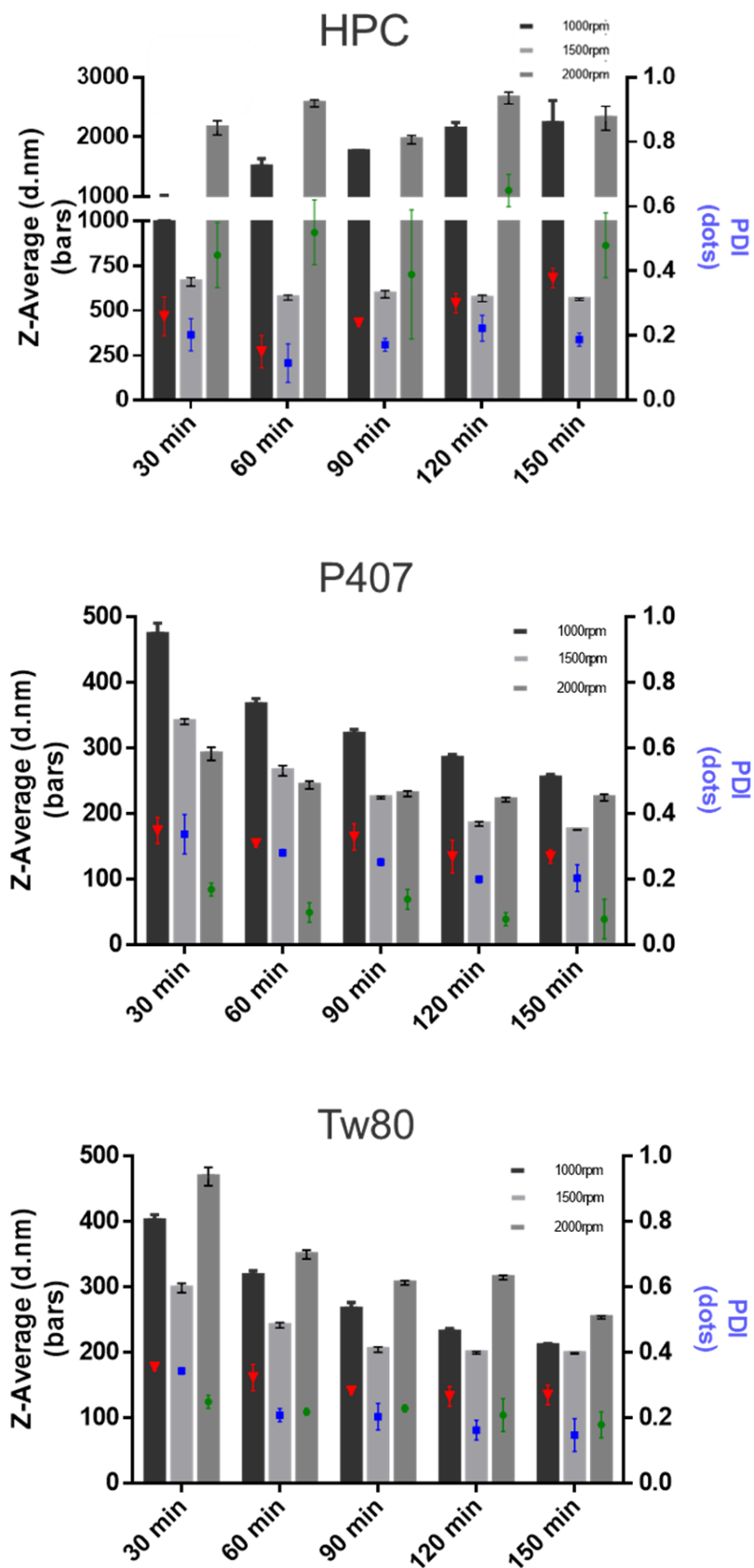
Fig. 3.7. Particle size and PDI of nanosuspension with different stabilizers as a function of milling time and speed.

3.1.3.6. Long term stability study of optimized nanosuspension

Nanosuspension stabilized by Tw80 exhibited a slight increase in particle size from 220 nm to 250 nm and 290 nm within 30 days at 4 and 25 °C, respectively (Fig. 3.8). In addition, the particle size increased from 220 nm to almost 600 nm within 7 days at 40 °C. Moreover, HPC stabilized nanosuspension showed increased particle size from 500 nm to 700 nm within 7 days at 25 °C. However, nanosuspension stabilized by P407 was relatively stable during at least 30 days of storage at 4, 25, and 40 °C. The physical stability of the itraconazole nanosuspension depended on storage conditions and the stabilizers. The relative increase in average particle size on day 30 compared to the initial particle size was highest for nanosuspension stabilized with Tw80 and HPC stored at 40 °C, followed by 25 °C. No significant increase in size was observed at 4 °C.

Ostwald ripening, a process whereby the larger particles grow by "devouring" smaller particles, might contribute to nanocrystals' instability. By increasing storage temperature, the saturation solubility of drugs was increased; thus, the driving force of Ostwald ripening arose because more drugs were dissolved, followed by precipitation and particle growth (Wang et al., 2013). In addition, the nanosuspension system is thermodynamically unstable and tended to minimize its total energy. Hence, storage at higher temperatures introduced more energy in the system, and particle collision and aggregation were more likely to happen. In order to prevent possible particle aggregation or growth, nanosuspension is recommended to be stored at a lower temperature. Compared with Tw80 and HPC, no significant increase in size was observed on day 30 for nanosuspension stabilized with P407 stored at even 40 °C. When a suitable stabilizer was selected, the optimized nanosuspension could even be stable for a longer period under higher temperature storage conditions. Therefore, nanosuspension stabilized with P407 was the optimal itraconazole nanocrystal formulation with a small particle size of 200 nm and PDI of 0.22 and good long-term physical stability under different storage conditions.
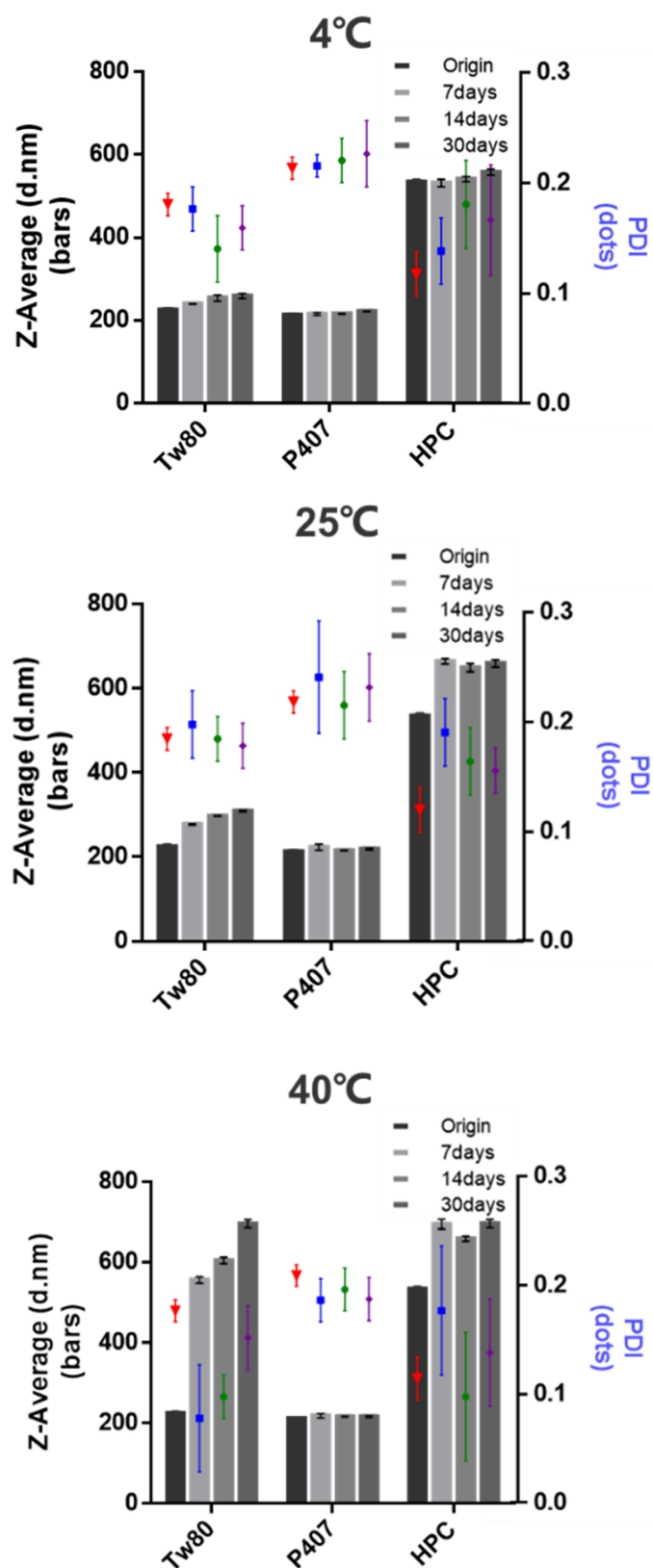
Fig. 3.8. Particle size and PDI of itraconazole nanosuspensions after 30 days storage at 4, 25, and 40 °C.

3.1.4. Characterization of optimized itraconazole nanosuspension

3.1.4.1. Particle size

The particle size of itraconazole nanosuspension stabilized with poloxamer 407 showed a PCS size average of 205 ± 5 nm and a polydispersity index of 0.22 ± 0.01. Data from the particle size analysis could be confirmed by light microscopic pictures, where no large particles were observed after effective milling with dual centrifugation (Fig. 3.9a, b). In addition, there was no significant increase in particle size after the redispersion of freeze-dried sample (Fig. 3.9b, c).
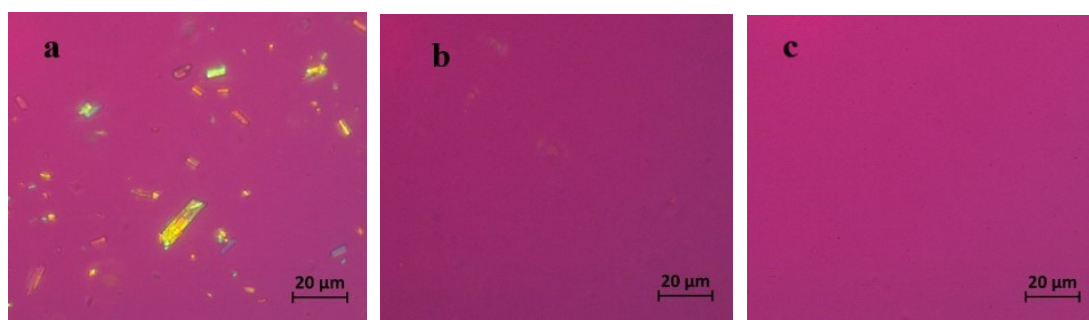
Fig. 3.9. Light microscopic pictures: (a) itraconazole and poloxamer 407 physical mixture, (b) itraconazole nanosuspension, (c) redispersed freeze-dried itraconazole nanocrystal

3.1.4.2. Solid state characterization

The thermograms showed an endothermic melting peak of crystalline itraconazole at 170 °C (Fig. 3.10a). The physical mixture and prepared nanocrystal displayed a small peak at 58 °C indicated the existence of poloxamer 407 (Fig. 3.10b, c). Compared with pure drug or physical mixture, the onset melting temperatures of itraconazole nanocrystals slightly shifted to lower temperatures at 165 °C (Fig. 3.10c). Two reasons could explain this phenomenon; first, the stabilizer melted at lower temperatures, and the drug dissolved to form eutectic mixtures during temperature increase; and second, the reduced degree of crystallinity of nanocrystals (Kocbek et al., 2006; Lai et al., 2009). DSC analysis suggested that the solid-state of itraconazole remained crystalline after milling with poloxamer 407.
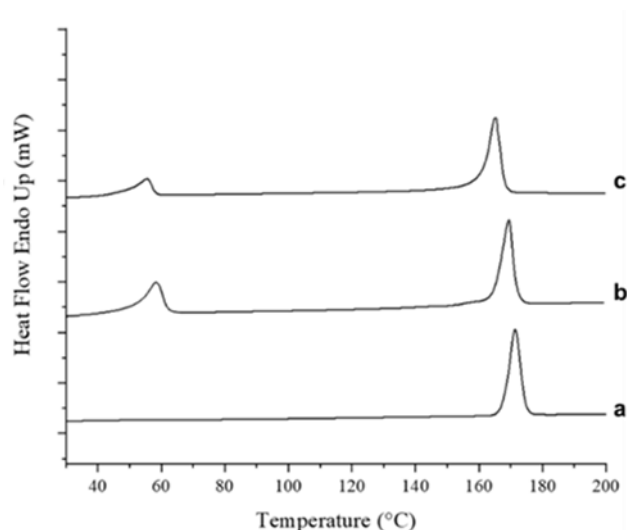
Fig. 3.10. Differential scanning calorimetry profiles of (a) itraconazole, (b) physical mixture (PM), (c) itraconazole nanocrystal with poloxamer 407.

The XRPD spectra of the itraconazole, physical mixture, and nanocrystals were evaluated to confirm the results obtained by DSC. Itraconazole raw powder showed distinct crystalline peaks at 14.4, 17.4, 20.5, 23.5, and 25.7° (Fig. 3.11a). The XRPD patterns of physical mixture and nanocrystals did not change after wet milling (Fig. 3.11b, c). The peak intensity of nanocrystal formulations showed a slight decrease which indicated a slight reduction of crystallinity during wet milling.
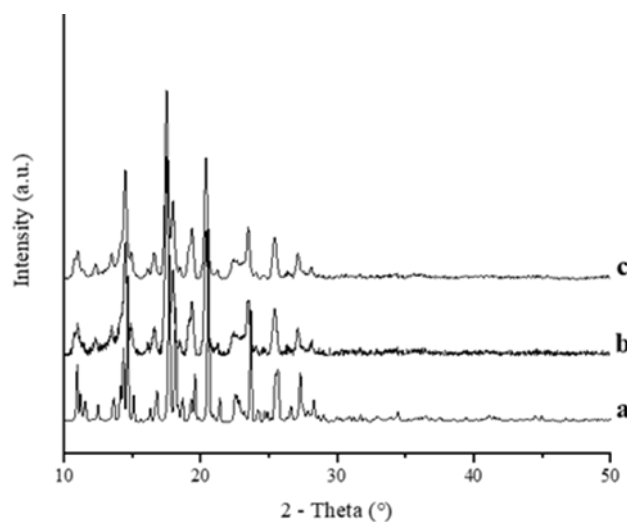
Fig. 3.11. XRPD patterns of (a) itraconazole, (b) physical mixture (PM), (c) itraconazole nanocrystal with poloxamer 407.

3.1.4.3. In vitro *dissolution*

The dissolution studies were conducted under sink and non-sink conditions. The solubility of crystalline itraconazole was determined in different dissolution media at 37 °C (Table 3.3).

Table 3.3. Solubility of itraconazole in different dissolution media (mean ± SD; n=3).

Medium	Solubility (µg/mL)
Phosphate buffer pH 6.8	Below detection limit
0.1N HCl	4.8 ± 0.2
0.1N HCl with 0.1% SDS	36.5 ± 4.3
0.1N HCl with 0.25% SDS	112.0 ± 15.5
0.1N HCl with 0.5% SDS	321.8 ± 20.2
0.1N HCl with 0.7% SDS	634.4 ± 51.1

Samples equivalent to 100 mg itraconazole were evaluated in 900 mL 0.1 HCl with 0.7% SDS to maintain sink condition (< 20% of drug solubility in medium). The dissolution rate of pure itraconazole was slow, with only less than 40 % drug released within the first 15 minutes, and the physical mixture only improved to 50 %. Sporanox® exhibited a higher drug release of 70% at 15 min, while nanocrystals release was even faster and completed within a few minutes (Fig. 3.12). The dissolution rates displayed a rank order of nanocrystal > Sporanox® > physical mixture > raw drug. *In vitro* dissolution study under sink condition suggested that itraconazole nanocrystal formulation might be more promising than commercial product Sporanox®.

In order to evaluate the effect of nanosizing on the solubility of itraconazole, the amount of drug released under non-sink conditions (corresponding to 100 mg drug in 500 mL 0.1N HCl) from raw drug, physical mixture, nanocrystal, and Sporanox® was compared. Under non-sink conditions, Sporanox® improved drug release dramatically with the rank order of Sporanox® > nanocrystal > physical mixture > raw drug (Fig. 3.12). Sporanox® is composed of sugar pellets coated with itraconazole amorphous solid dispersion (Hong et al., 2006). Amorphous solid dispersion could dramatically improve the kinetic solubility of the poorly soluble drug; thus, the degree of supersaturation was 35-fold compared to saturation solubility of raw drug itraconazole. The dissolution profile of nanocrystal under non-sink conditions indicated that the extent of the nanosizing effect on solubility was limited. Furthermore, itraconazole nanocrystal's reported *in vivo* performance was much more

consistent with *in vitro* dissolution under non-sink conditions than sink conditions (Sarnes et al., 2016). The main reason was that itraconazole belonged to "solubility-limited drug". Since there was inadequate fluid within the GI tract to dissolve the administered dose, "solubility-limited drug" will be incompletely absorbed unless the drug was formulated in an already solubilized form like amorphous solid dispersion (Jermain et al., 2018). Therefore, although itraconazole nanocrystal exhibited a faster dissolution rate than Sporanox® under sink conditions, it displayed limited solubility improvement under non-sink conditions. As a solubility-limited drug, itraconazole was not suitable to formulate as a nanocrystal formulation to effectively improve oral bioavailability. A combination of nanosizing techniques with other solubilization formulation strategies like cocrystals or amorphous which could improve the solubility might be more suitable for delivering poorly soluble drugs like itraconazole. The study also suggested that selecting a suitable *in vitro* dissolution test to evaluate nanocrystal formulation was crucial to obtain a high-fit correlation with *in vivo* performance.
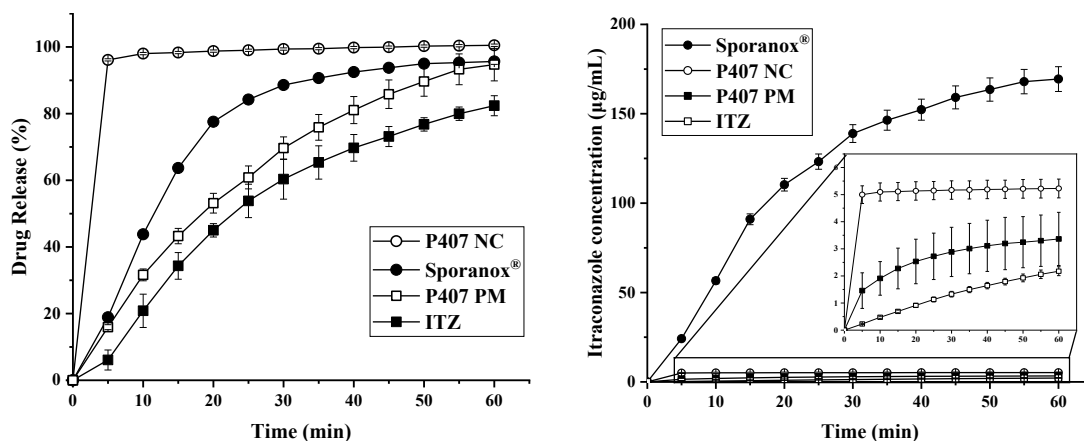
Fig. 3.12. *In vitro* dissolution analysis of the itraconazole (ITZ) formulations: Sporanox®, ITZ, ITZ NC, and physical mixture (left: sink condition; right: non-sink condition).

3.1.5. Conclusion

In the present study, different laboratory-scale nanocrystal preparation methods were compared for milling efficiency and process attributes. Dual centrifugation milling was considered the most promising method with higher milling efficiency, formulation screening efficiency, and broader controllable process attributes. Applying the dual centrifugation milling method to efficiently screen stabilizers and adjust process parameters, optimized itraconazole nanocrystal stabilized by poloxamer 407 was produced with a mean particle size of 200 nm and PDI 0.2. The nanosuspension was physically stable at 4, 25 and 40 °C

for one month. The optimized nanocrystal formulation exhibited a faster dissolution rate than the physical mixture and raw drug under sink or non-sink conditions in *in vitro* dissolution study. While compared with commercial product Sporanox®, nanocrystal formulation exhibited faster drug release under sink conditions but lower and limited solubility increment under non-sink conditions. Itraconazole nanocrystal formulation might not exhibit advantageous *in vivo* behavior compared to the commercial product. Some other solubilization methods like cocrystal or amorphization could be combined with the nanocrystal approach and utilized to offer a valuable approach for delivering orally poorly soluble drugs like itraconazole.

3.2. Combination of cocrystal and nanocrystal techniques to improve the solubility and dissolution rate of poorly soluble drugs

3.2.1. Introduction

Active pharmaceutical ingredients (APIs) are categorized on the basis of the Biopharmaceutics Classification System (BCS) indicating solubility and intestinal permeability as important factors for controlling the rate and extent of oral bioavailability. Recently, most novel APIs have been classified as poorly soluble in BCS class II. According to FDA guidance, an API is considered to be poorly soluble when the highest dose strength cannot be dissolved over the pH range of 1.0-6.8 in 250 mL aqueous media. The Developability Classification System (DCS) further divided BCS class II into IIa (dissolution-limited) and IIb (solubility-limited) based on the dose/solubility ratio, providing more useful information on suitable formulation strategies. Formulation approaches for improving IIa drugs focus primarily on improving dissolution rates including particle size reduction (Jinno et al., 2006; Rabinow, 2004; Sigfridsson et al., 2009), whereas IIb drugs need to increase solubility like complexation (Becket et al., 1999), polymorphs (Nair et al., 2002), amorphous (Blagden et al., 2007) and cocrystals (Babu and Nangia, 2011).

Nanosuspensions (nanocrystals) consist of nano-sized pure drug particles and stabilizers. One of the most common approaches to nanocrystal preparation is wet bead milling. Several studies have demonstrated that nanocrystals could improve oral bioavailability by increasing the dissolution rate of poorly soluble drugs (Rabinow, 2004; Sun et al., 2012; Zhang et al., 2011). The dissolution rate of API is proportional to its surface area, thus reducing the particle size to nano range significantly increases the dissolution rate (Noyes and Whitney, 1897). However, the solubility enhancement by nanocrystal technique is reported only less than 15% (Van Eerdenbrugh et al., 2010). Another research also reported that the saturation solubility of 300 nm nanocrystals increased only by factor 1.3-2.8 compared with raw drug powders (Colombo et al., 2017b). More specifically, this improvement in solubility is closely related to the crystallinity of drug crystals after milling; the benefit of increased solubility on the basis of decreased crystallinity will be lost during storage. Considering the low solubility of the drug itself this slight nanocrystal enhancement is negligible. Sarnes et al. formulated an itraconazole solid oral nanocrystal delivery system and compared to the market product *in vitro* and *in vivo*, and the efficient *in vitro* dissolution enhancement of nanocrystals compared to market product was not reflected in the *in vivo* drug absorption (Sarnes et al., 2014), certifying that nanocrystals did not substantially

improve solubility. In the previous chapter, compared with commercial product Sporanox®, itraconazole nanocrystal formulation exhibited faster drug release under sink conditions but lower and limited solubility increment under non-sink conditions. Therefore, nanocrystal preparation may not be an effective method to increase drug solubility, where solubility is the rate-limiting step after oral administration.

A pharmaceutical cocrystal is composed of an API and an acceptable pharmaceutical molecule. Various methods of cocrystal preparation have been reported, e.g., solvent evaporation, grinding and fusion methods. Jayasankar et al. prepared carbamazepine and saccharin cocrystals by neat grinding (Jayasankar et al., 2006). Dhumal et al. prepared ibuprofen-nicotinamide cocrystals by hot melt extrusion (Dhumal et al., 2010). Itraconazole has been reported to form cocrystals with a number of C4 dicarboxylic acids by solvent evaporation method (Shevchenko et al., 2013). The formation of cocrystals alters the original molecular arrangement and lattice packing of drugs, reduces lattice energy and improves drug solubility (Elder et al., 2013; Schultheiss and Newman, 2009). However, drug concentration in the cocrystal diffusion layer is significantly increased and the supersaturation occurs on the surface of the cocrystal during dissolution. Nucleation and crystal growth coincide with cocrystal dissolution and dissolved cocrystals transform into original crystal structure or precipitate on the surface of the cocrystal particles, preventing a rapid dissolution process and losing the advantage of cocrystal solubility (Almeida et al., 2016; Childs et al., 2013).

Combining cocrystals and nanocrystals could be a promising strategy to increase the solubility and dissolution rate of poorly soluble drugs by overcoming the limitation of each technique. The combination of cocrystal and nanocrystal techniques is not well investigated. Itraconazole, in combination with Tween 80 as stabilizer and excess adipic acid as coformer, was wet milled together at 150 rpm for 60 h to form nano-cocrystals with a particle size of 549 nm (De Smet et al., 2014). Compared to a market product, this formulation yielded equal or faster release. In another study, nano-cocrystal suspensions were successfully prepared by wet milling of cocrystals with stabilizers; optimized nano-cocrystal suspensions were physically stable for at least one month and dissolution profiles were significantly improved (Karashima et al., 2016). Phenazopyridine and phthalimide nano-cocrystals were reported using a sonochemical anti-solvent precipitation method; release and oral bioavailability studies exhibited superior release rate and oral absorption compared to the hydrochloride salt and original cocrystal (Huang et al., 2017). However, the robust preparation processes of nano-cocrystal formulations are still in the exploratory

stage and the mechanism of increasing solubility and dissolution rate through the integration of nanocrystal and cocrystal technology has not been fully understood. In addition, methods of non *in situ* solubility determination like centrifugation/filtration that have been widely applied in common formulations may not be suitable for nanocrystals, cocrystals and nano-cocrystals. A fraction of nanoparticles would exist in the supernatant after centrifugation and filtration; precipitation and dissolution occur simultaneously on the cocrystal surface. Thus, non *in situ* methods do not present sufficient kinetic solubility values in time and result in incorrect values. In order to obtain a more realistic value for kinetic solubility and a deeper understanding of the formulation, *in situ* solubility analyses are superior to non *in situ* methods (Fagerberg et al., 2010; Kuentz, 2015; Teleki et al., 2020).

In situ kinetic solubility determination of different nanocrystals was successfully performed on the basis of UV-VIS spectroscopy (Colombo et al., 2017b). The equipment not only dynamically detects changes in solubility (as short as every 5 s), but the automated platform also provides a Tyndall-Rayleigh scattering correction to exclude scattering from undissolved particles and to obtain the absorbance of dissolved drug only. The aim of this study was therefore to prepare nano-cocrystals and determine their solubility and dissolution rate *in situ*. Itraconazole (ITZ) and indomethacin (IND) were used as model drugs not only because of their low solubility and dissolution rate but also their widely used to form nanocrystals or cocrystals (Elder et al., 2013; Shevchenko et al., 2013). Efficient wet bead milling was applied to obtain nano-cocrystal formulations (Hagedorn et al., 2017). Solid state and particle size of various cocrystals and nano-cocrystals were investigated. The synergistic effect of nanocrystals and cocrystals on increased kinetic solubility was evaluated. In order to understand how nanocrystal technique promotes the kinetic solubility of cocrystals, further *in situ* solubility studies were conducted by comparing macro-, micro- and nano-cocrystals; and the maximum kinetic solubility of different nano-cocrystals was determined under different excess conditions.

3.2.2. Preparation and characterization of drug nanocrystals, macro-, micro- and nano-cocrystals

ITZ forms cocrystals with a range of aliphatic dicarboxylic acids by solvent evaporation-based crystallization (Lahtinen et al., 2013; Shevchenko et al., 2013). Stable cocrystals were formed with fumaric acid and succinic acid as coformers in this study (ITZ-FUM, ITZ-SUC). Subsequently, they were wet milled into micro- and nano range. Formulations were stabilized with poloxamer 407, which was commonly used in nanocrystal formulations

(Cerdeira et al., 2013). ITZ raw powder and its two macro-cocrystals were all in the larger micron range (around 30-100 µm). After 0.5 h milling, the particle sizes of the two macro-cocrystals decreased to smaller micron range (around 10-20 µm); and after 4 h, the particle sizes of ITZ-FUM and ITZ-SUC were around 400 nm with a narrow distribution (Table 3.4).

Table 3.4. Particle size characterization of ITZ particles (±S.D., n = 3).

Sample	Size measurement, µm	Particle size after redispersion of freeze-dried powder	
	D50	z-average, nm	PDI
ITZ raw powder	50 ± 6	-	-
ITZ nanocrystal	-	223 ± 5	0.24 ± 0.02
ITZ-FUM macro	107 ± 5	-	-
ITZ-FUM micro	18 ± 2	-	-
ITZ-FUM nano	-	443 ± 7	0.35 ± 0.02
ITZ-SUC macro	36 ± 5	-	-
ITZ-SUC micro	13 ± 2	-	-
ITZ-SUC nano	-	455 ± 9	0.24 ± 0.01

The morphological evaluation displayed a substantial difference between ITZ raw powder and two macro-cocrystals (Fig. 3.13a-c). The ITZ particles were irregular crystals and the drug clusters were formed by static electricity. However, the ITZ-FUM cocrystals were rod crystals; and the ITZ-SUC cocrystals were hexagonal plate like crystals, in accordance with the literature (Remenar et al., 2003). No large particles were observed after milling, which was consistent with PCS measurements (Fig. 3.13d-f).
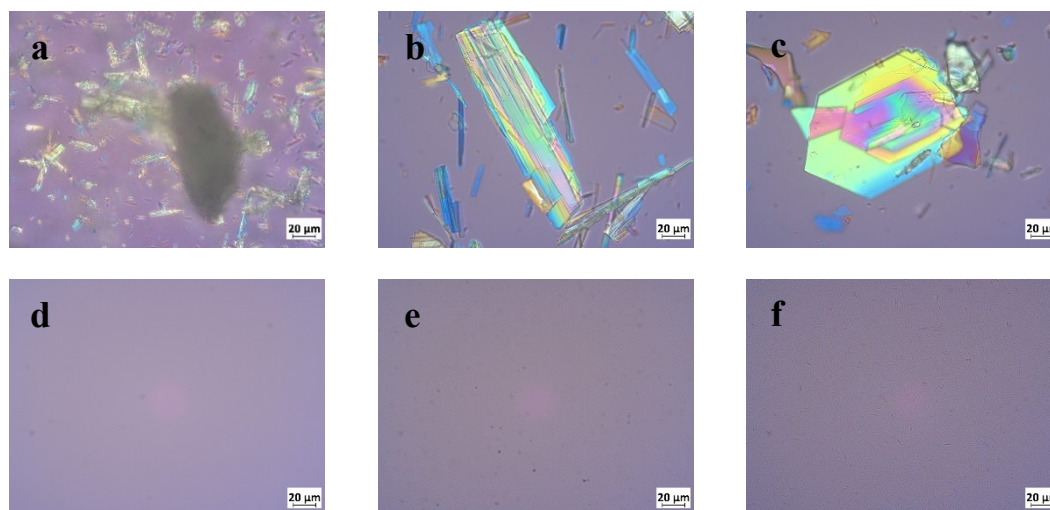
Fig. 3.13. Optical microscopy pictures of (a) ITZ raw powder, (b) ITZ-FUM macro-cocrystal, (c) ITZ-SUC macro-cocrystal, (d) ITZ nanocrystal, (e) ITZ-FUM nano-cocrystal, (f) ITZ-SUC nano-cocrystal.

The preservation of the solid state cocrystal structure, despite being subjected to high energy stress in aqueous media, must be confirmed after wet milling. ITZ-FUM macro-cocrystals exhibited an endothermic peak at 184 °C that differed from the melting peak of ITZ (170 °C) and the physical mixture (165 °C) (Fig. 3.14a, c, d); whereas ITZ-FUM macro-cocrystals showed a second small endothermic peak at around 135 °C, it was possible that a small part of ITZ and FUM did not form cocrystals or formed other isotropic crystal structures. ITZ-SUC macro-cocrystals displayed a single melting peak at 165 °C, which differs from the melting peak of ITZ and the endothermic melting peak of the physical mixture (157 °C and 180 °C) (Fig. 3.14a, f, g). After milling, a small peak at 55 °C indicated the small fraction of poloxamer 407 and the onset melting temperatures of ITZ-FUM and ITZ-SUC nano-cocrystals slightly shifted to lower temperatures compared to their macro-cocrystals (Fig. 3.14e, h). The stabilizer melted at lower temperatures dissolved the drug to form eutectic mixtures or the reduced degree of crystallinity may explain melting peak shift (Colombo et al., 2017a; Kocbek et al., 2006). ITZ-FUM macro-cocrystals owned the highest melting point representing harder crystal lattice structure and processed less crystallinity reduction after milling into ITZ-FUM nano-cocrystals, resulting in the smallest peak shift compared to ITZ nanocrystals and ITZ-SUC nano-cocrystals. In majority, the cocrystal structure of both nano-cocrystals remained unchanged after wet milling.
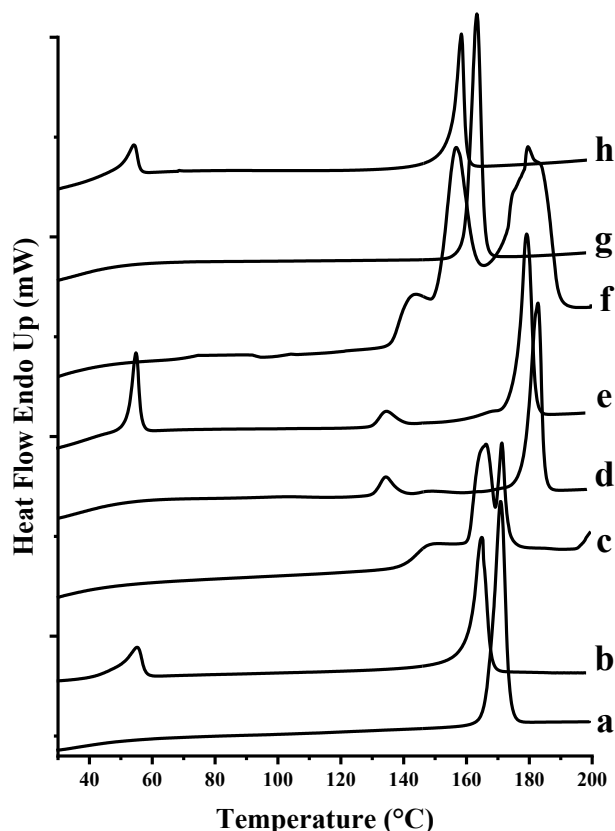
Fig. 3.14. Differential scanning calorimetry profiles of different ITZ formulations: (a) ITZ raw powder, (b) ITZ nanocrystal, (c) ITZ and FUM physical mixture, (d) ITZ-FUM macro-cocrystal, (e) ITZ-FUM nano-cocrystal, (f) ITZ and SUC physical mixture, (g) ITZ-SUC macro-cocrystal and (h) ITZ-SUC nano-cocrystal.

The XRPD spectra of the ITZ raw powder, ITZ-FUM and ITZ-SUC macro-cocrystals were evaluated in order to confirm the cocrystal structure and crystallinity before and after wet milling (Fig. 3.15). ITZ raw powder showed distinct crystalline peaks at 14.4, 17.4, 20.5, 23.5 and 25.7°, while ITZ-FUM and ITZ-SUC macro-cocrystals showed different crystalline peaks indicating different crystal structure (Shevchenko et al., 2012). The XRPD patterns of ITZ nanocrystals and ITZ-FUM and ITZ-SUC nano-cocrystals did not change after wet milling, however, the peak intensity of all the nanocrystal formulations showed a slight decrease which indicated a slight reduction of crystallinity during wet milling. ITZ cocrystals were able to maintain the crystalline structure during wet milling process due to their high binding energies in the crystal lattice. XRPD analysis further confirmed the results obtained by DSC.

79
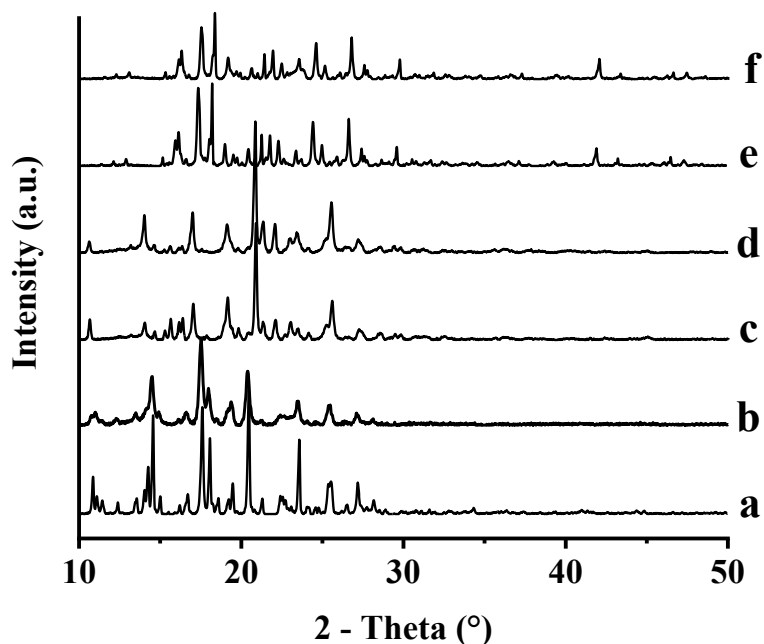
Fig. 3.15. XRPD patterns of different ITZ formulations: (a) ITZ raw powder, (b) ITZ nanocrystal, (c) ITZ-FUM macro-cocrystal, (d) ITZ-FUM nano-cocrystal, (e) ITZ-SUC macro-cocrystal and (f) ITZ-SUC nano-cocrystal.

Obtained particle sizes of various IND samples are listed in Table 2. IND raw powder and its two macro-cocrystals were all in the larger micron range (around 30-70 μm). The resulted mean particle sizes of the IND-SAC and IND-NCT nano-cocrystals were around 300 nm and the particle size distributions were narrow.

Table 3.5. Particle size characterization of IND particles (±S.D., n = 3).

Sample	Size measurement, μm	Particle size after redispersion of freeze-dried powder	
	D50	z-average, nm	PDI
IND raw powder	70 ± 9	-	-
IND nanocrystal	-	163 ± 1	0.14 ± 0.02
IND-SAC macro	68 ± 10	-	-
IND-SAC nano	-	329 ± 10	0.20 ± 0.02
IND-NCT macro	29 ± 8	-	-
IND-NCT nano	-	280 ± 4	0.29 ± 0.01

The morphological evaluation displayed a substantial difference between IND raw powder and two macro-cocrystals (Fig. 3.16). IND raw powder crystals were irregular. However, the IND-SAC cocrystals were plate crystals; and the IND-NCT cocrystals resulted in needle like crystals (Fig. 3.16a-c). After milling, large particles were not observed, which was consistence with the particle size measurements (Fig. 3.16d-f).
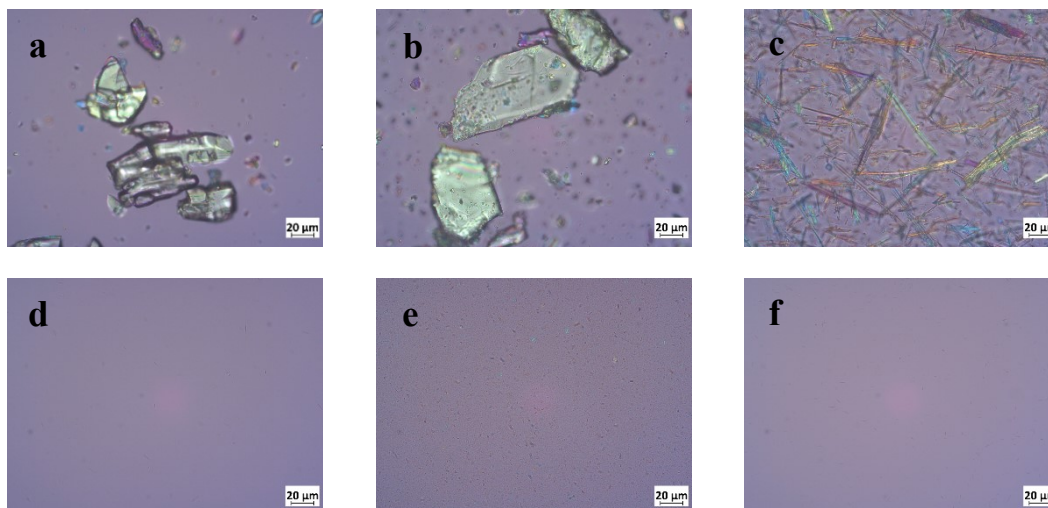
Fig. 3.16. Optical microscopy pictures of (a) IND raw powder, (b) IND-SAC macro-cocrystal, (c) IND-NCT macro-cocrystal, (d) IND nanocrystal, (e) IND-SAC nano-cocrystal, (f) IND-NCT nano-cocrystal.

The melting temperatures of IND raw powder, IND-SAC and IND-NCT macro-cocrystals were at 165 °C, 180 °C and 120 °C, respectively (Fig. 3.17a, d, g). The physical mixture of IND with saccharin exhibited multi-melting transition points and the physical mixture of IND with nicotinamide exhibited overlaid melting peaks (Fig. 3.17c, f). After wet milling, the small peak at around 50 °C indicated a small fraction of poloxamer 407. Compared to IND raw powder, the endothermic melting peak of IND nanocrystals not only shifted to lower temperatures, but also turned broader (Fig. 3.17a, b). IND is susceptible to undergo polymorphism and partial amorphization during milling (Colombo et al., 2018). The onset melting temperatures of IND-SAC and IND-NCT nano-cocrystals slightly shifted to lower temperatures without significant peak broadening (Fig. 3.17e, h).
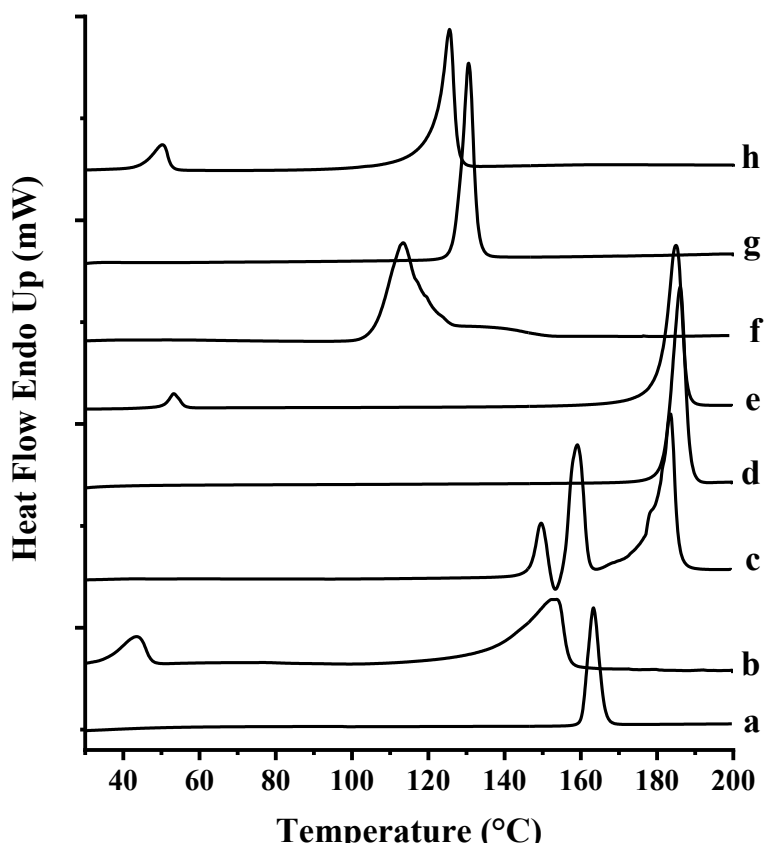
Fig. 3.17. Differential scanning calorimetry profiles of different IND formulations: (a) IND raw powder, (b) IND nanocrystal, (c) IND and SAC physical mixture, (d) IND-SAC macro-cocrystal, (e) IND-SAC nano-cocrystal, (f) IND and NCT physical mixture, (g) IND-NCT macro-cocrystal and (h) IND-NCT nano-cocrystal.

IND raw powder exhibited distinct crystalline peaks at 11.6, 19.6, 21.8, 26.6 and 29.3°, while IND-SAC macro-cocrystals exhibited crystalline characteristic peaks at 11.0, 14.3 and 24.9°, consistent with literature (Fig. 3.18) (Chun et al., 2014; Padrela et al., 2012). In addition, IND-NCT macro-cocrystals demonstrated different characteristic peaks from IND raw powder and IND-SAC. After milling, IND nanocrystal XRPD pattern indicated a dramatic decrease in the intensity of crystalline peaks and disappearance of some distinct characteristic peaks. While both nano-cocrystals presented similar crystalline characteristic peaks compared to their macro-cocrystals with only a slight decrease in intensity.
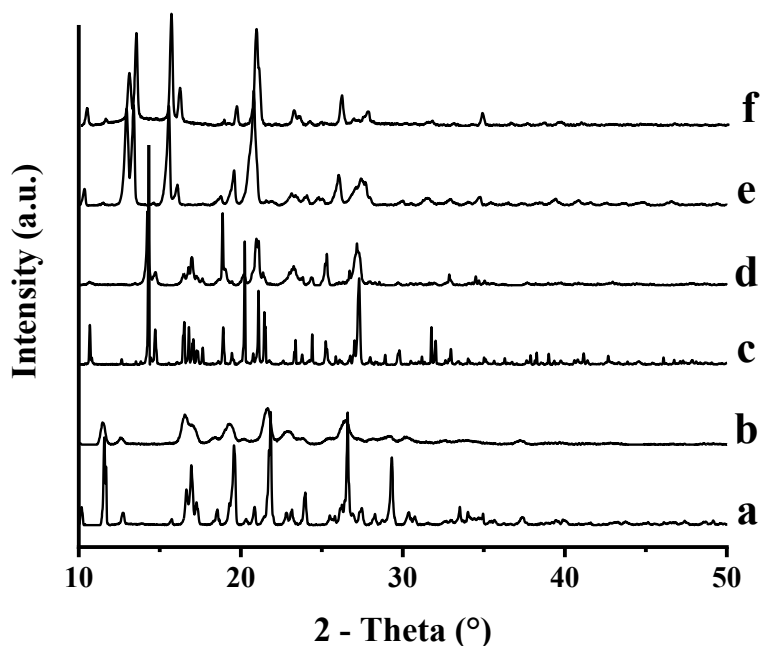
Fig. 3.18. XRPD patterns of different IND formulations: (a) IND raw powder, (b) IND nanocrystal, (c) IND-SAC macro-cocrystal, (d) IND-SAC nano-cocrystal, (e) IND-NCT macro-cocrystal and (f) IND-NCT nano-cocrystal.

Compared to macro-cocrystals, the melting peak of both nano-cocrystals slightly shifted to lower temperature and the intensity of XRPD pattern decreased slightly, both indicating that the reduction of crystallinity during wet milling was unavoidable. However, the transformation of API into its cocrystal form still suggested a new strategy for the preparation of nano-formulations that are physically or chemically unstable during wet milling. Amorphization during nano milling was significantly lower for IND cocrystals than for raw powder. The same result was found during nano milling of ITZ raw powder and cocrystals even though the trend was not so pronounced. The formation of cocrystals may alter some physical properties of drug like hardness by crystal lattice structure transformation. The hydrogen bonding, which is the majority interaction between the drug and coformers, not only fixed the structure of crystals but also prevent the drugs' hydrogen bonding sites from hydration with water during wet milling. Cocrystal formulation is therefore another promising strategy to avoid phase transformation during wet milling processes.

3.2.3. Comparison of dissolution profiles of raw drug powder, nanocrystals, macro- and nano-cocrystals

The solubility and dissolution rate of ITZ-FUM and ITZ-SUC nano-cocrystals were compared to ITZ raw powder, macro-cocrystals and nanocrystals in the presence of equal concentrations of poloxamer 407 (Fig. 3.19). The solubility of crystalline ITZ was low up to 30 min (around 1 µg/mL) and reached a plateau of 5.1 µg/mL after 6 h. While the solubility of nanocrystals was around 7.1 µg/mL, with an increase factor of 1.4 (Colombo et al., 2017b). No significant increase in crystalline drug nanosuspensions solubility is expected. Nanocrystals, however still exhibited a superior dissolution rate as they reached the solubility plateau within 1 min. ITZ-FUM and ITZ-SUC macro-cocrystals resulted in a higher solubility of 35.1 µg/mL and 42.4 µg/mL after 30 min, with an increase factor of 6.9 and 8.3, respectively. ITZ-FUM and ITZ-SUC nano-cocrystals exhibited superior solubility and dissolution rate than nanocrystals and macro-cocrystals. Specifically, ITZ-FUM and ITZ-SUC nano-cocrystals had a maximum solubility of 127.0 µg/mL and 156.9 µg/mL, with an increase factor of 24.9 and 30.8; additionally, nano-cocrystals reached the plateau in less than 5 min, indicating that nanosized formulations owned superior dissolution rate due to their great increased surface area. Nano-cocrystals successfully combined nanocrystal and cocrystal technologies to overcome the limitation of nanocrystals with regard to solubility improvement and of cocrystal with regard to rate of dissolution.
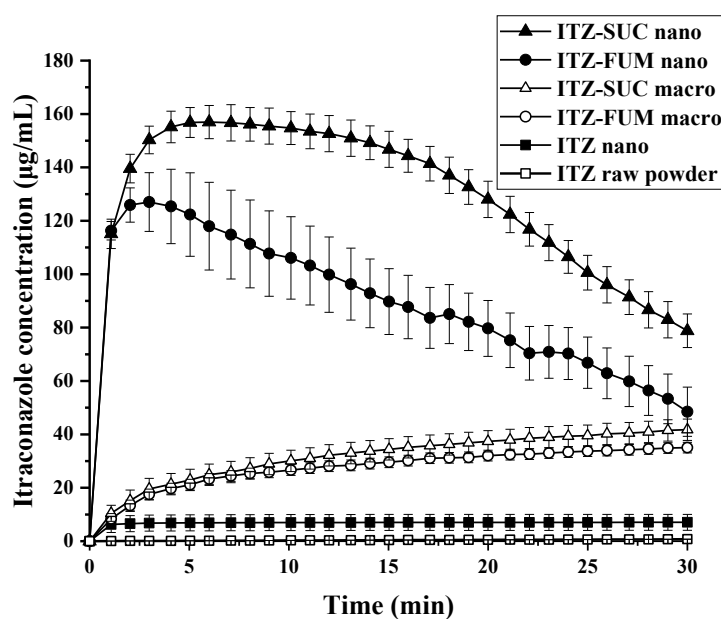
Fig. 3.19. Solubility profiles of ITZ raw powder, ITZ nanocrystal, ITZ-FUM macro-cocrystal, ITZ-SUC macro-cocrystal, ITZ-FUM nano-cocrystal and ITZ-SUC nano-cocrystal.

The solubility of IND raw powders, nanocrystals, macro- and nano-cocrystals in the presence of equal concentrations of poloxamer was tested. The saturation solubility of IND raw powder and nanocrystal powder was 9.0 µg/mL after 5 h (equilibrium solubility) and 15.6 µg/mL after 1 min (Fig. 3.20). Compared to raw powder, the solubility of IND nanocrystals increased by a factor of 1.7; IND-SAC and IND-NCT macro-cocrystals reached solubility plateau of 21.3 µg/mL and 27.3 µg/mL, with increase by a factor of 2.4 and 3.0. The reduction of the particle size of macro-cocrystals to nano range strongly increases kinetic solubility. The maximum solubility of IND-SAC and IND-NCT nano-cocrystals was 91.1 µg/mL and 112.2 µg/mL with an increase of 10.1 and 12.4. IND-SAC nano-cocrystals showed a short-live peak solubility and dropped to low solubility which was considered as "spring and parachute". In contrast, IND-NCT nano-cocrystals showed a high supersaturation state that was maintained for a long time and was considered as "spring and hover" (Wei et al., 2018). The solubility of API is increased and maintained by complexation in the presence of some specific coformers (Song et al., 2015; Wei et al., 2018). IND may have greater interaction with NCT but has less interaction with SAC after dissolution, thus explaining why IND-NCT exhibited longer parachute time than IND-SAC nano-cocrystals. These *in situ* results indicated that synergistic effects of nanocrystals and cocrystals were realized by the nano-cocrystal formulation, which each technology cannot achieve independently.
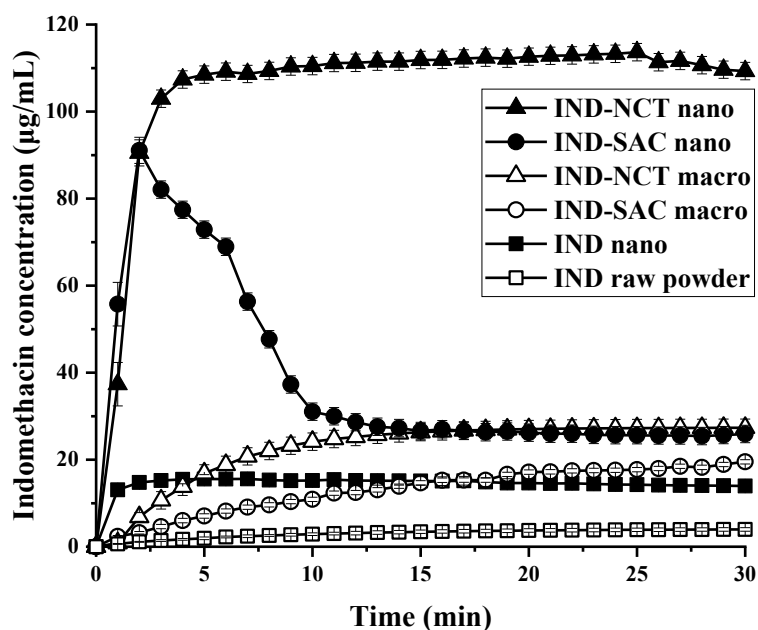
Fig. 3.20. Solubility profiles of IND raw powder, IND nanocrystal, IND-SAC macro-cocrystal, IND-NCT macro-cocrystal, IND-SAC nano-cocrystal and IND-NCT nano-cocrystal.

3.2.4. Effect of particle size on the solubility profiles of ITZ cocrystals

In order to further understand the mechanism of synergistic effect of nanocrystals and cocrystals with regard to increased solubility and dissolution rate, different cocrystal particle sizes were investigated with *in situ* solubility profiles. Same excess amounts (corresponding to 10 mg ITZ) of macro-, micro- and nano-cocrystals were added to the dissolution media and their kinetic solubility were analysed. As shown above, ITZ-FUM and ITZ-SUC macro-cocrystals resulted in a solubility of approximately 40 µg/mL. According to previous research, nanocrystal solubility would increase with minor factor (around 1.5) resulting from a small fraction of nanoparticles (< 100 nm) and a reduction of crystallinity (Colombo et al., 2017b). The theoretical solubility value of nano-cocrystals should not be more than 60 µg/mL (1.5 * 40 µg/mL). While the experimental solubility of ITZ-FUM and ITZ-SUC nano-cocrystal (127 and 157 µg/mL) was more than twice higher than 60 µg/mL (Fig. 3.21). Upon water contact, the diffusion layer of cocrystal particle is highly concentrated and reaches a supersaturation state. The process of dissolution and precipitation would therefore occur simultaneously. The dissolution rate of macro-cocrystals is not high enough to overcome precipitation occurred on the cocrystal surface, which prevents further dissolution (Childs et al., 2013). By integrating nanotechnology, the dissolution rate is highly promoted and overweighs the precipitation process, resulted in the highest maximum solubility. ITZ micro-cocrystals with medium particle size were compared to its macro- and nano-cocrystals. As expected, the kinetic solubility of micro-cocrystals was higher than macro-cocrystals and lower than nano-cocrystals. Therefore, the kinetic solubility of cocrystal formulations increased with reduced particle size (Fig. 3.21). The particle size can be further reduced by optimizing the preparation method and formulation. However, stability issues during nano-cocrystal formulations storage and downstream process need to be considered. In general, nanocrystal technique effectively promotes the potential of cocrystal supersaturation effect by its superior dissolution rate, explained by the competition between dissolution rate and precipitation rate.
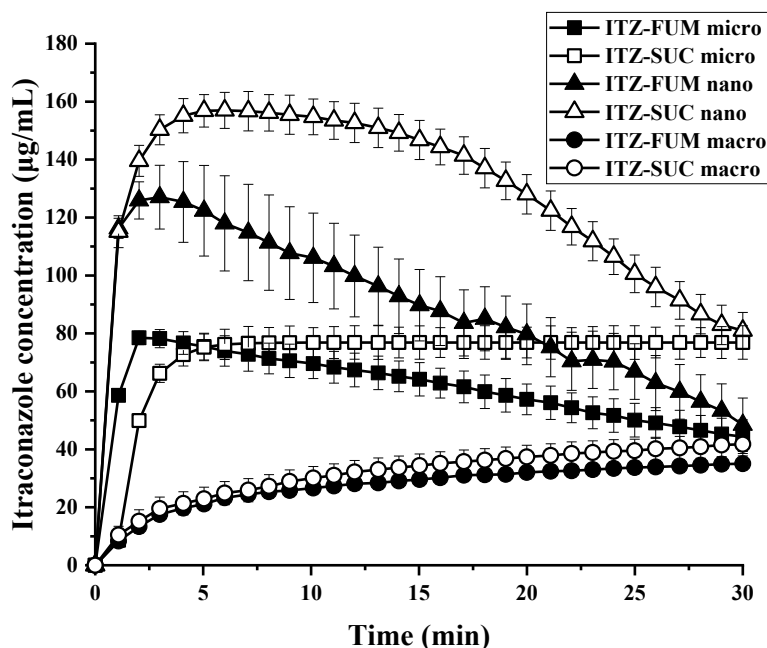
Fig. 3.21. Solubility profiles of ITZ macro-, micro and nano-cocrystal formulations.

3.2.5. Maximum solubility of nano-cocrystals

ITZ and IND nano-cocrystals were used to investigate the maximum solubility of nano-cocrystals under various excess conditions. As the influence of the small amount of poloxamer 407 on the solubility is negligible, the kinetic solubility profiles of nano-cocrystals were determined with drug loadings 5-100 times higher than the equilibrium solubility of the raw drug powder.

The maximum solubility of ITZ-FUM and ITZ-SUC nano-cocrystals was determined with 10, 20, 40, 80 and 10, 20, 40, 80, 100 times excess conditions respectively. The solubility profiles are plotted using the supersaturation level as the right vertical axis (Fig. 10). The maximum supersaturation level of ITZ-FUM nano-cocrystals is approximately 26. The maximum solubility of ITZ-FUM nano-cocrystal was 127μg/mL and did not further increase from 40 to 80 times excess (Fig. 3.22A). For ITZ-SUC nano-cocrystals, the maximum supersaturation level is approximately 55. The maximum solubility of ITZ-SUC nano-cocrystal was 260 μg/mL and did not further increase from 80 to 100 times excess (Fig. 3.22B). ITZ-SUC nano-cocrystals possessed much higher kinetic solubility than ITZ-FUM nano-cocrystals under same excess conditions. Since succinic acid has remarkably higher solubility than fumaric acid in the dissolution media, succinic acid separates faster from the cocrystal structure and causes higher crystal arrangement disruption; hence achieved higher supersaturated solubility.
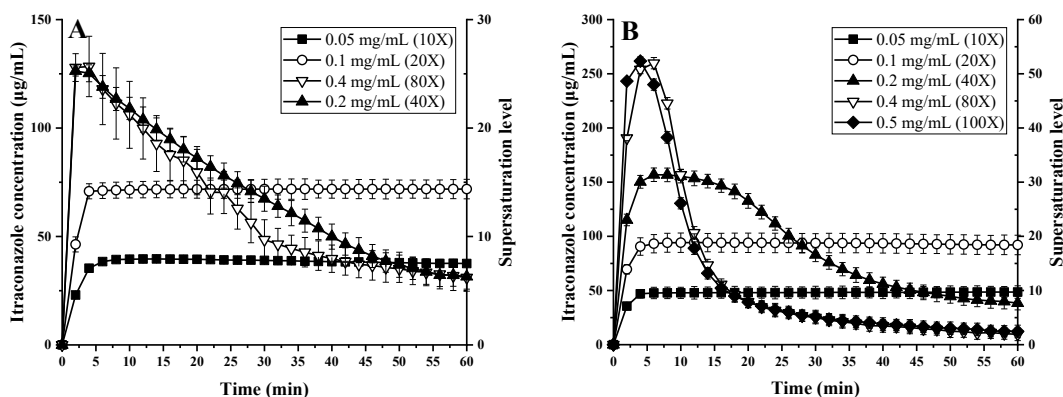
Fig. 3.22. The maximum solubility achievable with increasing excess conditions of (A) ITZ-FUM nano-cocrystals and (B) ITZ-SUC nano-cocrystals.

The maximum solubility of IND-SAC and IND-NCT nano-cocrystals was determined with 5, 10, 20, 40, 50 and 5, 10, 20, 40 times excess conditions respectively. The maximum supersaturation level of IND-SAC and IND-NCT nano-cocrystals is approximately 12 and 13 (Fig. 3.23). The addition of more nano-cocrystals to higher excess did not increase the solubility further in both cases.
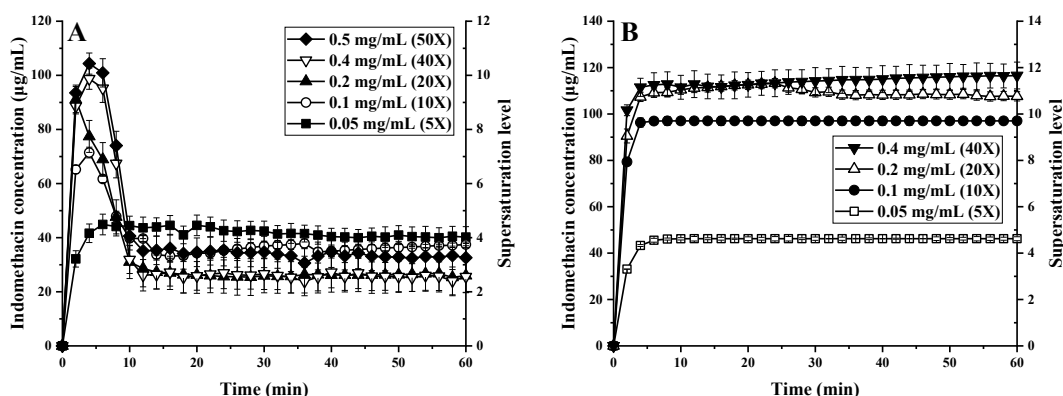
Fig. 3.23. The maximum solubility achievable with increasing excess conditions of (A) IND-SAC nano-cocrystals and (B) IND-NCT nano-cocrystals.

For all these nano-cocrystals, lower excess conditions exhibited longer supersaturation maintaining time. At 10- and 20-times excess condition, ITZ-FUM and ITZ-SUC nano-cocrystals maintained supersaturation for more than 1 h, while at 40 times excess precipitation started after 5 min. IND-SAC nano-cocrystals maintained supersaturation for more than 1 h at 5 times excess, while all the higher excess started precipitating in less than 5 min. The exception is IND-NCT nano-cocrystals, where no precipitation is observed under all excess conditions. IND-NCT may form a stable complexation during these

dissolution experiments and precipitation is expected for longer observation time. Nano-cocrystal precipitation induction time decreased as excess conditions increased. At the step of nucleation and crystal growth in a supersaturated system, each supersaturated solution has a maximum supersaturation limit, defined as metastable zone width. When the concentration exceeds this limitation, precipitation occurs; whereas if the concentration is within the metastable zone, the induction time for precipitation is longer (Wu et al., 2014). Additionally, rapid and heterogeneous precipitation occurred as more undissolved particles in higher excess conditions act as crystallization nucleus in the supersaturated system (Plum et al., 2020). Comparing ITZ and IND nano-cocrystals, under 40 times excess, IND nano-cocrystals only achieved the supersaturation level of around 10, while ITZ-FUM and ITZ-SUC nano-cocrystals achieved the supersaturation level of 26 and 30. Different compounds have different supersaturation properties and ITZ owns higher supersaturation properties than IND (Palmelund et al., 2016). Precipitation and recrystallization clearly existed in nano-cocrystal formulations; thus, further studies are required to extend the time of increased kinetic solubility. One potential approach is *in situ* recrystallization inhibitors investigation.

3.2.6.   Stability studies of nano-cocrystal suspension and powder

The stability data of suspension and powder form of ITZ-FUM, ITZ-SUC, IND-SAC and IND-NCT nano-cocrystals over a period of 90 days at different temperature are summarized respectively (Table 3.6-3.9). The particle size and PDI of ITZ-FUM nano-cocrystal suspensions were undetectable even after 30 days at 4 °C due to both crystal growth and particles aggregation. The particle size and PDI of ITZ-SUC, IND-SAC and IND-NCT nano-cocrystal suspensions slightly increased with increase of storage temperature after 30 days; while after 90 days, non-dispersible aggregates was observed indicated the particle aggregation. The maximum solubility concentration of suspension form decreased with the storage time and the increase of storage temperature. While both the powder form of all nano-cocrystals were relatively stable in not only particle size and PDI but also maximum solubility concentration during at least 90 days storage at 4, 25 and 40 °C. Nanosuspension were more prone to physical instability like Ostwald ripening or agglomeration during storage compared to its powder forms. Moreover, suspension form is more susceptible to microbial instability. Thus, nano-cocrystal suspensions were suggested to be converted into solid dosage forms for stabilization.

Table 3.6. Stability data of ITZ-FUM nano-cocrystal suspension and powder

		Initial	4 °C		25 °C		40 °C	
			30 d	90 d	30 d	90 d	30 d	90 d
Suspension	z-average, nm	343 ± 7	-	-	-	-	-	-
	PDI	0.36 ± 0.03	-	-	-	-	-	-
	C_{max}, µg/mL	112 ± 2	79 ± 3	70 ± 5	66 ± 1	58 ± 3	39 ± 2	30 ± 1
Powder	z-average, nm	443 ± 7	406 ± 10	456 ± 5	464 ± 8	440 ± 12	435 ± 3	428 ± 6
	PDI	0.35 ± 0.02	0.32 ± 0.03	0.31 ± 0.01	0.42 ± 0.01	0.40 ± 0.02	0.38 ± 0.01	0.37 ± 0.02
	C_{max}, µg/mL	108 ± 5	107 ± 6	107 ± 5	108 ± 7	107 ± 3	106 ± 4	92 ± 10

Table 3.7. Stability data of ITZ-SUC nano-cocrystal suspension and powder

		Initial	4 °C		25 °C		40 °C	
			30 d	90 d	30 d	90 d	30 d	90 d
Suspension	z-average, nm	294 ± 6	283 ± 5	-	470 ± 10	-	913 ± 52	-
	PDI	0.29 ± 0.03	0.30 ± 0.02	-	0.20 ± 0.02	-	0.46 ± 0.05	-
	C_{max}, µg/mL	150 ± 10	154 ± 8	54 ± 9	66 ± 1	58 ± 3	39 ± 2	30 ± 1
Powder	z-average, nm	355 ± 9	412 ± 6	435 ± 5	446 ± 10	433 ± 6	418 ± 12	509 ± 22
	PDI	0.24 ± 0.01	0.25 ± 0.01	0.28 ± 0.02	0.30 ± 0.01	0.30 ± 0.02	0.33 ± 0.01	0.39 ± 0.05
	C_{max}, µg/mL	157 ± 5	154 ± 3	151 ± 3	154 ± 10	158 ± 9	158 ± 4	145 ± 10

Table 3.8. Stability data of IND-SAC nano-cocrystal suspension and powder

		Initial	4 °C		25 °C		40 °C	
			30 d	90 d	30 d	90 d	30 d	90 d
Suspension	z-average, nm	322 ± 6	459 ± 23	-	418 ± 15	-	328 ± 12	-
	PDI	0.15 ± 0.01	0.43 ± 0.05	-	0.38 ± 0.04	-	0.29 ± 0.05	-
	C_{max}, µg/mL	120 ± 8	100 ± 8	35 ± 5	86 ± 6	25 ± 2	62 ± 2	30 ± 3
Powder	z-average, nm	329 ± 10	322 ± 9	435 ± 5	364 ± 10	503 ± 6	411 ± 9	483 ± 22
	PDI	0.20 ± 0.02	0.21 ± 0.01	0.28 ± 0.02	0.30 ± 0.03	0.35 ± 0.03	0.33 ± 0.02	0.36 ± 0.04
	C_{max}, µg/mL	110 ± 10	114 ± 5	101 ± 4	105 ± 5	100 ± 11	108 ± 6	98 ± 2

Table 3.9. Stability data of IND-NCT nano-cocrystal suspension and powder

		Initial	4 °C		25 °C		40 °C	
			30 d	90 d	30 d	90 d	30 d	90 d
Suspension	z-average, nm	294 ± 6	396 ± 8	-	500 ± 7	-	782 ± 12	-
	PDI	0.29 ± 0.03	0.24 ± 0.01	-	0.26 ± 0.02	-	0.22 ± 0.01	-
	C_{max}, µg/mL	125 ± 2	110 ± 4	38 ± 5	86 ± 5	30 ± 1	78 ± 10	20 ± 2
Powder	z-average, nm	280 ± 4	321 ± 5	433 ± 9	303 ± 4	436 ± 10	395 ± 8	409 ± 9
	PDI	0.29 ± 0.01	0.26 ± 0.02	0.28 ± 0.02	0.25 ± 0.01	0.30 ± 0.02	0.30 ± 0.03	0.29 ± 0.02
	C_{max}, µg/mL	106 ± 4	103 ± 2	97 ± 3	104 ± 10	98 ± 9	100 ± 5	95 ± 6

3.2.7. Conclusions

Four itraconazole and indomethacin nano-cocrystals with mean particle diameters of around 450 nm were successfully prepared for the first time. Solid-state characterization suggested that by transforming raw drug powder into its cocrystal form is a new strategy for the preparation of nano-formulations which are physically or chemically unstable during wet milling. Furthermore, the kinetic solubility and dissolution rate of nano-cocrystals were investigated by *in situ* UV-VIS methods which were not performed before. *In situ* solubility studies indicated that nano-cocrystals showed remarkably higher solubility and dissolution rate compared to nanocrystals and cocrystals. The combination of cocrystals and nanocrystals could potentially overcome the limitation of nanocrystals in solubility improvement and the limitation of cocrystal in dissolution rate improvement. Nanocrystal technique efficiently promotes the potential of cocrystal solubilization effect by its superior dissolution rate. The maximum kinetic solubility of nano-cocrystals was determined under different excess conditions and reached a plateau. The optimization of the preparation process and *in situ* investigation of recrystallization inhibitors contributing to extend the kinetic solubility time of nano-cocrystals should be analysed in further studies. This expands the drug development strategies of poorly soluble drugs.

3.3. Itraconazole-succinic acid nano-cocrystals: Kinetic solubility improvement and influence of polymers on controlled supersaturation

3.3.1. Introduction

The biopharmaceutical classification system (BCS) has been widely applied to classify active pharmaceutical ingredients (API) based on their solubility and intestinal permeability (Amidon et al., 1995). The bioavailability of an orally administered drug depends primarily on its solubility in the gastrointestinal tract and its permeability across cell membranes. Most of these drug molecules permeate well through the intestinal wall despite their poor solubility in gastrointestinal fluids (BCS class II) (Buckley et al., 2013). Developability classification system (DCS) further divides the class II into IIa (dissolution-limited) and IIb (solubility-limited) based on dose/solubility ratio, which provides more useful information for appropriate formulation strategies (Butler and Dressman, 2010; Rosenberger et al., 2018). The use of supersaturation drug delivery system is one common strategy to overcome challenges associated with solubility-limited APIs (DCS IIb) (Brouwers et al., 2009). Supersaturation drug delivery system generates a higher concentration than the thermodynamic solubility of the crystalline drug (i.e., supersaturation) without compromising effective permeability across membranes; thus, an increase in the concentration at absorption sites can increase the flux of the drug across the gastrointestinal membrane according to Fick's First Law (Borbás et al., 2016; Poelma et al., 1991). Formulation strategies like cocrystals, salts, amorphous drugs and amorphous solid dispersion belong to the group of supersaturation drug delivery system (Hancock and Parks, 2000; Li et al., 2005; Thakuria et al., 2013; Serajuddin, 2007; Vo et al., 2013).

A pharmaceutical cocrystal is composed of an API and an appropriate pharmaceutical acceptable molecule. Compared with amorphous drugs or solid dispersion, cocrystals not only achieve the solubility benefits of high energy solids but also exist in crystalline form with high thermodynamic stability (Babu and Nangia, 2011). The mechanism by which cocrystals enhance solubility have been well investigated. One explanation is that the original molecular arrangement of the drugs is changed after cocrystal formation resulting in a decreased lattice energy (Good and Rodriguez-Hornedo, 2009). Another explanation is that upon dissolution, the rapid release of the coformer disrupts the cocrystal lattice forming randomly oriented drug molecules similar to amorphous drugs (Healy et al., 2017; Rodríguez-Spong et al., 2004). Theoretically, since cocrystals act similar to amorphous materials during dissolution, their extent of supersaturation should reach a comparable

level. However, the supersaturation of API cocrystals is significantly lower than their amorphous solid forms (Almeida et al., 2016; Bavishi and Borkhataria, 2016). The reason is that during cocrystals dissolution, supersaturation builds up at the surface of still undissolved drug cocrystals, inducing recrystallization at their surface. This results in a decreased dissolution rate (Childs et al., 2013; Shiraki et al., 2008). Therefore, during the dissolution of those high energy solid forms, the rate of dissolution has to be higher than the rate of precipitation/crystallization into low energy forms.

Nano-cocrystal formulations, which combine nano and cocrystal technologies, are proposed as a novel approach to improve supersaturation and thus possibly also oral bioavailability. Only few publications or patents have been reported on itraconazole-adipic acid, indomethacin-saccharin, carbamazepine-saccharin, phenazopyridine-phthalimide and myricetin-nicotinamide nano-cocrystal formulations (De Smet et al., 2014; Huang et al., 2017; Karashima et al., 2016; Liu et al., 2016). In the previous chapter, itraconazole-succinic acid and itraconazole-fumaric acid nano-cocrystal formulations have been prepared. These nano-cocrystals successfully combined nanocrystal and cocrystal technologies to overcome the limitation of nanocrystals with regard to solubility improvement and of cocrystal with regard to rate of dissolution. Nano-cocrystals resulted in a higher supersaturation solubility than its cocrystal forms. However, those nano-cocrystal formulations with improved solubility and dissolution rates were thermodynamically unstable once dissolved due to the supersaturation of the drug. In order to maintain the higher kinetic solubility, appropriate polymeric precipitation inhibitors are required to decrease the precipitation/crystallization rate. To our knowledge, there are no publications which investigated the effect of different polymeric precipitation inhibitors in nano-cocrystal formulations.

In this study, itraconazole-succinic acid (ITZ-SUC) nano-cocrystals were investigated as model formulation, as it has been successfully prepared, characterized and confirmed higher supersaturation but fast precipitation in the previous chapter. Therefore, a systematic investigation on the precipitation inhibition capacity of commonly used precipitation inhibitors in nano-cocrystal formulations was conducted. This study also provided insight into the mechanism of how nano-cocrystals obtain maximum supersaturation solubility in the presence and absence of precipitation inhibitors during dissolution as a function of addition rate and dose of nano-cocrystals. The key factors which influenced the supersaturation generation/maintenance of nano-cocrystal formulations were determined. The understanding of the mechanism was expected to

support subsequent formulation development processes of nano-cocrystal oral dosage forms to create prolonged supersaturation of poorly water-soluble drugs.

3.3.2. Solubility of itraconazole and ITZ-SUC cocrystals

The solubility of ITZ, ITZ-SUC cocrystals and its physical mixture was determined in different dissolution media at 37 °C (Table 3.10). The solubility of ITZ (4.9 ± 0.5 µg/mL) in 0.1 N HCl was similar to the solubility of the physical mixture of ITZ and succinic acid (5.0 ± 0.3 µg/mL), however, the solubility of ITZ-SUC cocrystals was about ten times higher (50.6 ± 5.0 µg/mL). As a supersaturated drug delivery system, cocrystal formulation was able to improve the solubility of a poorly water-soluble drug. To examine the solubilizing power of different polymers, either ITZ or ITZ-SUC cocrystal solubility in 0.1N HCl with 0.1 mg/mL of each polymer was similar to the ones determined without polymer. Therefore, all polymers have no impact on the solubilities of ITZ, ITZ-SUC cocrystals and its physical mixture.

Table 3.10. Solubility of ITZ, ITZ SUC physical mixture (PM) and ITZ-SUC cocrystals in 0.1N HCl with different dissolved polymer (0.1 mg/mL) (mean ± SD; n = 3).

Media	Solubility (µg/mL)		
	ITZ	ITZ SUC PM	ITZ-SUC
0.1 N HCl	4.9 ± 0.5	5.0 ± 0.3	50.6 ± 5.0
HPMC E5	5.1 ± 0.3	5.1 ± 0.5	53.4 ± 3.4
HPMC E50	4.8 ± 0.7	5.2 ± 0.1	51.7 ± 2.2
HPMCAS	5.0 ± 0.1	4.6 ± 0.2	48.6 ± 6.3
HPC	5.5 ± 0.2	4.9 ± 0.6	45.5 ± 4.9
PVPK30	5.4 ± 0.5	5.1 ± 0.2	47.4 ± 4.7
PVPVA64	5.2 ± 0.6	4.8 ± 0.5	43.1 ± 8.1

3.3.3. Precipitation inhibitor screening

3.3.3.1. Solvent shift method

The selection of a suitable precipitation inhibitor was conducted by generating supersaturation with the solvent shift method (Bevernage et al., 2013). Except for HPMCAS, no significant difference was observed for different polymer solutions acting as precipitation inhibitors (Fig. 3.24). Unlike other polymers that are completely dissolved at of 0.1 mg/mL, HPMCAS is insoluble in acid solution; thus, the actual HPMCAS concentration was significantly lower than 0.1 mg/mL and small polymer particles were observed in the

medium. Therefore, the data in the HPMCAS group might be explained as small amount of dissolved ITZ absorbed on those HPMCAS particles during filtration, also indicated in a higher standard deviation (Wang et al., 2018). The solvent shift method in 0.1 N HCl was not discriminatory for the different PPIs, which was in agreement with other studies. Speybroeck et al. reported that the capability of HPMC to inhibit precipitation of itraconazole could not be discriminated in simulated gastric fluid (Van Speybroeck et al., 2010). Since the drug was dissolved in the stock solution with the solvent shift method, a conclusion to the actual performance during powder dissolution is limited (Qiao et al., 2013).
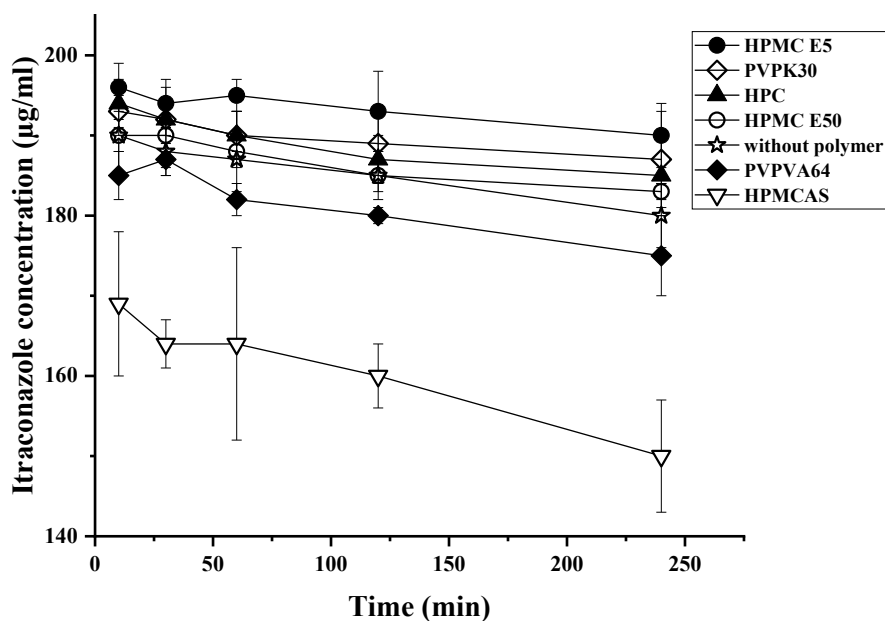
Fig. 3.24. Effect of inhibition of different polymers (0.1 mg/mL) on precipitation of a supersaturated solution of itraconazole (200 µg/mL) in 500 mL 0.1N HCl: (●) HPMC E5, (○) HPMC E50, (▽) HPMCAS, (▲) HPC, (◇) PVPK30, (◆) PVPVA64, (☆) without any polymer.

3.3.3.2. In situ *powder dissolution method*

Conventional non *in situ* methods do not present sufficient kinetic solubility values in time and result in incorrect values (Qiao et al., 2013). In order to obtain a more realistic value for the kinetic solubility of the supersaturated formulations, *in situ* kinetic solubility analyses was performed. Direct *in situ* powder dissolution under non-sink condition with dissolved precipitation inhibitor was applied for kinetic solubility studies, as this was closer to *in vivo* conditions (Colombo et al., 2018). In supersaturated drug delivery system, the precipitation and dissolution occurred simultaneously (Alonzo et al., 2010). The maximum supersaturated concentration and precipitation inhibition capacity were evaluated to

compare the influence of different types of polymers on the dissolution behaviour of nano-cocrystal formulations. In the absence of polymer, dissolution of ITZ-SUC nano-cocrystal powder (z-ave = 455 ± 9 nm, PDI = 0.24 ± 0.01), corresponding to 15 mg of ITZ, gave a maximum drug concentration of 250.5 µg/mL at 5 min. However, precipitation occurred immediately and rapidly after reaching the maximum (precipitation rate = 51.1 µg/mL/min). This performance is considered as "spring and fall off the cliff" and is commonly seen with supersaturated drug delivery system (Warren et al., 2010). Polymers could inhibit precipitation to varying degrees. The precipitation inhibition capacity, ranked from highest to lowest, was HPMC E5 > HPMC E50 > HPC > HPMCAS > PVPVA64 > PVPK30 (Fig. 3.25). Further comparison demonstrated that HPMC E5 and E50 maintained supersaturation with no precipitation even over 60 min, HPC and HPMCAS maintained supersaturation for around 15 min with slow precipitation rate of 0.9 and 1.0 µg/mL/min respectively. PVP and PVPVA64 prolonged supersaturation for 8 min and exhibited the weakest precipitation inhibition capacity with precipitation rate of 21.6 and 15.6 µg/mL/min. The dissolution process of supersaturated drug formulation was a balance between dissolution rate and precipitation rate (Plum et al., 2020). Therefore, if the polymer was not a suitable precipitation inhibitor to decrease the precipitation rate or overcome the crystallization and nucleation process, it was reasonable to conclude that also a lower maximum drug concentration was obtained as seen for HPMC E5 compared to HPC.
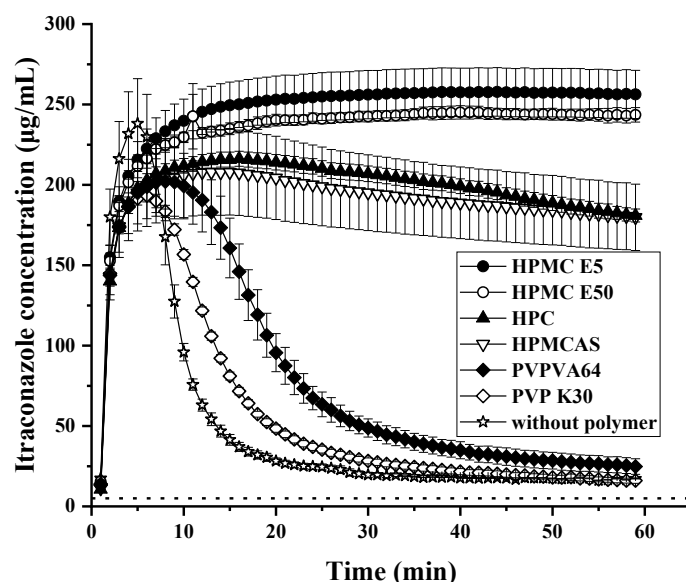

Fig. 3.25. Dissolution profiles of 15 mg ITZ-SUC nano-cocrystal powder in different polymer solutions (0.1 mg/mL) 50 mL 0.1N HCl: (●) HPMC E5, (○) HPMC E50, (▽) HPMCAS, (▲) HPC, (◇) PVPK30, (◆) PVPVA64, (☆) without polymer (dashed line indicates the thermodynamic solubility of ITZ).

Polymers can inhibit recrystallization of drug from a supersaturated solution by three mechanisms. The dissolved polymer can be adsorbed on the surface of the drug crystal by specific interactions, hence changing the microenvironment of the crystal-solution interface and reducing drug diffusion to the crystal surface. Adsorbed polymers can also interfere with adsorption and migration of drug molecules at the crystal surface, preventing drug molecules from entering the crystal lattice at the correct position, thus preventing crystal growth. Many studies have demonstrated that hydrophobicity and hydrogen bonding were common interactions between polymers and drugs and played an important role in inhibiting drug recrystallization (Baghel et al., 2016; Ilevbare et al., 2013). Schram et al. established a positive correlation between adsorption coverage and polymer precipitation inhibition using atomic force microscope (Schram et al., 2015). Second, in a supersaturated solution, degree of supersaturation of the drug is the fundamental driving force for crystallization (Gao and Shi, 2012; Palmelund et al., 2016; Taylor and Zhang, 2016). Therefore, the second mechanism is to increase the solubility of the crystalline drug through stabilizers or polymers to nominally reduce the degree of supersaturation. The third reason might be the higher viscosity in the presence of polymers, reducing diffusion and thereby inhibiting crystallization (Shi et al., 2019). This effect was negligible at the low polymer concentrations used in this study. Experiments above have proved that the investigated polymers did not affect the solubility of ITZ. Therefore, the different precipitation inhibition capacity could best be explained by the interactions of the polymers with itraconazole. HPMC E5, E50, HPC and HPMCAS all provide the same backbone structure of alkyl hydroalkyl cellulose. The faster precipitation rate with PVP and PVPVA confirmed that compared to the molecular structure of alkyl hydroalkyl cellulose, the molecular structure of PVP or PVPVA cannot form a stable intermolecular interaction with supersaturated itraconazole. Other studies also reported that the stabilizing effect of HPMC on supersaturated itraconazole solutions could be attributed to intermolecular interaction (Miller et al. 2007; Miller et al., 2008).

Polymers with an alkyl hydroalkyl cellulose structure resulted in smaller contact angles and thus better affinity to itraconazole than PVP (Table 3.11). The contact angle was a direct indicator of drug/polymer affinity, and it correlated well with drug supersaturation and crystallization inhibition during dissolution.

Table 3.11. Contact angles of 0.1 mg/mL polymer in 0.1N HCl solution on itraconazole compacts (mean SD; n=5).

Solution	Contact angle (°)
0.1 N HCl	70.5 ± 1.5
HPMC E5	53.3 ± 0.9
HPMC E50	57.4 ± 0.8
HPC	55.6 ± 1.1
HPMCAS*	-
PVPK30	64.7 ± 0.4
PVPVA64	61.0 ± 1.0

* HPMCAS was undissolved in 0.1N HCl solution

Recently, there is increasing evidence that a second phase transition, known as liquid−liquid phase separation (LLPS), can occur in highly supersaturated solutions of some compounds prior to crystallization (Ilevbare and Taylor, 2013). LLPS occurs when the concentration of the drug in the aqueous solution exceeds the boundary concentration at which the drug is no longer miscible with water. Those excess drug precipitates formed a dispersed, colloidal amorphous drug-rich phase. LLPS can occur if the dissolution rate of the formulation is exceeding the APIs amorphous solubility. This also explained why nano-cocrystals without any polymer could still reach a high supersaturated C_{max}. Through LLPS theory, suitable concentration of HPMC could maintain the stability of itraconazole-rich colloids as an excellent high-energy drug reservoir to supplement and maintain high-free drug concentration to prolong drug supersaturation. To evaluate the relationship between polymer concentration and precipitation inhibition capacity, three concentrations of HPMC E5 were investigated (Fig. 3.26). HPMC E5 concentrations of 0.1 and 0.025 mg/mL maintained the itraconazole supersaturation until 60 min, while at the lower concentration of 0.01 mg/mL, supersaturation was maintained only for 15 min. The precipitation inhibition capacity of a polymer was proportional to its concentration. This needs to be taken into consideration during the development of the nano-cocrystals into final solid dosage forms. After oral administration, gastrointestinal fluids could dilute the concentration of polymer to potentially cause failure of supersaturation-based delivery system by uncontrollable precipitation limiting absorption (Li and Taylor, 2018).
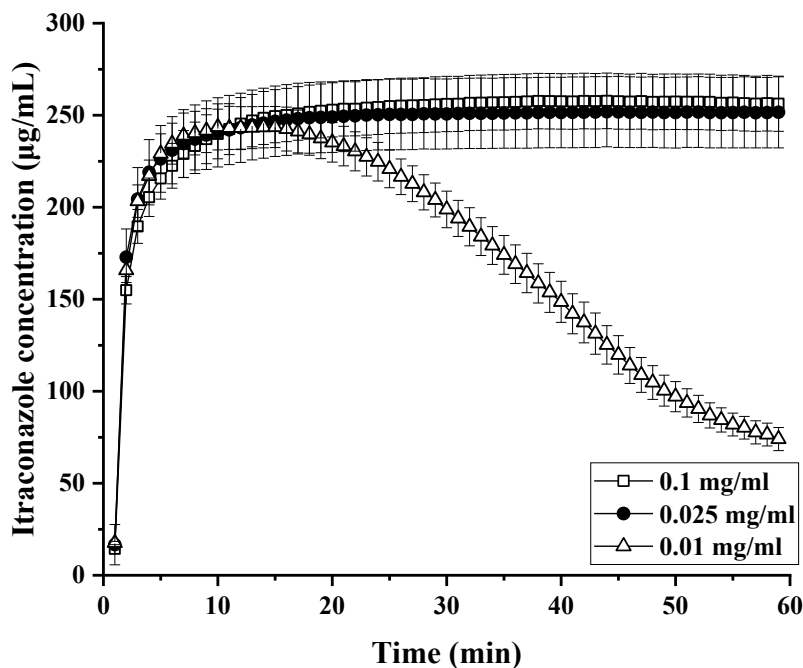
Fig. 3.26. Effect of HPMC E5 concentration on dissolution profiles of 15 mg ITZ-SUC nano-cocrystal powder in 50 mL 0.1N HCl: (□) 0.1mg/mL, (●) 0.025 mg/mL, (△) 0.01 mg/mL.

3.3.4. Effect of HPMC E5 on nano-cocrystals dissolution

The combined effect of precipitation inhibitors and the rate of supersaturation generation with a fixed dose was studied. Kinetic solubility profiles of ITZ-SUC nano-cocrystal powder (corresponding to 20 mg of ITZ) were generated by adding the powder into the dissolution medium at different time intervals. Without HPMC, a faster rate of drug addition (or rate of supersaturation generation) resulted in a higher maximum kinetic solubility, a shorter time to reach maximum solubility and a faster rate of precipitation (Fig. 3.27a). At the lowest addition rate of 1 mg/min, the drug concentration dropped after 13 min to 55 µg/mL and increased again after 17 min upon further drug addition. Again, the supersaturation of nano-cocrystals depended on the competition of dissolution and precipitation processes. As supersaturated solutions were in a thermodynamically unstable state, and precipitation was kinetically driven by a time-dependent process, a higher drug concentration could be achieved by a rapid supersaturation generation rate. Exceeding a certain supersaturation level resulted in faster precipitation, while dropping below a certain threshold reduced the higher degree of supersaturation and increased the risk of premature precipitation due to longer drug addition intervals. HPMC effectively retarded precipitation in supersaturated ITZ solution, as expressed in higher maximum drug concentrations and longer supersaturation times at the same addition rate (Fig. 3.27b). Nano-cocrystal also exhibited

possibility to be further applied to controlled-release formulations as seen for 1 mg/min group with HPMC E5. The continuous addition of drugs for 20 minutes is similar to the slow release of drugs during the controlled release process.
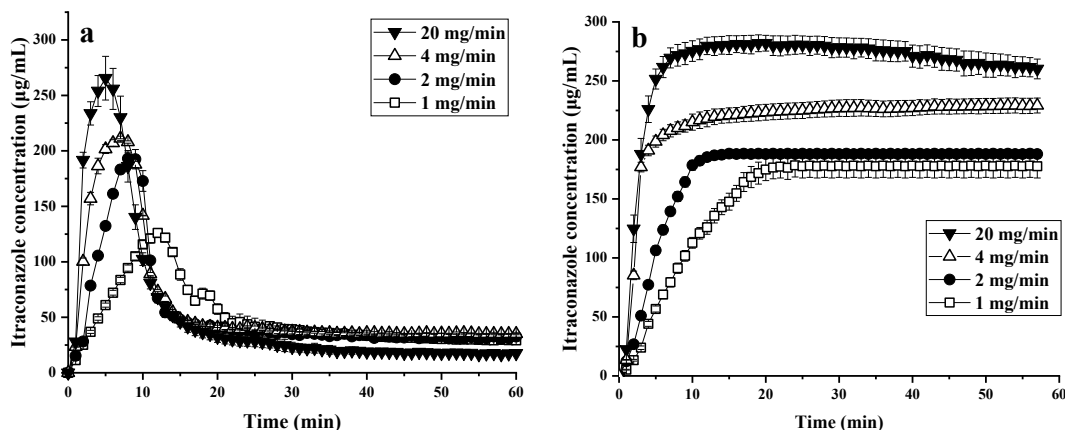
Fig. 3.27. Kinetic solubility profiles of ITZ-SUC nano-cocrystal powder (20 mg) added into 50 mL 0.1N HCl at different rates (a) no HPMC E5, (b) 0.1 mg/mL HPMC E5.

An increase in dose was a straightforward option to further increase the dissolution rate of nanosized formulations in supersaturated drug delivery system; it resulted in an increased absolute amount of nanoparticles with smaller particle size and faster dissolution rate. To evaluate the effect of the precipitation inhibitor on the extent of maximum supersaturation as a function of dose, various doses were added into the dissolution medium with and without HPMC E5. Without HPMC E5 and consistent with previous studies, the higher maximum supersaturation level at the higher dose led to a faster precipitation rate (Fig. 3.28a). Except for the highest dose of 30 mg, the high supersaturation solubility was maintained for prolonged time periods in the presence of HPMC due to its effective precipitation inhibition capacity (Fig. 3.28b). With the 30 mg dose, probably the large number of undissolved particles acted as recrystallization seeds.

Fig. 3.28. Dissolution of ITZ-SUC nano-cocrystals as a function of drug amount (dose) (a) no HPMC E5, (b) 0.1 mg/mL HPMC E5.

With and without HPMC, the maximum drug concentration increased with increasing drug amount from 10 mg to 20 mg and then reached a plateau at 30 mg (Fig. 3.29a). The area under the curve (AUC) of the concentration-time profile was also calculated to quantitatively evaluate the dissolution results. Without HPMC, AUC values increased with decreasing drug amount (Fig. 3.29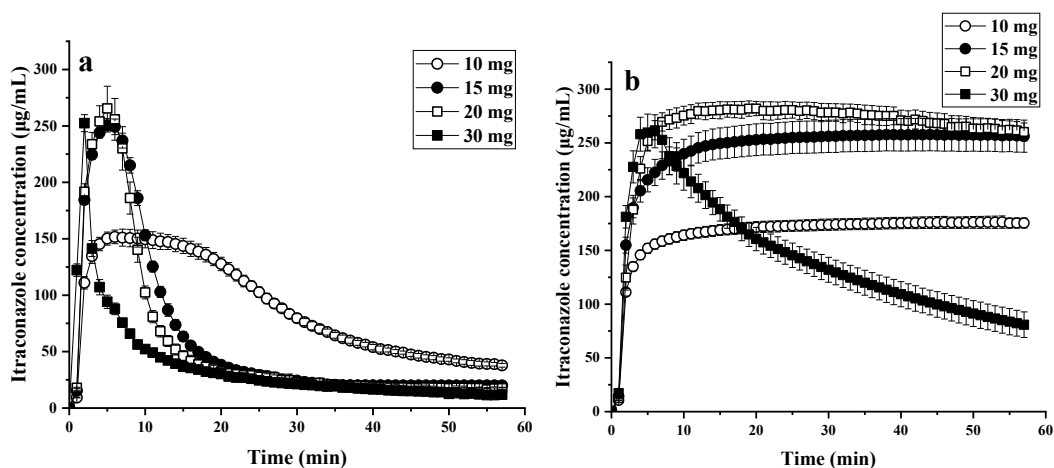b). Rapid precipitation rate led to a decrease in AUC, which explains why higher doses exhibited higher solubility but smaller AUC. With HPMC, AUC values ranked as follows: 20 mg > 15 mg > 10 mg > 30 mg (Fig. 3.29b). A higher AUC of the *in vitro* kinetic solubility profile did therefore not necessarily translate into a higher kinetic solubility. As mentioned before, the dissolution of nano-cocrystals depended on the balance between the dissolution and precipitation rates. Effective precipitation inhibitors adsorbed on crystal surfaces by intermolecular interaction to prevent precipitation. The polymer maintained supersaturation for prolonged time periods, as reflected by broadened AUC profiles. However, at a fixed polymer concentration, increasing the dose to 30 mg led to significant precipitation already after 3-4 min with the smallest AUC (Fig. 3.29b). By increasing polymer concentration in 30 mg dose group might be possible to maintain the supersaturated concentration for a longer time and broaden AUC. Thus, a rapid dissolution of supersaturated formulations did not always translate into optimal *in vivo* performance. Fast release not only provided higher kinetic solubility but also higher risk of rapid precipitation. Several studies have reported similar findings. Six et al. compared itraconazole ASD prepared with Eudragit E100, Eudragit E100/PVPVA64 and HPMC (Six et al., 2005). The results demonstrated ITZ/HPMC ASD which has a slower release rate actually produces enhanced oral bioavailability.
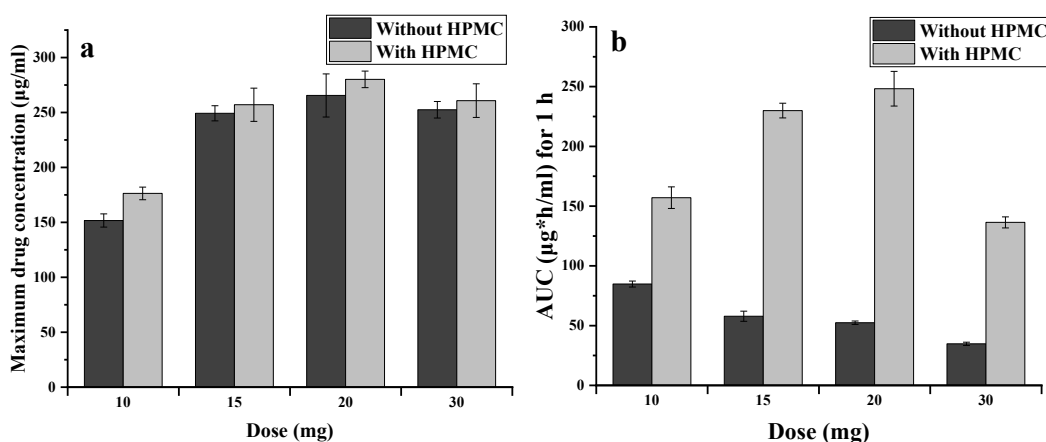
Fig. 3.29. Effect of various drug amounts on (a) maximum kinetic solubility and (b) area under the curve (AUC) of the kinetic solubility profile with and without HPMC E5 (0.1 mg/ml).

Nano-cocrystals exhibited faster dissolution rates compared to micronized cocrystals. This could offset the precipitation in the absence of precipitation inhibitors, thus explaining why nano-cocrystals achieved higher supersaturated solubility (internal data). The maximum supersaturated solubility of micronized cocrystals was considered to reach the similar level of nano-cocrystals since precipitation was inhibited by effective precipitation inhibitor. ITZ-SUC nano-cocrystal powder of 0.45 µm and micronized cocrystal powder of 5 µm average particle size (corresponding to 20 mg of ITZ) were added into the dissolution medium with HPMC E5. Nano-cocrystals exhibited higher dissolution rate and supersaturation solubility than micronized cocrystals (Fig. 3.30a). The only factor that affected the achievable maximum drug concentrations was the dissolution rate which was mainly controlled by the particle size. Total amount of 20 mg was equally divided into five doses and added when the concentration of each section reached a plateau. By adding micronized cocrystal powder, the increase in supersaturated concentration gradually decreased (Fig. 3.30b). Maximum supersaturation was reached at 135 µg/mL, where additional cocrystals could not increase the kinetic solubility further. Supersaturation could however be further increased by changing from micro- to nano cocrystals, which reached a higher plateau in a shorter time than the micronized cocrystals after each dose addition. Based on Noyes Whitney equation, the difference between the concentration of the particle surface and the bulk concentration determines the rate of solubility build up. This applies to the generation of supersaturated solubility which is a diffusion-controlled process. Therefore, in combination with previous findings, faster dissolution rate and the use of precipitation inhibitors were two key factors that determined whether higher supersaturated

concentration could be achieved and maintained for a longer period of time. Thus, in the further formulation development process of nano-cocrystal drug delivery system, it is necessary to ensure fast disintegration and release of the nano-cocrystal powder and suitable precipitation inhibitors from the final oral dosage forms.
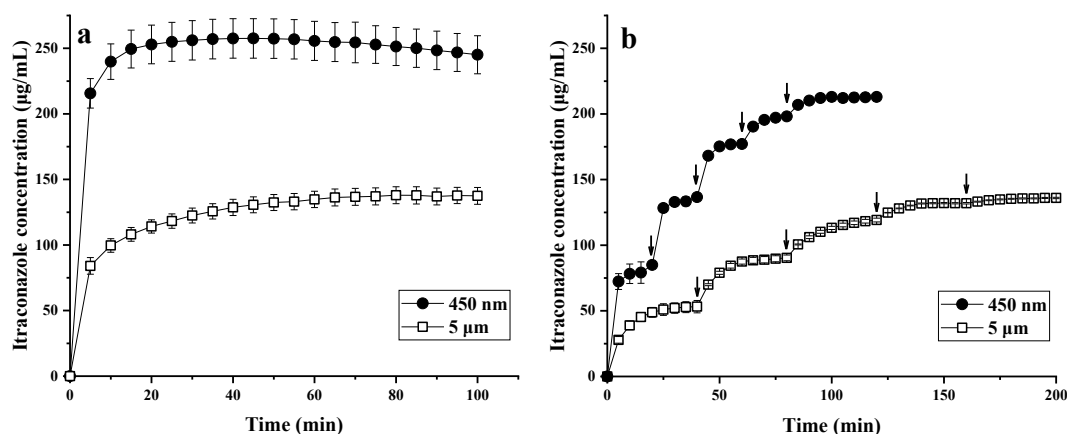
Fig. 3.30. Supersaturation generation profiles of ITZ-SUC micronized cocrystals (5 µm) and nano-cocrystals (0.45 µm) in 0.1N HCl with 0.1 mg/mL HPMC E5 at (a) one dose 20 mg, (b) incremental doses addition to 20 mg (arrows indicate time of dose induction).

As mentioned above, with HPMC, higher dose still resulted in faster precipitation rate and shorter induction time. The effect of precipitation from undissolved particles was investigated by varying the dose of different sized particles to manipulate the excess surface area of undissolved particles. 20 mg of ITZ-SUC nano-cocrystal powder were added into 0.1 mg/mL HPMC E5 0.1N HCl dissolution medium. Two groups of particles with different minimum size (0.45 µm vs. 5 µm) were added at 15 min until maximum drug concentration was stable (275 µg/mL). The total surface area of excess particles is inversely proportional to the particle size. 5 mg of 0.45 µm instantly induced concentration drop at infusion and further dropped to 180 µg/mL after 60 min. 10 mg of 0.45 µm even induced steeper concentration drop to 25 µg/mL after 60 min. While 50 mg of 5 µm maintained for 60 min without any concentration drop (Fig. 3.31). Theoretically, 5 mg of 0.45 µm and 50 mg of 5 µm gave approximately the same total excess surface area. Therefore, the main factor that induced precipitation might depend on the specific surface area of the excess particles rather than the total area of the excess particles. Que et al. demonstrated that critical nucleus size, seed origin, morphology, and interface properties as well as the extent of supersaturation generated during dissolution impacted precipitation from a supersaturated solution (Que et al., 2018). During the dissolution study of nano-

cocrystal formulation, faster dissolution rates were achieved by smaller particles with larger specific surface area, resulting in increased supersaturated solubility. While too much excess smaller particles led to higher risk of precipitation. Therefore, in the subsequent formulation development process, the relationship between particle size and dose of the nano-cocrystals and the achievable degree of supersaturation should be considered comprehensively.
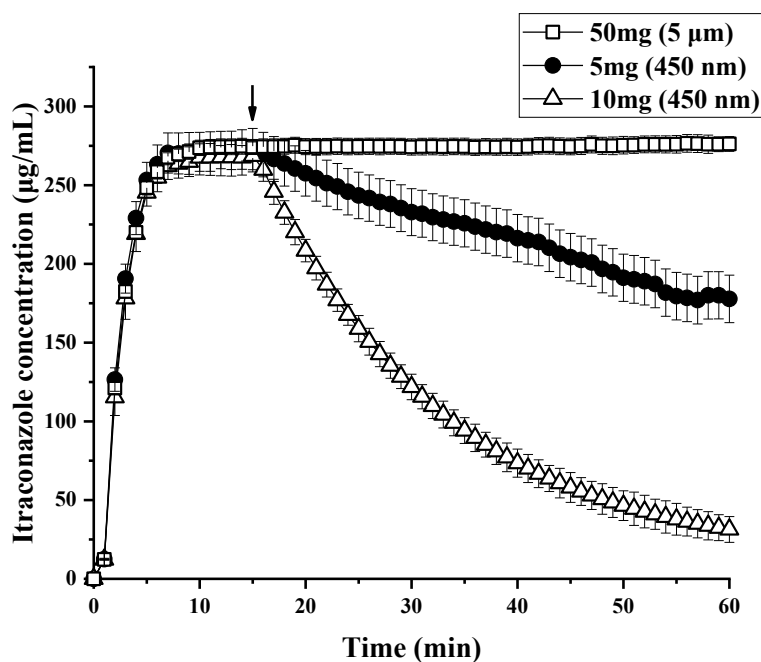
Fig. 3.31. Precipitation profiles induced by different seed crystal suspension. Degree of supersaturation 50 was maintained from dissolution of 20 mg ITZ-SUC nano-cocrystal powder in 0.1N HCl with 0.1 mg/mL HPMC E5. Arrows indicate the time at which the seed crystal suspension is induced.

3.3.5.   Conclusions

In the present study, for the first time, a systematic experimental investigation was conducted to explore the precipitation inhibition capacity of a range of commonly used PPIs in itraconazole-succinic acid nano-cocrystal formulation. The study provided an improved mechanistic understanding of nano-cocrystals performance during powder dissolution. HPMC E5 achieved greatest extended nano-cocrystals dissolution and maintenance of supersaturation based on specific drug/polymer intermolecular interaction. Dissolved polymer not only increased maximum achievable supersaturation, but also maintained supersaturation for prolonged times, resulting in significantly broadened AUC maxima. To achieve higher and sustained supersaturation from nano-cocrystal formulation during

dissolution, faster dissolution rate and proper application of precipitation inhibitors were two driving factors. The relationship between particle size, dose and polymer ratio and their synergic impact on the supersaturation must be considered. Generally, these insights and findings would contribute to the design of optimally performing oral solid dosage formulations with incorporated nano-cocrystals.

3.4. Incorporation of itraconazole nano-cocrystal into granulated or bead-layered solid dosage forms

3.4.1. Introduction

In recent years, more than 40% of drugs in the development pipelines have low aqueous solubility (Lipinski, 2002). For oral dosage forms, drug absorption is highly dependent on the free drug dissolved in the gastrointestinal medium, poorly soluble drugs resulting in low oral bioavailability and high fed-to-fasted absorption variation (Shegokar and Müller, 2010). Formulation strategies such as solid dispersion, cyclodextrin complexes, liposomes, co-solvents, and self-emulsifying systems are commonly used to improve the solubility of drugs (Allen and Cullis, 2013; Chiou and Riegelman, 1971; Pouton, 1997; Stella et al., 1999). Although these formulation strategies have achieved particular success, in some cases, due to the drugs' different physical and chemical properties, these traditional formulation methods still have some limitations like low drug loading and insufficient drug dissolution (Hanafy et al., 2007).

Nano-cocrystal formulations, which integrated nanocrystal technique into cocrystal formulations, were proposed as a novel approach to increase solubility, dissolution rate, and oral bioavailability (Tan et al., 2021). Nano-cocrystal could potentially overcome the limitation of nanocrystal and cocrystal; thus, leading to higher supersaturation solubility compared to single nanocrystal or cocrystal formulation. Recently, only a few nano-cocrystal publications or patents had been reported, referred to itraconazole-adipic acid, indomethacin-saccharin, carbamazepine-saccharin, phenazopyridine-phthalimide, and myricetin-nicotinamide nano-cocrystal formulations (De Smet et al., 2014; Huang et al., 2017; Karashima et al., 2016; Liu et al., 2016). In the previous chapter, itraconazole-succinic acid, itraconazole-fumaric acid, indomethacin-saccharin, and indomethacin-nicotinamide nano-cocrystal formulations have been successfully prepared and characterized. In order to achieve higher and prolonged supersaturation from nano-cocrystal formulation, a faster dissolution rate and suitable application of precipitation inhibitors are required. Nano-cocrystal was prepared by wet milling of prepared cocrystals, resulting in nanosized drug particles suspended in the aqueous medium. However, the nano-cocrystal suspension was highly thermodynamically unstable in cocrystal structure and particle size for long-term stability. Moreover, the suspension form processes microbial instability during storage and has less patient compliance in clinical application. Therefore, it is necessary to convert suspensions into solid dosage forms.

During the drying process, the aggregation of the drug nanoparticles would profoundly impact the properties of the final products. Thus, a suitable drying process should prevent irreversible particle aggregation and result in performance comparable to suspension form. Spray-drying or freeze-drying are the most commonly used two approaches to convert a nanosuspension into dried powder form (Kumar et al., 2014; Ma et al., 2020; Van Eerdenbrugh et al., 2008). However, both of the techniques have their limitations. The freeze-drying process has a longer drying cycle, thus is time and energy-consuming, while spray drying may cause low sample yield and decreased drug loading due to the addition of a large amount of dispersants (Arzi and Sosnik, 2018; Walters et al., 2014). Furthermore, the spray or freeze-dried powder should be blended with other excipients and further processed into solid dosage forms like tablets or capsules. Downstream processing of nanosized powders prepared from spray or freeze drying would be more complicated due to their low density, poor flowability, and high hygroscopicity. It may also lead to safety issues, such as more dust or powder leakage during the production pipeline (Tahara, 2020; Tuomela et al., 2015). Therefore, alternative methods with low production cost, simple downstream steps, and excellent product properties should be explored.

Spray granulation and bead layering processes are considered the new alternative methods for converting nanosuspension into solid dosage forms. The main concept is combining commonly utilized spray drying techniques with granulation process, thus is more straightforward, time and energy-saving (Kayaert et al., 2011). Nanosuspensions were directly used as granulation liquid with or without binder polymers to form granules with sugar or microcrystalline cellulose (MCC) as excipient carrier in the spray granulation process. In a fluidized bed coating process, nanosuspensions were used as layering dispersion along with binder polymers to form film coating onto sugar and MCC beads (Basa et al., 2008). The obtained granules or beads can be easily filled into capsules or compressed into tablets due to their excellent flowability and suitable density. Bose et al. demonstrated the feasibility of using spray granulation as a processing method to convert a nanosuspension into a solid dosage form with improved *in vivo* exposure compared to the coarse suspension formulation (Bose et al., 2012). Parmentier et al. observed that bead layering was a suitable method to process an itraconazole nanosuspension into a solid form without compromising release (Parmentier et al., 2017). Azad et al. prepared immediate release sugar beads by drug layering as a function of carrier particle size. The small carrier particles exhibited faster dissolution and redispersion than large carriers due to the large surface area and thinner coating layer (Azad et al., 2015). Meruva et al.

prepared solid dosage forms of irbesartan nanosuspension by bead layering or spray granulation and further processed into mini-tablets while retaining rapid release characteristics (Meruva et al., 2019). However, very few reports compared conventional wet granulation, spray granulation, and bead layering as the downstream process of nanosuspension; and the impact of different types of substrates (water-soluble or insoluble) has not been well investigated. In addition, none of the published reports investigated the possibility of converting nano-cocrystal suspension into solid dosage forms.

In this work, itraconazole-succinic acid (ITZ-SUC) nano-cocrystal was used as model formulation. HPMC E5, a low viscosity cellulose polymer, was employed as a binder and precipitation inhibitor. The optimized nano-cocrystal/HPMC suspension was dried via wet granulation, spray granulation, and bead layering. The dried samples were used to assess the influence of different drying processes, types of substrates, and drug loading on drug dissolution under non-sink conditions. Further, the optimized dried dosage forms were stored at 40 °C/75% relative humidity (RH) in blistered and non-blistered conditions for three months and evaluated for *in vitro* dissolution performance.

3.4.2. Comparison of ITZ and ITZ-SUC nanosuspension

The granulation or layering dispersion for the downstream process was prepared by adding HPMC E5 (2% w/v) to the nanosuspension. In order to identify the impact of adding polymer, Table 3.12 compared the particle size and distribution of nanosuspensions with or without HPMC E5. ITZ or ITZ-SUC nanosuspension had an acceptable size distribution with a mean particle size of 211 nm or 365 nm. After adding HPMC E5, there were negligible differences regarding particle size and distribution compared to original suspension, indicating that adding HPMC E5 into nanosuspension did not influence particle size.

Table 3.12. Particle size of prepared nanosuspensions and granulation/layering dispersion containing HPMC E5.

Formulation	Z-average (nm)	PDI
ITZ NS	211 ± 5	0.22 ± 0.01
ITZ NS/HPMC	225 ± 3	0.21 ± 0.01
ITZ-SUC NS	365 ± 9	0.25 ± 0.01
ITZ-SUC NS/HPMC	345 ± 8	0.26 ± 0.02

The dissolution of ITZ nanosuspension and ITZ-SUC nano-cocrystal suspension were determined under non-sink conditions (Fig. 3.32). Although ITZ nanosuspension had a

superior dissolution rate, the achieved maximum solubility in 0.1N HCl was only about 5-6 µg/mL whereas the equilibrium solubility of ITZ in 0.1N HCl is 6 µg/mL (Brewster et al., 2008). After the subsequent addition of HPMC E5, the dissolution rate and maximum solubility were unchanged, indicating HPMC E5 could not improve the solubility of ITZ. Compared with ITZ nanocrystals, ITZ-SUC nano-cocrystal had the same superior dissolution rate under the same conditions but reached a maximum solubility of 250 µg/mL (50 times higher than equilibrium solubility of ITZ). However, as a supersaturated system, the increased solubility was thermodynamically unstable and precipitation happened simultaneously. By adding HPMC E5, the precipitation rate was significantly inhibited, and the supersaturated solubility was maintained for more than 1 h. HPMC could act as a binder in preparing nano-cocrystal solid formulations and plays a substantial role in precipitation inhibition during the dissolution process.
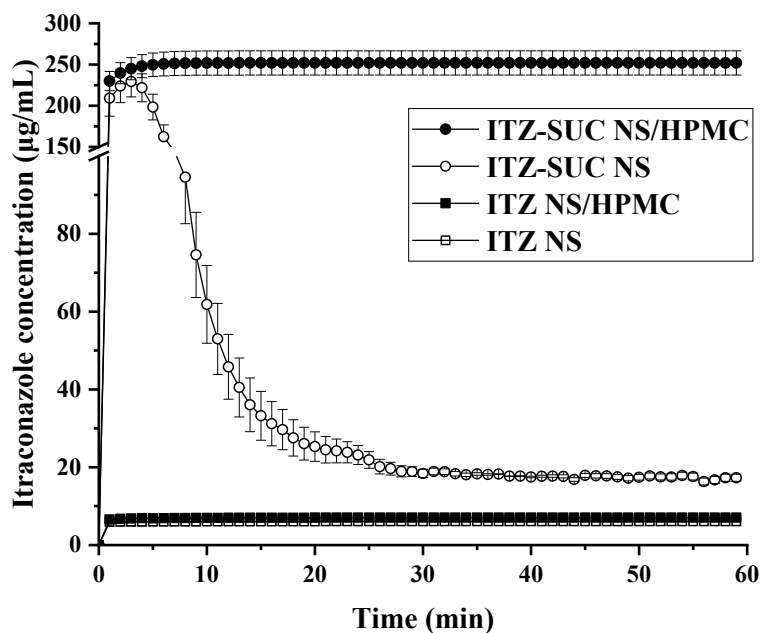
Fig. 3.32. Dissolution profiles of ITZ, ITZ-SUC nanosuspensions and their granulation/layering dispersion with HPMC.

3.4.3. Wet granulation

3.4.3.1. Characterization of granules

Microscopy images of granules with incorporated ITZ-SUC nano-cocrystals processed by conventional wet granulation and of the disintegration of granules while contacting water were taken. Although wet granulation of ITZ-SUC nano-cocrystal yielded spherical-like granules with both MCC and lactose (Fig. 3.33a, d), granules consisting of different

substrates exhibited significantly different disintegration characteristics after contact with water. In the case of the water-insoluble substrate, WG-MCC granules swelled slightly after being in contact with water for 1 minute, and the particles did not disintegrate after 5 minutes with no observation of any released nanoparticles (Fig. 3.33b, c). A small amount of water may not be enough to form a high osmotic pressure to disintegrate the granules (Berggren and Alderborn, 2001). During the wet granulation process, water converts part of the MCC from crystalline into a gel structure where nanoparticles were embedded in the matrix. The subsequent drying process causes the MCC solid matrix to be more stable and difficult to disintegrate after contact with water (Kleinebudde, 1997). While granules-based on water-soluble excipient, lactose, disintegrated after contact with water, and water has completely penetrated the WG-Lac granules after 5 minutes (Fig. 3.33e, f). A closer view of the corresponding WG-Lac granules surfaces revealed drug nanoparticles redispersed into water.

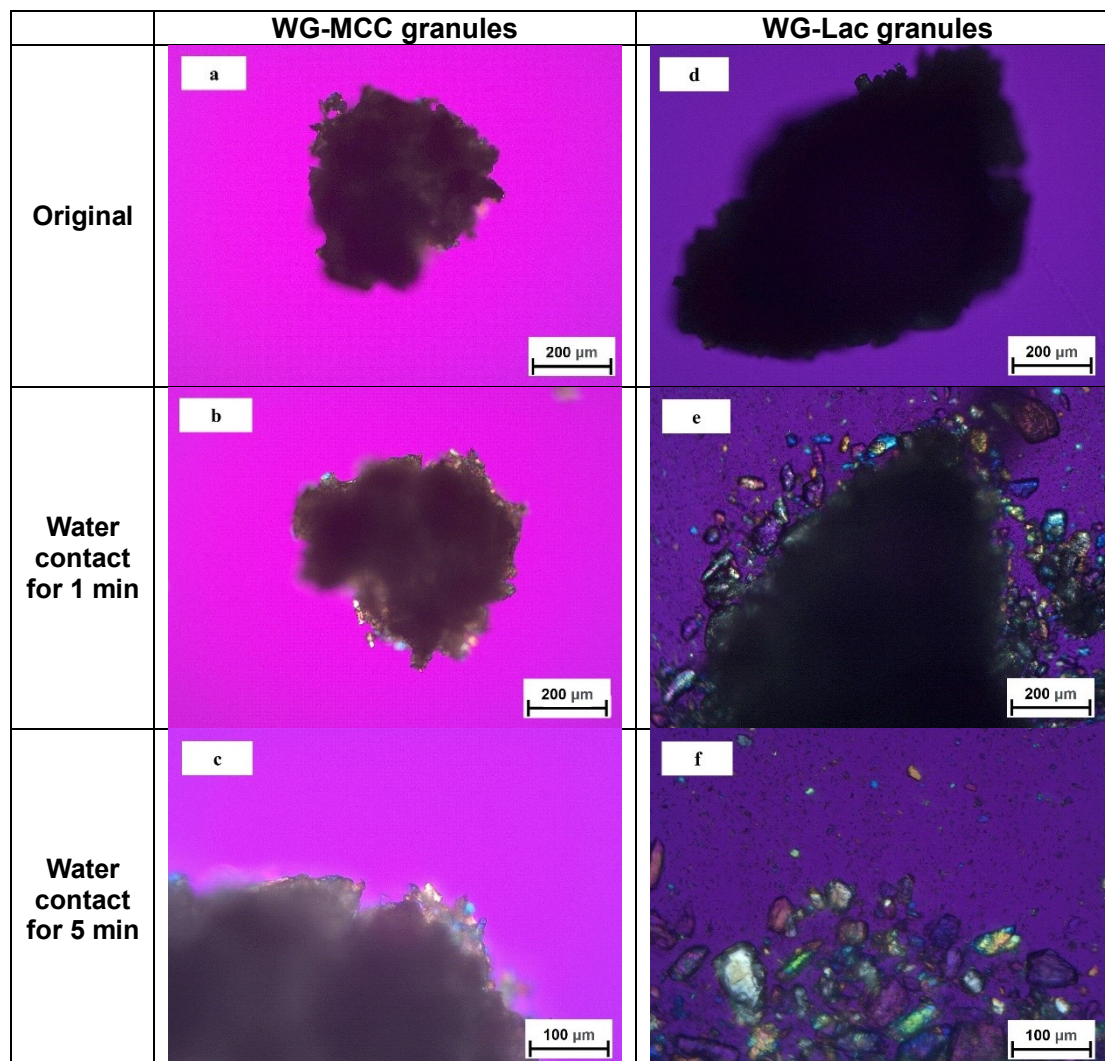|	WG-MCC granules	WG-Lac granules
Original	a 200 µm	d 200 µm
Water contact for 1 min	b 200 µm	e 200 µm
Water contact for 5 min	c 100 µm	f 100 µm

Fig. 3.33. Microscopy images of WG-MCC granules and WG-Lac granules before and after water contact.

Compared with the nano-cocrystal/HPMC dispersion, both WG-MCC and WG-Lac granules exhibited a lower dissolution rate and achievable maximum solubility (Fig. 3.34). The solid dosage forms need to be released after wetting and disintegration during the dissolution process, where the suspension was readily available for dissolution (Figueroa and Bose, 2013). After granules were redispersed and filtered, the average particle size of the nano-cocrystal released from WG-Lac granules was 800 nm; in contrast, nano-cocrystal released from WG-MCC granules cannot be measured indicated no release or a strong agglomeration. Agglomeration of nanoparticles would lead to a significant decrease in the dissolution rate. The achievable maximum solubility of nano-cocrystal was directly proportional to the dissolution rate. Compared with different substrates, WG-MCC granules exhibited a slower dissolution rate and maximum solubility of around 130 µg/mL within 60 min. In contrast, WG-Lac granules exhibited a faster dissolution rate and maximum solubility of around 190 µg/mL within 60 min. The water-soluble lactose granules have a faster dissolution rate and higher maximum solubility than the water-insoluble MCC granules. However, due to the limitation of the preparation conditions, the theoretical maximum drug loading of the WG-Lac granules was only 2 %. The assay for drug content post wet granulation was found to be between 90-95% for MCC with 10% w/w drug loading and 92-96% for lactose with 2% w/w drug loading. The loss on drying (LOD) values were <1% for all the formulations. Overall, the conventional wet granulation method was not suitable for the downstream process of nano-cocrystal into solid dosage forms.
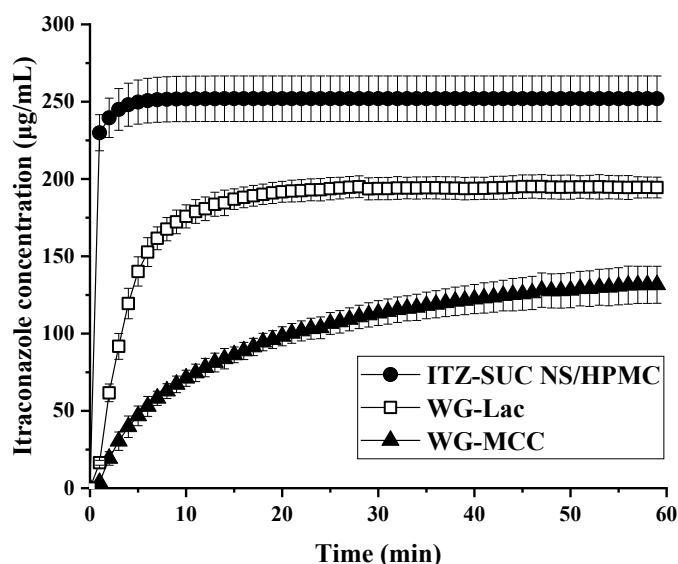

Fig. 3.34. Dissolution profiles of WG-Lac and WG-MCC granules containing ITZ-SUC nano-cocrystal. Additionally, the dissolution of ITZ-SUC NS/HPMC was used for comparison.

3.4.4. Spray granulation

3.4.4.1. Characterization of spray granulation processed granules

MCC and lactose granules incorporated with ITZ-SUC nano-cocrystal were processed by spray granulation, in which several smaller granules were bound to each other in the presence of HPMC as the binder during drying (Fig. 3.35a, d). The extent and location of ITZ-SUC nano-cocrystal released from a single granule after contact with water can be observed as a function of the different substrates. Nanoparticles released and formed a cloud around the surface of both SG-MCC or SG-Lac granules within 1 min (Fig. 3.35b). As time progressed, SG-MCC granules disintegrated into few smaller fragments (Fig. 3.35c). There was a high risk that a small part of nano-cocrystals was trapped in those fragments, impacting drug release. In contrast, most lactose dissolved and formed a hollow surrounded by nanoparticles in the case of SG-Lac granules after contacting water for 5 min (Fig. 3.35f). To retain the original nanosuspension's fast dissolution profile after drying, the formation of friable granules with fast disintegration was desirable. Most of the nanoparticles were coated instead of embedded in the substrate during the spray granulation process. Here was the first visual evidence for the positive impact of the spray granulation downstream method on the redispersiblity of the nanoparticles.

	SG-MCC granules	SG-Lac granules
Original	a	d
Water contact for 1 min	b	e
Water contact for 5 min	c	f
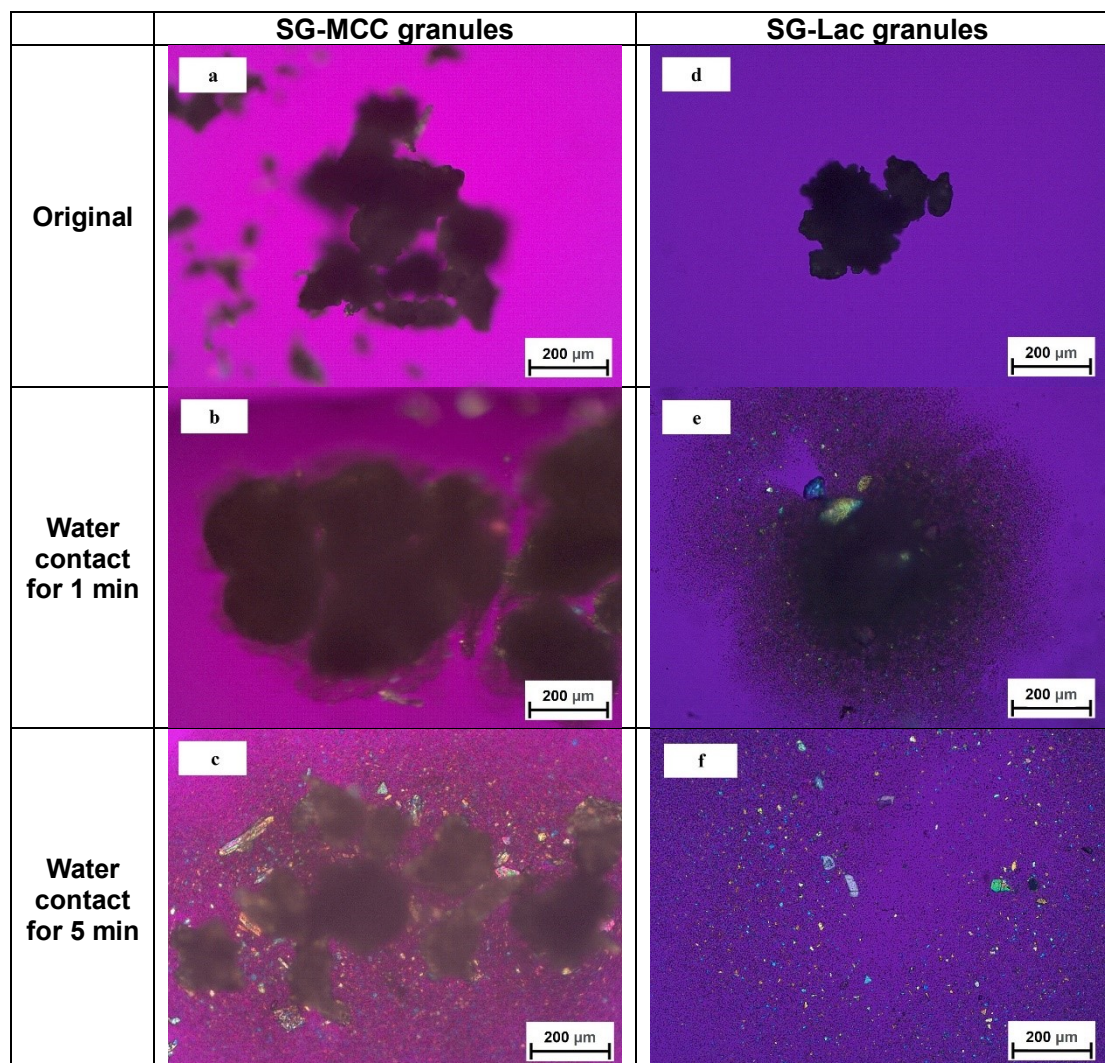
Fig. 3.35. Microscopy images of SG-MCC granules and SG-Lac granules (all 20% w/w drug loading) before and after water contact.

During the fluid bed spray granulation process, the nanosuspension was atomized at a high pressure to produce very fine droplets, which could be distributed uniformly over the powder bed and lead to minimal localized wetting. The nanosuspension droplets were instantaneously dried by the flowing hot air, reducing the availability of nanoparticles to form liquid bridges between particles. Less liquid bridges would lead to the formation of friable granules (Figueroa and Bose, 2013). Therefore, theoretical 10%-20% w/w drug loading was available for either MCC or lactose as granulating substrate with spray granulation. Hence, spray granulation was more suitable when high drug loading was required (Meruva et al., 2019; Meruva et al., 2021). Drug content post spray granulation was around 80-90% of the theoretical drug loading for both substrates. The LOD values of all the granules were < 1% at both drug loading. After granules were redispersed and

filtered, the average particle size of the nano-cocrystal released from SG-MCC and SG-Lac granules was 600 nm and 550 nm, respectively. DSC and XRPD analysis of granules with 20% drug loading compared with physical mixture also indicated no polymorphic or cocrystal structure changes post spray granulation (Fig. 3.36, 3.37).
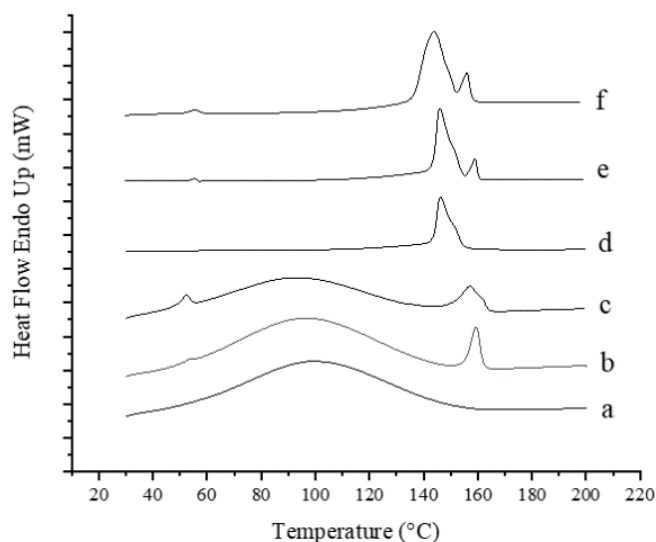
Fig. 3.36. DSC profiles for 20% w/w drug loading of (a) MCC, (b) MCC and ITZ-SUC nano-cocrystal/HPMC physical mixture, (c) SG-MCC granules, (d) lactose, (e) lactose and ITZ-SUC nano-cocrystal/HPMC physical mixture, (f) SG-Lac granules.
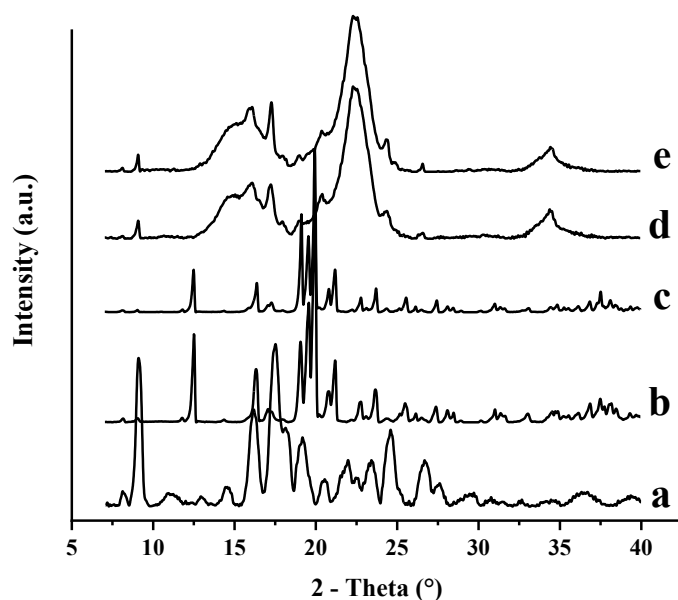

Fig. 3.37. XRPD patterns for 20% w/w drug loading of (a) ITZ-SUC nano-cocrystal/HPMC, (b) MCC and ITZ-SUC nano-cocrystal/HPMC physical mixture, (c) SG-MCC granules, (d) lactose and ITZ-SUC nano-cocrystal/HPMC physical mixture, (e) SG-Lac granules.

3.4.4.2. *Effect of granulation substrate and drug loading on dissolution performance*

The substrate utilized for the spray granulation and drug loading influenced the dissolution behavior of the dried product. Both of the granules presented a fast dissolution rate (Fig. 3.38). However, compared to ITZ-SUC nano-cocrystal/HPMC dispersion, SG-Lac granules slightly decreased achievable maximum solubility from 250 µg/mL to 230 µg/mL. In contrast, SG-MCC granules exhibited a maximum solubility of less than 200 µg/mL. The slight increment of particle size after redispersion combined with the wetting process of the solid dosage forms resulted the lower achievable maximum solubility than nano-cocrystal suspension. However, comparing the performance of different substrates, water-soluble lactose exhibited faster dissolution and higher solubility than water-insoluble MCC (Meruva et al., 2019). During dissolution, due to the swelling properties of MCC after contact with water, the dissolution medium cannot penetrate the internal MCC granules immediately; thus, a small part of the nano-cocrystal may not be released (Kleinebudde, 1994).

The drug release rate from SG-MCC or SG-Lac granules containing 20% drug loading was slower than corresponding granules with 10% drug loading. The maximum solubility of 180 µg/mL was observed within 5 min from SG-MCC granules at 20% w/w drug loading compared to 200 µg/mL at 10% w/w drug loading. The similar maximum solubility of 225 µg/mL was observed within 5 min from SG-Lac granules at 10% and 20% w/w drug loading. The spray granulation process combines wetting and nucleation, consolidation and growth, and breakage and attrition (Panda et al., 2001). In order to increase drug loading, more nanosuspension was sprayed onto the substrate, which prolonged the processing time, resulted in the risk of more binder forming liquid bridges between the granules. More liquid bridges led to granules with a tighter internal structure that was more resistant to water penetration during the dissolution process, thereby compromising the dissolution rate.
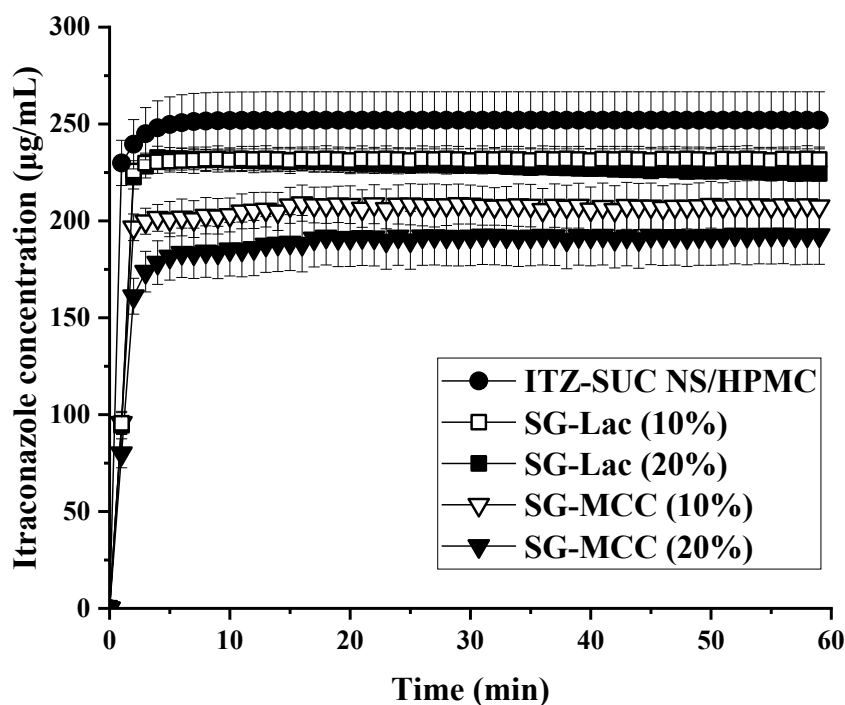
Fig. 3.38. Dissolution profiles of SG-Lac and SG-MCC granules containing ITZ-SUC nano-cocrystal with 10% and 20% w/w drug loading. Additionally, the dissolution of ITZ-SUC NS/HPMC was used for comparison.

The dissolution curve of SG-MCC granules with 20% drug loading exhibited a slow solubility increment from 180 to nearly 200 µg/mL from 5 to 15 minutes, indicating that drug has not been released completely at the beginning. Due to MCC's swelling and water-insoluble inherent properties, small MCC particles tended to accumulate in the bottom of the dissolution vessel; hence, part of nano-cocrystals was embedded by those MCC particles to prevent them from releasing in time. With the stirring of the paddle during the dissolution process, embedded nano-cocrystals were further released from the MCC particle accumulative, and the solubility will increase slowly. In order to verify this assumption, SG-MCC granules were added into dissolution media and tested with different rotation speeds. As expected, the maximum solubility of SG-MCC granules was only about 150 µg/mL at a rotating speed of 50 rpm, and by increasing the speed to 300 rpm, the maximum solubility of MCC granules reaches 250 µg/mL, which was as high as the nano-cocrystal/HPMC dispersion (Fig. 3.39a). SG-MCC granules were also added into the dissolution medium with an initial rotating speed of 50 rpm; the speed was increased to 100 rpm after 60 minutes and 300 rpm after another 30 minutes. As the rotation speed increased, more nano-cocrystals covered by MCC were released (Fig. 3.39b). The achievable maximum solubility of MCC granules with a beginning rotation speed of 300

rpm reaches 250 µg/mL. However, the achievable maximum solubility of MCC granules with an increasing rotation speed from 50 to 300 rpm only achieves 200 µg/mL. Therefore, the achievable maximum solubility of a supersaturated drug delivery system for nano-cocrystal was proportional to the supersaturation generation rate (Sun and Lee, 2013).
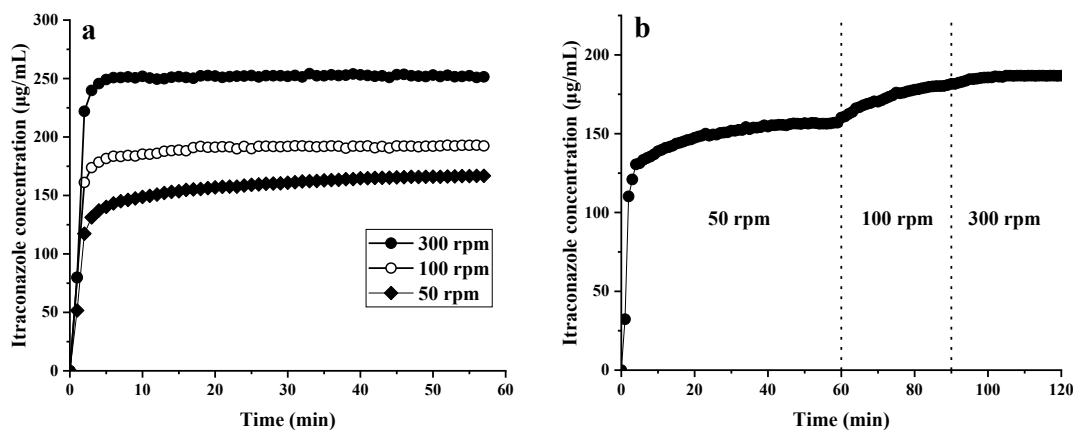
Fig. 3.39. Dissolution profiles of (a) SG-MCC granules with different rotation speed, (b) SG-MCC granules with increasing rotation speed

3.4.5. Bead layering

3.4.5.1. Characterization of ITZ-SUC nano-cocrystal coated beads

ITZ-SUC nano-cocrystal coated beads with different substrates were spherical (Fig. 3.40a, c). The surface of the beads was smooth, indicating that the nanoparticles were evenly layered on the surface of the beads. A small amount of nanoparticles were released from the surface of BL-MCC beads within 1 min (Fig. 3.40b). After 5 min, nanoparticles released from BL-MCC beads formed a dense cloud around the surface, indicating a core-shell structure with an MCC inert core and a shell composed of dried nanoparticles and coating polymer (Fig. 3.40c). In the case of BL-Sugar beads, after being in contact with water for 1 minute, the release of nanoparticles and the erosion of the polymer which covers the surface of the core occurs firstly (Fig. 3.40e). After 5 minutes, water has completely penetrated into the interior of the sugar beads, causing the disintegration of the core structure (Fig. 3.40f). Unlike granules, nanoparticles were layered on the beads during the fluidized bed coating process. The release of nanoparticles may not be affected by the substrate used due to the distribution of nanoparticles on the outer layer of beads.

	BL-MCC beads	BL-Sugar beads
Original	a	d
Water contact for 1 min	b	e
Water contact for 5 min	c	f
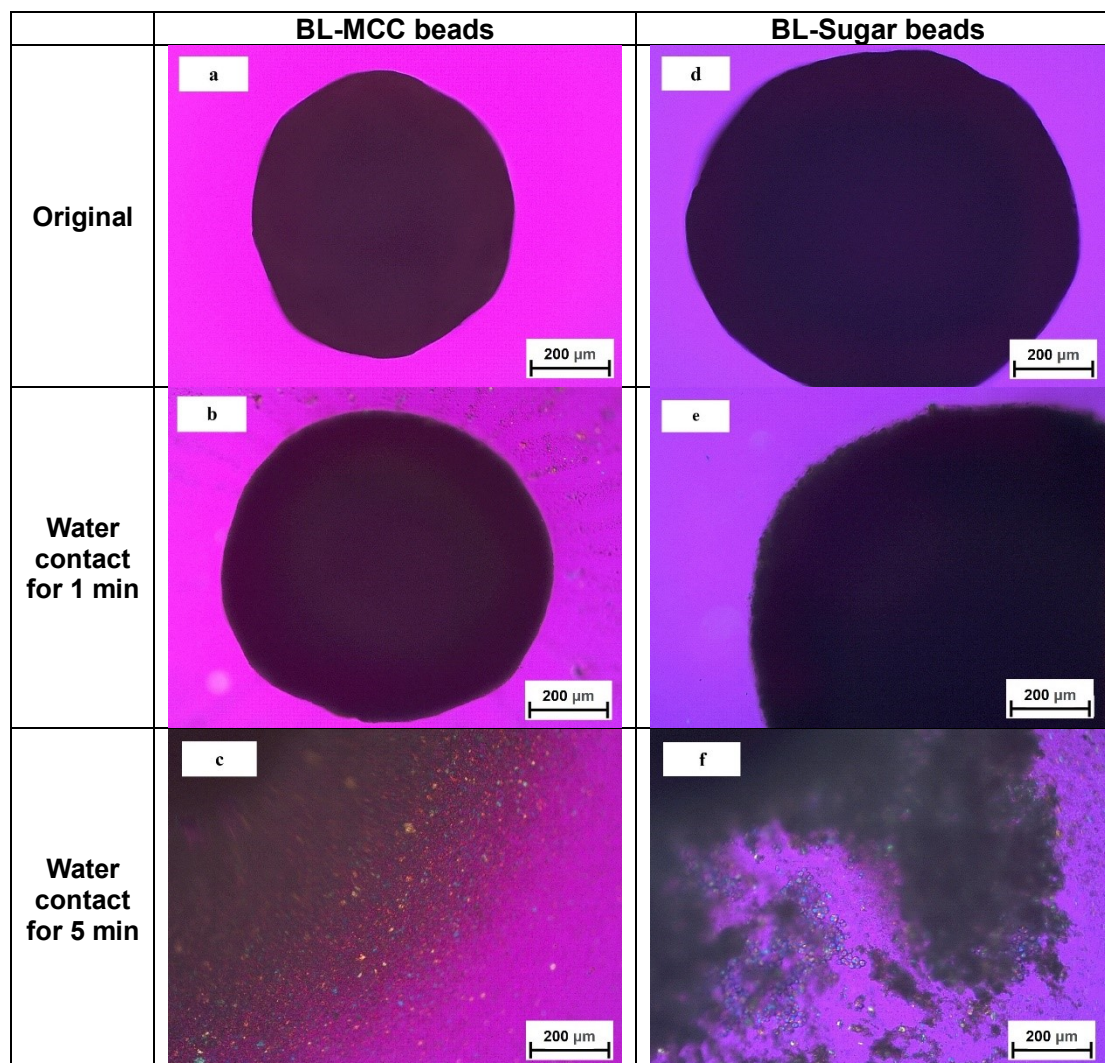
Fig. 3.40. Microscopy images of BL-MCC beads and BL-Sugar beads (all 20% w/w drug loading) before and after water contact.

Theoretically, more drug was available to layer on either MCC or sugar blank beads; for comparison, beads with 10% and 20% drug loading were prepared and investigated in this study. The assay for drug content post bead layering was around 75 – 80% of the theoretical drug loading. The LOD values of the beads were < 1% at both drug loading. After granules were dispersed in water and filtered, the average particle size of the nano-cocrystal released from MCC or sugar beads was around 600 nm. DSC and XRPD analysis of 20% drug loading beads indicated no polymorphic or cocrystal structure changes post layering process (Fig. 3.41, 3.42).
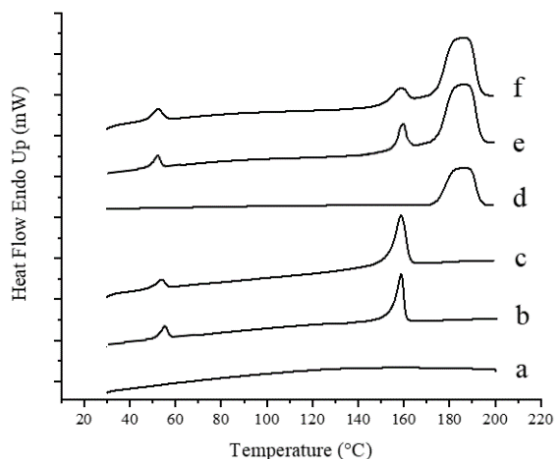
Fig. 3.41. DSC profiles for 20% w/w drug loading of (a) MCC beads, (b) MCC beads and ITZ-SUC nano-cocrystal/HPMC physical mixture, (c) MCC beads containing ITZ-SUC nano-cocrystal, (d) sugar beads, (e) sugar beads, and ITZ-SUC nano-cocrystal/HPMC physical mixture, (f) sugar beads containing ITZ-SUC nano-cocrystal.
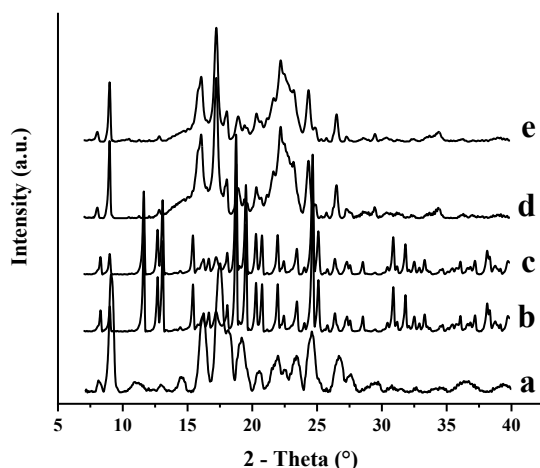
Fig. 3.42. XRPD patterns for 20% w/w drug loading of (a) ITZ-SUC nano-cocrystal/HPMC, (b) MCC beads and ITZ-SUC nano-cocrystal/HPMC physical mixture, (c) MCC beads containing ITZ-SUC nano-cocrystal, (d) sugar beads, and ITZ-SUC nano-cocrystal/HPMC physical mixture, (f) sugar beads containing ITZ-SUC nano-cocrystal.

3.4.5.2. Dissolution of ITZ-SUC nano-cocrystal layered beads

ITZ-SUC nano-cocrystal coated beads obtained a similar maximum solubility compared to the nano-cocrystal/HPMC dispersion (Fig. 3.43). Furthermore, the dissolution curve of the drug-coated MCC beads had no difference with sugar beads. Due to the nanoparticles forming the layer on the bead surface, using a water-soluble or water-insoluble core had little impact on the drug dissolution. Parmentier et al. investigated the influence of bead

material (sugar vs. MCC) on the dissolution performance of beads layered with itraconazole nanocrystal. They also demonstrated that the drug release from the beads was not influenced by bead type (Parmentier et al., 2017).

A higher drug loading indicated a thicker layer. With a thicker coating layer, the polymer's erosion would impact the release of the nanoparticle. Many studies had shown that when poorly soluble drugs were coated on beads, thicker layers resulted in slower release (Azad et al., 2015; Parmentier et al., 2017). The polymer can impact the dissolution rate either directly by its swelling and dissolution behavior or indirectly by the drug particle size after drying. However, in this study, no significant difference between drug loading and drug release was found. The possible reason was that the difference in thickness of beads prepared with 10% and 20% drug loading was not obvious, leading to insufficient dissolution discrimination. Another possible reason was that HPMC E5 as a suitable polymer resulted in fast swelling and dissolution behavior, thus having little impact on the dissolution rate of nanoparticles (Dukić-Ott et al., 2007).
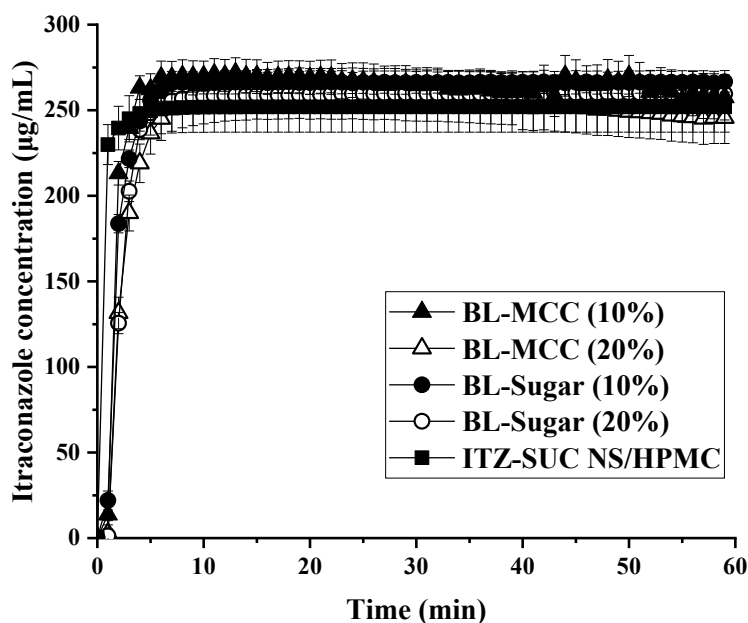
Fig. 3.43. Dissolution of ITZ-SUC nano-cocrystal from BL-Sugar and BL-MCC beads with 10% and 20% w/w drug loading. Additionally, the dissolution of ITZ-SUC NS/HPMC was used for comparison.

3.4.6. Comparison of downstream process

Different parameters such as the number of steps, yield, time, drug loading per batch, and dissolution profiles were summarized and compared for ITZ-SUC nano-cocrystal incorporated solid dosage forms prepared with three different downstream processes. Wet

granulation consists of separated granulation and drying two-step process, while spray granulation and bead layering integrated granulation and drying in one step. Although the time required for the granulation from the wet granulation process was relatively short, the subsequent drying process usually takes overnight or even 24 hours. In contrast, the spray granulation and bead layering required only 0.5-2.5 h for the whole process, significantly shortening the downstream processing time. Furthermore, spray granulation requires many droplets to form a liquid bridge to bond the dispersed excipient materials to form fine granules; the suspension feed rate was generally 3-4 times faster than that of bead layering. The process yield of three downstream methods was all higher or near 80%.

Unlike granules, the nano-cocrystal was almost completely coated on the surface of the beads to form a core-shell structure. Therefore, theoretically, as long as the appropriate polymer and drug concentration were selected, the drug loading of the coated beads could increase with the coverage of nanoparticles layer by layer. However, in the spray granulation process, increasing the drug loading means longer preparation time and the formation of more liquid bridges between the excipients, resulting in more nanoparticles being embedded inside the excipients and affecting drug dissolution. This slower dissolution with the increase of drug loading was more obvious in using water-insoluble excipients such as MCC than water-soluble excipients like lactose. Furthermore, the ratio of suspension to excipient was usually fixed to obtain a suitable wet mass that can be wet granulated. Therefore, the only way to increase drug loading in granules was by increasing the initial drug concentration, while higher concentrations of nanosuspensions were challenging to prepare with a high risk of agglomeration.

The location and distribution of nanoparticles in solid dosage forms had a significant impact on drug dissolution. High maximum solubility meant fast dissolution, as shown with a rank order of solid forms prepared by wet granulation < spray granulation < bead layering (Fig. 3.44). In the granules prepared with wet granulation, most nanoparticles were embedded inside the tighten granules; hence the dissolution rate was the slowest. In the spray granulation process, most of the nanoparticles were evenly distributed on small granules that assembled large granules. A small part of the nanoparticles was either embedded in those small granules or located in the particle junction. Therefore, the dissolution rate was faster than wet granulation but lower than layered beads. Drug layered beads obtained the fastest drug dissolution rate because all nanoparticles were layered on the surface of the beads and could be released when contacted with the dissolution medium. The maximum solubility of granules prepared with wet and spray granulation achieved from the water-

soluble lactose was higher than that of the water-insoluble MCC.

It was necessary to develop a desirable downstream process for nano-cocrystals and maintain dissolution and supersaturated solubility benefits obtained from particle size reduction and cocrystal structure. The bead layering method displayed promising outcomes: one-step process, high drug loading, broader excipient applicability, and rapid dissolution. Therefore, the bead layering method is recommended to be the first choice for developing nano-cocrystal-based solid dosage products. The second choice is spray granulation, while traditional wet granulation is not recommended.
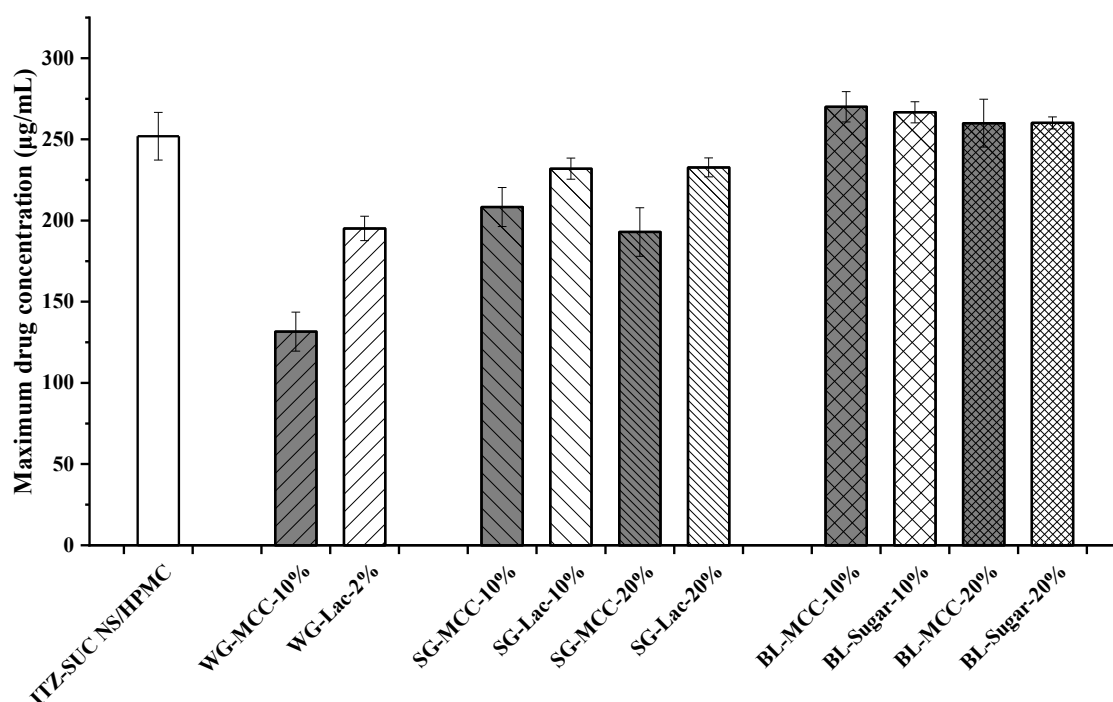
Fig. 3.44. Comparison of the maximum solubilities of ITZ-SUC nano-cocrystal released from granules and beads with different drug loading.

3.4.7. Stability of nano-cocrystal incorporated granules or beads

The largest challenge of the nanosized pharmaceutical formulation to be a commercial drug product is the problematic stability. Not only the preparation process but also the long-term storage should be taken into consideration. Stability was the first requirement for nano-cocrystal based products to enter the industrial stage. Therefore, this study investigated the accelerated stability of prepared solid dosage forms containing ITZ-SUC nano-cocrystals.

Dissolution tests were taken to evaluate the release of nano-cocrystal from sprayed granules and coated beads. In order to figure out the influence of temperature and moisture

on stability, all the tested solid dosage forms were packed in double polyethylene-lined aluminum pouches or placed in open bottles (blistered or non-blistered) and stored in 40 °C/75% RH. From all the samples in blisters, the dissolution results were similar to that of the freshly prepared ones within 3-month storage (Fig. 3.45b, d, f, and g). Nano-cocrystal was physically stable, and particle aggregation did not occur during storage in blistering conditions. The temperature had no impact on the stability of nano-cocrystal incorporated into solid dosage forms. However, a decrease in dissolution rate and maximum solubility was observed from sprayed granules in non-blistered conditions after 3-month storage (Fig. 3.45a, c). The LOD values of SG-MCC and SG-Lac granules increased from 0.92% to 6.02% and from 0.48% to 4.72% after exposure in 75% RH for 3 months, respectively.

On the other hand, the dissolution profile of nano-cocrystal was not affected by long-term storage in non-blistered conditions from layered beads (Fig. 3.45e, g). The LOD values of either BL-MCC or BL-Sugar beads were still < 1% after exposure in 75% RH for 3 months. Core-shell structured beads provided less surface of excipient for moisture absorption than sprayed granules. In the case of sprayed granules, as with increasing moisture content, an increase in cohesion from stronger interparticle liquid bridges formed tighter internal structure; nano-cocrystal particle aggregation or entrapment in the excipient were more likely to happen. While in the case of layered beads, a dense drug layer played a role in preventing the internal excipient core from absorbing too much moisture and affecting the stability. The influence of moisture on the stability of nano-cocrystal solid dosage forms was more significant than that of temperature. Therefore, formulations with weaker hygroscopicity were recommended in the downstream composition, like tablets or capsules.
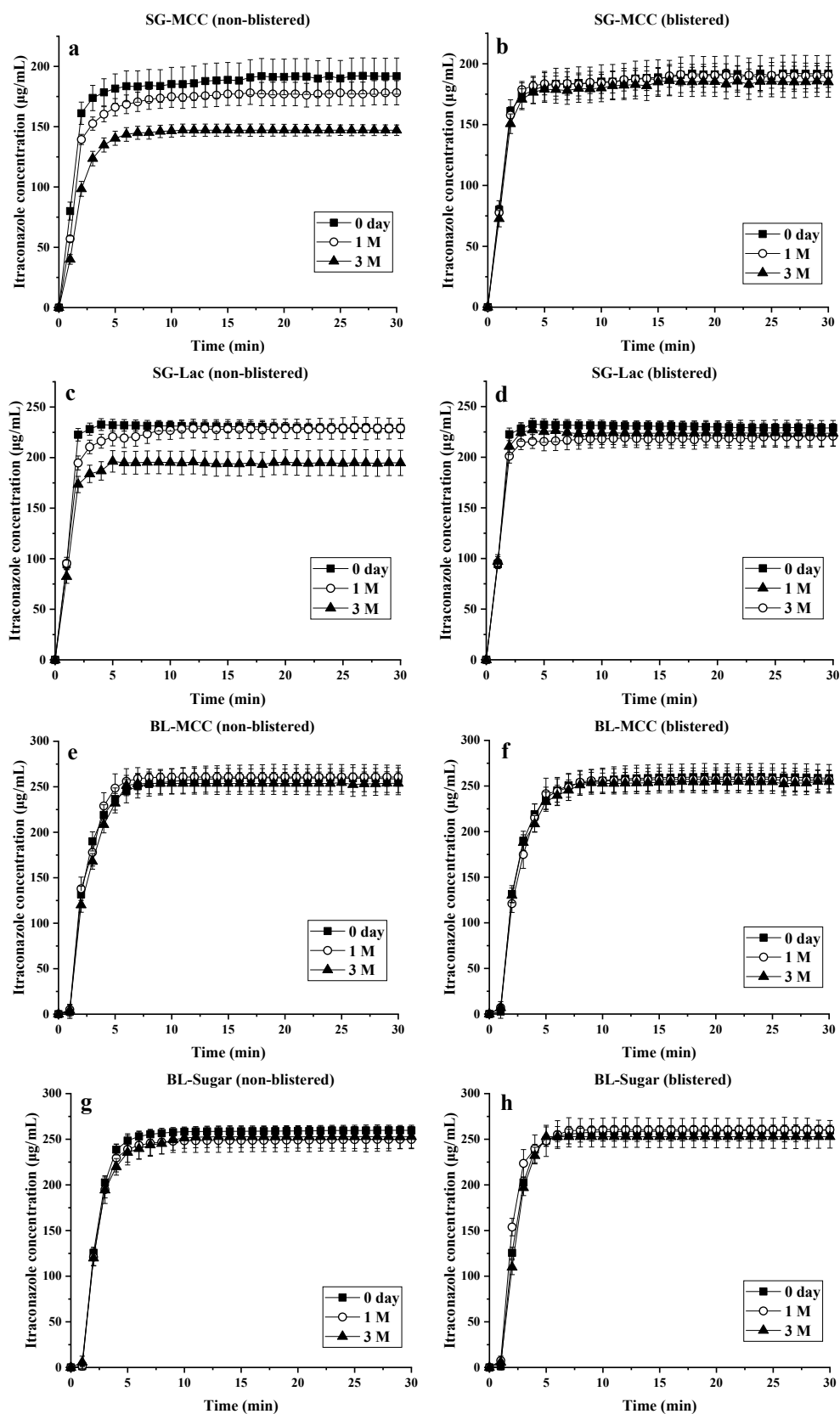
Fig. 3.45. Stability of ITZ-SUC nano-cocrystal dissolution upon 3 months storage at 40 °C/75% RH from its formulated granules and beads in blistered and non-blistered conditions.

3.4.8. Comparison of layered sugar beads with Sporanox®

BL-Sugar with incorporated ITZ-SUC nano-cocrystal formulation released remarkably faster than the marketed product Sporanox®. Sugar beads layered with nano-cocrystal reached to a maximum drug concentration plateau of around 250 µg/mL within 10 min. And for commercial product Sporanox®, it had reached the same concentration after 17 min. However, drug concentration from the Sporanox® reached a slightly higher plateau after 25 min. Sporanox® capsules contain ITZ, that is layered onto the sugar beads by dissolving the drug and HPMC in an organic solvent and dried, which are finally protected by a layer of PEG (20,000), which explained the dissolution behavior of Sporanox® formulation (Kapsi and Ayres, 2001). Overall, compared with Sporanox®, BL-Sugar with incorporated ITZ-SUC nano-cocrystal formulation exhibited faster dissolution rate and could almost reach the same maximum concentration. Therefore, nano-cocrystal downstream with bead layering method is an alternative or even better choice in the development of novel solid oral ITZ formulations. The results of its research in vivo are worth studying and promising.
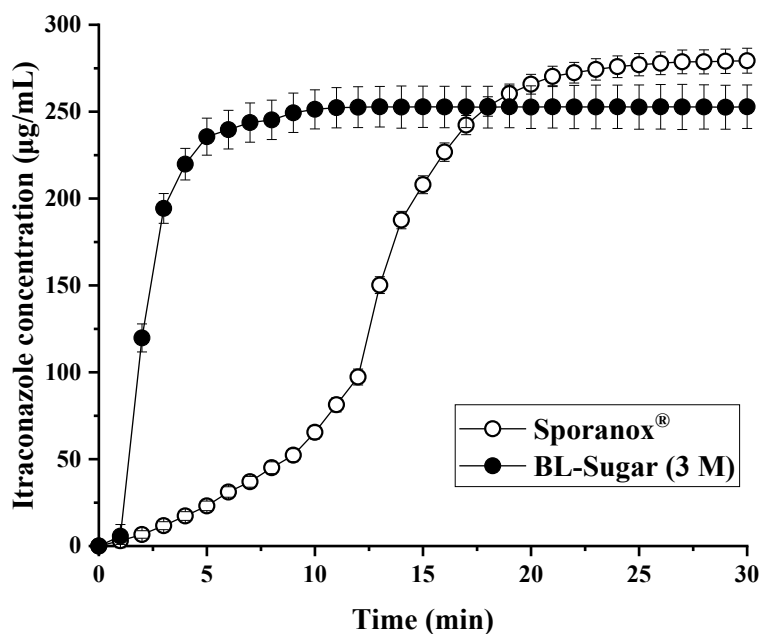
Fig. 3.46. Dissolution analysis of BL-Sugar (20% w/w drug loading) after 3-month storage and Sporanox®.

3.4.9. Conclusions

The present study investigated the impact of drying methods, type of substrate, and drug loading on the dissolution behavior of nano-cocrystals from their solid dosage forms. Limited by low drug loading and slow dissolution profile, traditional wet granulation was not

suitable for downstream processing of nano-cocrystal formulation. Spray granulation and bead layering could increase the drug loading without strongly compromising the rapid dissolution behavior of nano-cocrystal. However, the type of substrate used for spray granulation impacted the dissolution performance from the granules. Faster dissolution profiles and higher maximum solubility were obtained when the water-soluble substrate was used. While the type of substrate has no impact on the dissolution behavior of beads layered with nano-cocrystals. Furthermore, during the accelerated stability studies, the nano-cocrystal processed by spray granulation was less stable than nano-cocrystal processed by bead layering upon 3 months storage at 40 °C/75% RH in non-blistered condition. Overall, bead layering was the most suitable method for the downstream process of nano-cocrystal suspensions with the overall performance of a solid product.

4. SUMMARY

Solubility and dissolution rate are essential for the oral absorption and thus bioavailability of poorly soluble drugs. Currently, there are various formulation approaches available to overcome issues in solubility and dissolution rate. However, single formulation approach always has its drawback. The purpose of this work was to explore the nano-cocrystal formulation by combining cocrystal and nanocrystal formulation technologies and to optimize the formulation by investigating its dissolution mechanism. A downstream process investigation was also explored to transform the nano-cocrystal formulation into a final oral solid dosage form.

Preparation and optimization of nanocrystal formulations with different lab-scale wet milling methods

Different laboratory-scale nanocrystal preparation methods were compared as milling efficiency and process attributes. Dual centrifugation milling was considered the most promising method with higher milling efficiency, formulation screening efficiency, and broader controllable process attributes. Applying the dual centrifugation milling method to efficiently screen stabilizers and adjust process parameters, optimized itraconazole nanocrystal stabilized by poloxamer 407 was produced with a mean particle size of 200 nm and PDI 0.2. The nanosuspension was physically stable at 4, 25 and 40 °C for one month. The optimized nanocrystal formulation exhibited a faster dissolution rate than the physical mixture and raw drug under sink or non-sink conditions in *in vitro* dissolution study. While compared with commercial product Sporanox®, nanocrystal formulation exhibited faster drug release under sink conditions but lower and limited solubility increment under non-sink conditions. Itraconazole nanocrystal formulation might not exhibit advantageous *in vivo* behavior compared to the commercial product. A selection of a suitable *in vitro* dissolution test to evaluate nanocrystal formulation was crucial. In addition, nanocrystalline formulation significantly improved the dissolution rate of poorly soluble APIs, while its increases in solubility were limited. Finally, some other solubilization methods like cocrystal or amorphization could be combined with the nanocrystal approach and utilized to offer a practical approach for delivering orally poorly soluble drugs.

Combination of cocrystal and nanocrystal techniques to improve the solubility and dissolution rate of poorly soluble drugs

Four itraconazole and indomethacin nano-cocrystals with mean particle diameters of around 450 nm were successfully prepared. Solid-state characterization suggested that by

transforming raw drug powder into its cocrystal form is a new strategy for the preparation of nano-formulations which are physically or chemically unstable during wet milling. Furthermore, *in situ* solubility studies indicated that nano-cocrystals showed remarkably higher solubility and dissolution rate compared to nanocrystals and cocrystals. The maximum kinetic solubility of nano-cocrystals increased with excess conditions until reaches a plateau. The highest increase was obtained with itraconazole-succinic acid nano-cocrystals with a solubility of 263.5 ± 3.9 µg/mL which is 51.5 and 6.6 times higher than the solubility of itraconazole crystalline and itraconazole-succinic acid cocrystal. The combination of cocrystals and nanocrystals could potentially overcome the limitation of nanocrystals in solubility improvement and the limitation of cocrystal in dissolution rate improvement. Nanocrystal technique efficiently promotes the potential of cocrystal solubilization effect by its superior dissolution rate. This nano-cocrystal formulation expands the drug development strategies of poorly soluble drugs.

Itraconazole-succinic acid nano-cocrystals: Kinetic solubility improvement and influence of polymers on controlled supersaturation

A systematic experimental investigation was conducted to explore the precipitation inhibition capacity of a range of commonly used precipitation inhibitors (HPMC E5, HPMC E50, HPMCAS, HPC-SSL, PVPK30 and PVPVA64) in itraconazole-succinic acid nano-cocrystal formulation. HPMC E5 achieved greatest extended nano-cocrystals dissolution and maintenance of supersaturation based on specific drug/polymer intermolecular interaction. Dissolved polymer not only increased maximum achievable supersaturation, but also maintained supersaturation for prolonged times, resulting in significantly broadened AUC maxima. The maximum achievable supersaturation was proportional to the dissolution rate which can be modulated by the rate of supersaturation generation (i.e., addition rate or dose). Supersaturation could be prolonged significantly resulting in 2-5-fold increased area under the dissolution curves compared to nano-cocrystals alone. This effect was however limited by a critical excess of undissolved particles with high specific surface area which acted as crystallization seeds resulting in faster precipitation. To achieve higher and sustained supersaturation from nano-cocrystal formulation during dissolution, faster dissolution rate and proper application of precipitation inhibitors were two driving factors. The relationship between particle size, dose and polymer ratio and their synergic impact on the supersaturation must be considered. Generally, these insights and findings would

contribute to the design of optimally performing oral solid dosage formulations with incorporated nano-cocrystals.

Incorporation of itraconazole nano-cocrystal into granulated or bead-layered solid dosage forms

Three downstream processes (wet granulation, spray granulation, and bead layering) were evaluated on the performance of itraconazole-succinic acid nano-cocrystal suspension. Limited by low drug loading and slow dissolution profile, traditional wet granulation was not suitable for downstream processing of nano-cocrystal formulation. Spray granulation and bead layering could increase the drug loading without significantly compromising the rapid dissolution behavior of nano-cocrystal. However, the type of substrate used for spray granulation impacted the dissolution performance from the granules containing nano-cocrystals. Faster dissolution profiles and higher maximum solubility were obtained when the water-soluble substrate was used. While the type of substrate has no impact on the dissolution behavior of beads layered with nano-cocrystals. Furthermore, during the accelerated stability studies, the nano-cocrystal processed by spray granulation was less stable than nano-cocrystal processed by bead layering upon 3 months storage at 40 °C/75% RH in non-blistered condition. Overall, bead layering was the most suitable method for the downstream process of nano-cocrystal suspensions with the overall performance of a solid product.

In conclusion, this entire work indicated that the combination of cocrystals and nanocrystals could potentially overcome the limitation of nanocrystals in solubility improvement and the limitation of cocrystal in dissolution rate improvement. Nano-cocrystal formulations could be optimized with adding specific precipitation inhibitor. Bead layering was a superior downstream process approach for incorporating nano-cocrystals into an oral solid dosage form without compromising release.

5. ZUSAMMENFASSUNG

Löslichkeit und Auflösungsgeschwindigkeit sind für die orale Absorption und damit für die Bioverfügbarkeit von schwer löslichen Arzneimitteln von wesentlicher Bedeutung. Derzeit gibt es verschiedene Formulierungsansätze um Probleme mit Löslichkeit und Auflösungsgeschwindigkeit zu überwinden. Einzelne Ansätze haben jedoch jeweils auch Restriktionen. Ziel dieser Arbeit war es, die Nano-Kristall-Formulierung durch die Kombination von Co-Kristall- und Nanokristall-Formulierungstechnologien zu untersuchen und die Formulierung anhand des Auflösungsmechanismus zu optimieren. Außerdem wurde ein nachgeschalteter Prozess beschrieben, um die Nano-Kristallformulierung in eine endgültige orale feste Darreichungsform zu überführen.

Herstellung und Optimierung von Nanokristallformulierungen mit verschiedenen Nassmahlverfahren im Labormaßstab

Verschiedene Methoden zur Herstellung von Nanokristallen im Labormaßstab wurden hinsichtlich ihrer Mahlleistung und ihrer Prozesseigenschaften verglichen. Die duale Zentrifugation wurde als die vielversprechendste Methode mit höherer Vermahlungseffizienz, effizienterem Formulierungsscreening und breiter kontrollierbaren Prozesseigenschaften angesehen. Durch effizientes Screening von Stabilisatoren und Optimierung der Prozessparameter wurden mittels dualer Zentrifugation, durch Poloxamer 407 stabilisierte Itraconazol-Nanokristalle mit einer mittleren Partikelgröße von 200 nm und einem PDI von 0,2 hergestellt. Die Nanosuspension war bei 4, 25 und 40 °C einen Monat lang physikalisch stabil. Die optimierte Nanokristallformulierung wies in der *in-vitro*-Auflösungsstudie unter Sink- und Nicht-Sink-Bedingungen eine schnellere Auflösungsrate auf als die reine Substanz oder die physikalische Mischung . Im Vergleich zum kommerziellen Produkt Sporanox® zeigte die Nanokristallformulierung eine schnellere Wirkstofffreisetzung unter Sinkbedingungen, aber einen geringeren und begrenzten Löslichkeitszuwachs unter Nicht-Sinkbedingungen. Die Itraconazol-Nanokristallformulierung könnte im Vergleich zum kommerziellen Produkt kein verbessertes *in-vivo*-Verhalten aufweisen.

Die Auswahl eines geeigneten *in-vitro*-Auflösungstests ist ein zentraler Punkt zur Bewertung der Nanokristallformulierung. Darüber hinaus verbesserte die nanokristalline Formulierung die Auflösungsgeschwindigkeit von schwer löslichen Wirkstoffen erheblich, während die Erhöhung der Löslichkeit begrenzt war. Schließlich könnten andere Solubilisierungsmethoden wie co-kristalline oder amorphe Formulierungen mit dem

nanokristallinen Ansatz kombiniert und genutzt werden, um einen praktischen Ansatz für die orale Verabreichung schwer löslicher Arzneimittel zu bieten.

Kombination von Co-kristall- und Nanokristalltechniken zur Verbesserung der Löslichkeit und Auflösungsgeschwindigkeit schwerlöslicher Arzneimittel

Vier Itraconazol- und Indomethacin-Nanokristalle mit einem mittleren Partikeldurchmesser von etwa 450 nm wurden erfolgreich hergestellt. Die Festkörpercharakterisierung deutete darauf hin, dass die Umwandlung des Roharzneimittelpulvers in seine co-kristalline Form eine neue Strategie für die Herstellung von Nanoformulierungen darstellt, welche bei Nassmahlung physikalisch oder chemisch instabil wären. Darüber hinaus zeigten *in-situ*-Löslichkeitsstudien, dass Nano-Co-kristalle im Vergleich zu Nanokristallen und Co-kristallen eine deutlich höhere Löslichkeit und Auflösungsgeschwindigkeit aufweisen. Die maximale kinetische Löslichkeit der Nano-Kristalle nahm mit den Überschussbedingungen zu, bis sie ein Plateau erreichte. Der höchste Anstieg wurde bei Itraconazol-Bernsteinsäure-Nanokristallen mit einer Löslichkeit von 263,5 ± 3,9 µg/ml erzielt, was 51,5- bzw. 6,6-mal höher ist als die Löslichkeit von kristallinem Itraconazol und Itraconazol-Bernsteinsäure-Co-Kristallen. Die Kombination von Co-Kristallen und Nanokristallen könnte die Beschränkung von Nanokristallen bei der Verbesserung der Löslichkeit und die Beschränkung von Co-Kristallen bei der Verbesserung der Auflösungsgeschwindigkeit überwinden. Die Nanokristalltechnik fördert effizient das Potenzial der Solubilisierung von Co-Kristallen durch ihre überlegene Auflösungsgeschwindigkeit. Eine Nanokristallformulierung erweitert die Strategien der Arzneimittelentwicklung für schwerlösliche Arzneimittel.

Itraconazol-Bernsteinsäure-Nanokristalle: Verbesserung der kinetischen Löslichkeit und Einfluss der Polymere auf die kontrollierte Übersättigung

Es wurde eine systematische experimentelle Untersuchung durchgeführt, um die Ausfällungsinhibitionskapazität einer Reihe von üblicherweise verwendeten Ausfällungsinhibitoren (HPMC E5, HPMC E50, HPMCAS, HPC-SSL, PVPK30 und PVPVA64) in Itraconazol-Bernsteinsäure-Nanokristallformulierungen zu erkunden. Speziell HPMC E5 verlängerte die Auflösung der Nano-Kristalle und die Aufrechterhaltung der Übersättigung aufgrund der spezifischen intermolekularen Wechselwirkung zwischen Arzneimittel und Polymer. Das aufgelöste Polymer erhöhte nicht nur die maximal erreichbare Übersättigung, sondern hielt die Übersättigung auch über einen längeren

Zeitraum aufrecht, was zu einer signifikanten Verbreiterung der AUC-Maxima führte. Die maximal erreichbare Übersättigung war proportional zur Auflösungsrate, die durch die Rate der Übersättigungserzeugung (Zugaberate oder Dosis) moduliert werden kann. Die Übersättigung konnte hierdurch deutlich verlängert werden, was zu einer 2-5-fachen Vergrößerung der AUC im Vergleich zu Nanokristallen allein führte. Dieser Effekt wurde jedoch durch einen kritischen Überschuss an ungelösten Partikeln mit hoher spezifischer Oberfläche begrenzt, die als Kristallisationskeime fungierten und zu einer schnelleren Ausfällung führten. Um eine höhere und anhaltende Übersättigung der Nanokristallformulierung während der Auflösung zu erreichen, waren eine schnellere Auflösungsrate und die richtige Anwendung von Ausfällungsinhibitoren zwei entscheidende Faktoren. Die Beziehung zwischen Partikelgröße, Dosis und Polymerverhältnis und ihre synergetischen Auswirkungen auf die Übersättigung müssen berücksichtigt werden. Generell würden diese Erkenntnisse und Ergebnisse zur Entwicklung optimal funktionierender oraler fester Dosierungsformulierungen mit eingearbeiteten Nanokristallen beitragen.

Einarbeitung von Itraconazol-Bernsteinsäure-Nanokristallen in granulierte oder wirkstoffbeschichtete feste Darreichungsformen

Drei nachgeschaltete Verfahren (Nassgranulierung, Sprühgranulierung und Perlenschichtung) wurden hinsichtlich der Leistung der Itraconazol-Bernsteinsäure Nanokristallsuspension bewertet. Aufgrund der geringen Wirkstoffbeladung und des langsamen Auflösungsprofils war die herkömmliche Nassgranulation für die nachgeschaltete Verarbeitung der Nano-Kristallformulierung nicht geeignet. Durch Sprühgranulation und Coating konnte die Wirkstoffbeladung erhöht werden, ohne das schnelle Auflösungsverhalten der Nanokristalle wesentlich zu beeinträchtigen. Die Art des für die Sprühgranulation verwendeten Substrats wirkte sich jedoch auf die Auflösungsleistung der Nanokristalle enthaltenden Granulate aus. Schnellere Auflösungsprofile und eine höhere maximale Löslichkeit wurden erzielt, wenn ein wasserlösliches Substrat verwendet wurde. Die Art des Substrats hatte jedoch keinen Einfluss auf das Auflösungsverhalten der mit Nanokristallen beschichteten Perlen. In den beschleunigten Stabilitätsstudien waren die durch Sprühgranulation hergestellten Nanokristalle nach dreimonatiger Lagerung bei 40 °C und 75 % relativer Luftfeuchtigkeit weniger stabil als die durch Coating hergestellten Nanokristalle. Insgesamt war die

Perlenschichtung die am besten geeignete Methode für die Weiterverarbeitung von Nano-Kristallsuspensionen in eine finale feste Darreichungsform.

Zusammenfassend lässt sich sagen, dass die Kombination von Co-Kristallen und Nanokristallen die Beschränkung von Nanokristallen bei der Verbesserung der Löslichkeit und die Beschränkung von Co-Kristallen bei der Verbesserung der Auflösungsgeschwindigkeit überwinden könnte. Nano-Kristall-Formulierungen könnten durch Zugabe eines spezifischen Ausfällungsinhibitors optimiert werden. Die Perlenschichtung war ein überlegener nachgeschalteter Prozessansatz, um Nano-Kristalle in eine feste orale Darreichungsform einzubringen, ohne die Freisetzung zu beeinträchtigen.

6. REFERENCES

REFERENCES

Aakeröy, C.B., Salmon, D.J., 2005. Building co-crystals with molecular sense and supramolecular sensibility. CrystEngComm 7, 439-448.

Agrawal, S., Guest, J.S., Cusick, R.D., 2018. Elucidating the impacts of initial supersaturation and seed crystal loading on struvite precipitation kinetics, fines production, and crystal growth. Water Res. 132, 252-259.

Alhalaweh, A., Roy, L., Rodríguez-Hornedo, N., Velaga, S.P., 2012. pH-dependent solubility of indomethacin–saccharin and carbamazepine–saccharin cocrystals in aqueous media. Mol. Pharm. 9, 2605-2612.

Alhalaweh, A., Velaga, S.P., 2010. Formation of cocrystals from stoichiometric solutions of incongruently saturating systems by spray drying. Crystal growth & design 10, 3302-3305.

Ali, S., 2001. Adsorption of the poloxamer surfactants onto model hydrophobic surfaces in suspension systems. University of London, University College London (United Kingdom).

Allen, T.M., Cullis, P.R., 2013. Liposomal drug delivery systems: from concept to clinical applications. Adv. Drug Del. Rev. 65, 36-48.

Almarsson, Ö., Zaworotko, M.J., 2004. Crystal engineering of the composition of pharmaceutical phases. Do pharmaceutical co-crystals represent a new path to improved medicines? Chem. Commun., 1889-1896.

Almeida e Sousa, L., Reutzel-Edens, S.M., Stephenson, G.A., Taylor, L.S., 2016. Supersaturation potential of salt, co-crystal, and amorphous forms of a model weak base. Crystal Growth & Design 16, 737-748.

Alonzo, D.E., Zhang, G.G., Zhou, D., Gao, Y., Taylor, L.S., 2010. Understanding the behavior of amorphous pharmaceutical systems during dissolution. Pharm. Res. 27, 608-618.

Amidon, G.L., Lennernäs, H., Shah, V.P., Crison, J.R., 1995. A theoretical basis for a biopharmaceutic drug classification: the correlation of in vitro drug product dissolution and in vivo bioavailability. Pharm. Res. 12, 413-420.

Annapragada, A., Adjei, A., 1996. Numerical simulation of milling processes as an aid to process design. Int. J. Pharm. 136, 1-11.

Arzi, R.S., Sosnik, A., 2018. Electrohydrodynamic atomization and spray-drying for the production of pure drug nanocrystals and co-crystals. Adv. Drug Del. Rev. 131, 79-100.

Atkins, P., Paula, J.d., 2014. Physical chemistry thermodynamics, structure, and change. WH Freeman and Company New York.

Azad, M., Arteaga, C., Abdelmalek, B., Davé, R., Bilgili, E., 2015. Spray drying of drug-swellable dispersant suspensions for preparation of fast-dissolving, high drug-loaded, surfactant-free nanocomposites. Drug Dev. Ind. Pharm. 41, 1617-1631.

Babu, N.J., Nangia, A., 2011. Solubility advantage of amorphous drugs and pharmaceutical cocrystals. Crystal Growth & Design 11, 2662-2679.

Badawi, A.A., El-Nabarawi, M.A., El-Setouhy, D.A., Alsammit, S.A., 2011. Formulation and stability testing of itraconazole crystalline nanoparticles. AAPS PharmSciTech 12, 811-820.

Baghel, S., Cathcart, H., O'Reilly, N.J., 2016. Polymeric amorphous solid dispersions: a review of amorphization, crystallization, stabilization, solid-state characterization, and aqueous solubilization of biopharmaceutical classification system class II drugs. J. Pharm. Sci. 105, 2527-2544.

Bak, A., Gore, A., Yanez, E., Stanton, M., Tufekcic, S., Syed, R., Akrami, A., Rose, M., Surapaneni, S., Bostick, T., 2008. The co‑crystal approach to improve the exposure of a water‑insoluble compound: AMG 517 sorbic acid co‑crystal characterization and pharmacokinetics. J. Pharm. Sci. 97, 3942-3956.

Basa, S., Muniyappan, T., Karatgi, P., Prabhu, R., Pillai, R., 2008. Production and in vitro characterization of solid dosage form incorporating drug nanoparticles. Drug Dev. Ind. Pharm. 34, 1209-1218.

Basavoju, S., Boström, D., Velaga, S.P., 2008. Indomethacin–saccharin cocrystal: design, synthesis and preliminary pharmaceutical characterization. Pharm. Res. 25, 530-541.

Bavishi, D.D., Borkhataria, C.H., 2016. Spring and parachute: How cocrystals enhance solubility. Prog. Cryst. Growth Charact. Mater. 62, 1-8.

Becket, G., Schep, L.J., Tan, M.Y., 1999. Improvement of the in vitro dissolution of praziquantel by complexation with α-, β-and γ-cyclodextrins. Int. J. Pharm. 179, 65-71.

Beirowski, J., Inghelbrecht, S., Arien, A., Gieseler, H., 2011. Freeze-drying of nanosuspensions, 1: freezing rate versus formulation design as critical factors to preserve the original particle size distribution. J. Pharm. Sci. 100, 1958-1968.

Berggren, J., Alderborn, G., 2001. Drying behaviour of two sets of microcrystalline cellulose pellets. Int. J. Pharm. 219, 113-126.

Bevernage, J., Brouwers, J., Brewster, M.E., Augustijns, P., 2013. Evaluation of gastrointestinal drug supersaturation and precipitation: strategies and issues. Int. J. Pharm. 453, 25-35.

Bevernage, J., Forier, T., Brouwers, J., Tack, J., Annaert, P., Augustijns, P., 2011. Excipient-mediated supersaturation stabilization in human intestinal fluids. Mol. Pharm. 8, 564-570.

Bilgili, E., Hamey, R., Scarlett, B., 2006. Nano-milling of pigment agglomerates using a wet stirred media mill: Elucidation of the kinetics and breakage mechanisms. Chem. Eng. Sci. 61, 149-157.

References

Bilgili, E., Li, M., Afolabi, A., 2016. Is the combination of cellulosic polymers and anionic surfactants a good strategy for ensuring physical stability of BCS Class II drug nanosuspensions? Pharm. Dev. Technol. 21, 499-510.

Blagden, N., Berry, D.J., Parkin, A., Javed, H., Ibrahim, A., Gavan, P.T., De Matos, L.L., Seaton, C.C., 2008. Current directions in co-crystal growth. New J. Chem. 32, 1659-1672.

Blagden, N., de Matas, M., Gavan, P.T., York, P., 2007. Crystal engineering of active pharmaceutical ingredients to improve solubility and dissolution rates. Adv. Drug Del. Rev. 59, 617-630.

Bleicher, K.H., Böhm, H.-J., Müller, K., Alanine, A.I., 2003. Hit and lead generation: beyond high-throughput screening. Nature reviews Drug discovery 2, 369-378.

Borbás, E., Sinkó, B.l., Tsinman, O., Tsinman, K., Kiserdei, E.v., Démuth, B.z., Balogh, A., Bodák, B., Domokos, A.s., Dargó, G., 2016. Investigation and mathematical description of the real driving force of passive transport of drug molecules from supersaturated solutions. Mol. Pharm. 13, 3816-3826.

Borhade, V., Pathak, S., Sharma, S., Patravale, V., 2014. Formulation and characterization of atovaquone nanosuspension for improved oral delivery in the treatment of malaria. Nanomedicine 9, 649-666.

Bose, S., Schenck, D., Ghosh, I., Hollywood, A., Maulit, E., Ruegger, C., 2012. Application of spray granulation for conversion of a nanosuspension into a dry powder form. Eur. J. Pharm. Sci. 47, 35-43.

Brewster, M.E., Vandecruys, R., Peeters, J., Neeskens, P., Verreck, G., Loftsson, T., 2008. Comparative interaction of 2-hydroxypropyl-β-cyclodextrin and sulfobutylether-β-cyclodextrin with itraconazole: Phase-solubility behavior and stabilization of supersaturated drug solutions. Eur. J. Pharm. Sci. 34, 94-103.

Brouwers, J., Brewster, M.E., Augustijns, P., 2009. Supersaturating drug delivery systems: the answer to solubility-limited oral bioavailability? J. Pharm. Sci. 98, 2549-2572.

Bucar, D.-K., Henry, R.F., Lou, X., Duerst, R.W., MacGillivray, L.R., Zhang, G.G., 2009. Cocrystals of caffeine and hydroxybenzoic acids composed of multiple supramolecular heterosynthons: Screening via solution-mediated phase transformation and structural characterization. Cryst. Growth Des. 9, 1932-1943.

Buckley, S.T., Frank, K.J., Fricker, G., Brandl, M., 2013. Biopharmaceutical classification of poorly soluble drugs with respect to "enabling formulations". Eur. J. Pharm. Sci. 50, 8-16.

Butler, J.M., Dressman, J.B., 2010. The developability classification system: application of biopharmaceutics concepts to formulation development. J. Pharm. Sci. 99, 4940-4954.

Censi, R., Di Martino, P., 2015. Polymorph impact on the bioavailability and stability of poorly soluble drugs. Molecules 20, 18759-18776.

Cerdeira, A.M., Mazzotti, M., Gander, B., 2013. Formulation and drying of miconazole and itraconazole nanosuspensions. Int. J. Pharm. 443, 209-220.

Chamarthy, S.P., Pinal, R., 2008. The nature of crystal disorder in milled pharmaceutical materials. Colloids Surf. Physicochem. Eng. Aspects 331, 68-75.

Chan, H.-K., Kwok, P.C.L., 2011. Production methods for nanodrug particles using the bottom-up approach. Adv. Drug Del. Rev. 63, 406-416.

Chang, T.-L., Zhan, H., Liang, D., Liang, J.F., 2015. Nanocrystal technology for drug formulation and delivery. Frontiers of Chemical Science and Engineering 9, 1-14.

Chen, H., Khemtong, C., Yang, X., Chang, X., Gao, J., 2011. Nanonization strategies for poorly water-soluble drugs. Drug Discov. Today 16, 354-360.

Chen, X., Matteucci, M.E., Lo, C.Y., Johnston, K.P., Williams III, R.O., 2009. Flocculation of polymer stabilized nanocrystal suspensions to produce redispersible powders. Drug Dev. Ind. Pharm. 35, 283-296.

Childs, S.L., Kandi, P., Lingireddy, S.R., 2013. Formulation of a danazol cocrystal with controlled supersaturation plays an essential role in improving bioavailability. Mol. Pharm. 10, 3112-3127.

Chin, W.W.L., Parmentier, J., Widzinski, M., Tan, E.H., Gokhale, R., 2014. A brief literature and patent review of nanosuspensions to a final drug product. J. Pharm. Sci. 103, 2980-2999.

Chiou, W.L., Riegelman, S., 1971. Pharmaceutical applications of solid dispersion systems. J. Pharm. Sci. 60, 1281-1302.

Chun, N.-H., Lee, M.-J., Song, G.-H., Chang, K.-Y., Kim, C.-S., Choi, G.J., 2014. Combined anti-solvent and cooling method of manufacturing indomethacin–saccharin (IMC–SAC) co-crystal powders. J. Cryst. Growth 408, 112-118.

Cincic, D., Friscic, T., Jones, W., 2008. A stepwise mechanism for the mechanochemical synthesis of halogen-bonded cocrystal architectures. J. Am. Chem. Soc. 130, 7524-7525.

Colombo, M., Minussi, C., Orthmann, S., Staufenbiel, S., Bodmeier, R., 2018. Preparation of amorphous indomethacin nanoparticles by aqueous wet bead milling and in situ measurement of their increased saturation solubility. Eur. J. Pharm. Biopharm. 125, 159-168.

Colombo, M., Orthmann, S., Bellini, M., Staufenbiel, S., Bodmeier, R., 2017a. Influence of drug brittleness, nanomilling time, and freeze-drying on the crystallinity of poorly water-soluble drugs and its implications for solubility enhancement. AAPS PharmSciTech 18, 2437-2445.

Colombo, M., Staufenbiel, S., Rühl, E., Bodmeier, R., 2017b. In situ determination of the saturation solubility of nanocrystals of poorly soluble drugs for dermal application. Int. J. Pharm. 521, 156-166.

De Smet, L., Saerens, L., De Beer, T., Carleer, R., Adriaensens, P., Van Bocxlaer, J., Vervaet, C., Remon, J.P., 2014. Formulation of itraconazole nanococrystals and evaluation of their bioavailability in dogs. Eur. J. Pharm. Biopharm. 87, 107-113.

De Waard, H., Hinrichs, W., Frijlink, H., 2008. A novel bottom–up process to produce drug nanocrystals: controlled crystallization during freeze-drying. J. Control. Release 128, 179-183.

Derjaguin, B., Landau, L., 1993. Theory of the stability of strongly charged lyophobic sols and of the adhesion of strongly charged particles in solutions of electrolytes. Prog. Surf. Sci. 43, 30-59.

Desiraju, G.R., 2011. A bond by any other name. Angew. Chem. Int. Ed. 50, 52-59.

Dhumal, R.S., Kelly, A.L., York, P., Coates, P.D., Paradkar, A., 2010. Cocrystalization and simultaneous agglomeration using hot melt extrusion. Pharm. Res. 27, 2725-2733.

Dokoumetzidis, A., Macheras, P., 2006. A century of dissolution research: from Noyes and Whitney to the biopharmaceutics classification system. Int. J. Pharm. 321, 1-11.

Du, J., Li, X., Zhao, H., Zhou, Y., Wang, L., Tian, S., Wang, Y., 2015. Nanosuspensions of poorly water-soluble drugs prepared by bottom-up technologies. Int. J. Pharm. 495, 738-749.

Dukić-Ott, A., Remon, J.P., Foreman, P., Vervaet, C., 2007. Immediate release of poorly soluble drugs from starch-based pellets prepared via extrusion/spheronisation. Eur. J. Pharm. Biopharm. 67, 715-724.

Elder, D.P., Holm, R., de Diego, H.L., 2013. Use of pharmaceutical salts and cocrystals to address the issue of poor solubility. Int. J. Pharm. 453, 88-100.

Fagerberg, J.H., Tsinman, O., Sun, N., Tsinman, K., Avdeef, A., Bergström, C.A., 2010. Dissolution rate and apparent solubility of poorly soluble drugs in biorelevant dissolution media. Mol. Pharm. 7, 1419-1430.

Fahr, A., Liu, X., 2007. Drug delivery strategies for poorly water-soluble drugs. Expert opinion on drug delivery 4, 403-416.

Figueroa, C.E., Bose, S., 2013. Spray granulation: importance of process parameters on in vitro and in vivo behavior of dried nanosuspensions. Eur. J. Pharm. Biopharm. 85, 1046-1055.

Florence, A.T., Attwood, D., 2015. Physicochemical principles of pharmacy: In manufacture, formulation and clinical use. Pharmaceutical press.

Franks, F.t., Ives, D., 1966. The structural properties of alcohol–water mixtures. Quarterly Reviews, Chemical Society 20, 1-44.

Friscic, T., Jones, W., 2009. Recent advances in understanding the mechanism of cocrystal formation via grinding. Cryst. Growth Des. 9, 1621-1637.

Gao, L., Liu, G., Ma, J., Wang, X., Zhou, L., Li, X., Wang, F., 2013. Application of drug nanocrystal technologies on oral drug delivery of poorly soluble drugs. Pharm. Res. 30, 307-324.

Gao, P., Shi, Y., 2012. Characterization of supersaturatable formulations for improved absorption of poorly soluble drugs. The AAPS journal 14, 703-713.

Gao, Y., Zu, H., Zhang, J., 2011. Enhanced dissolution and stability of adefovir dipivoxil by cocrystal formation. J. Pharm. Pharmacol. 63, 483-490.

Garside, J., Davey, R., 2000. From molecules to crystallizers: An Introduction to crystallization. Oxford University Press.

Goldberg, A.H., Gibaldi, M., Kanig, J.L., 1965. Increasing dissolution rates and gastrointestinal absorption of drugs via solid solutions and eutectic mixtures I: Theoretical considerations and discussion of the literature. J. Pharm. Sci. 54, 1145-1148.

Good, D.J., Rodriguez-Hornedo, N., 2009. Solubility advantage of pharmaceutical cocrystals. Cryst. Growth Des. 9, 2252-2264.

Greco, K., Bogner, R., 2012. Solution-mediated phase transformation: significance during dissolution and implications for bioavailability. J. Pharm. Sci. 101, 2996-3018.

Guo, P., Huang, J., Zhao, Y., Martin, C.R., Zare, R.N., Moses, M.A., 2018. Nanomaterial preparation by extrusion through nanoporous membranes. Small 14, 1703493.

Hagedorn, M., Bögershausen, A., Rischer, M., Schubert, R., Massing, U., 2017. Dual centrifugation–a new technique for nanomilling of poorly soluble drugs and formulation screening by a DoE-approach. Int. J. Pharm. 530, 79-88.

Hagedorn, M., Liebich, L., Bögershausen, A., Massing, U., Hoffmann, S., Mende, S., Rischer, M., 2019. Rapid development of API nano-formulations from screening to production combining dual centrifugation and wet agitator bead milling. Int. J. Pharm. 565, 187-198.

Han, Y.R., Lee, P.I., 2017. Effect of extent of supersaturation on the evolution of kinetic solubility profiles. Mol. Pharm. 14, 206-220.

Hanafy, A., Spahn-Langguth, H., Vergnault, G., Grenier, P., Grozdanis, M.T., Lenhardt, T., Langguth, P., 2007. Pharmacokinetic evaluation of oral fenofibrate nanosuspensions and SLN in comparison to conventional suspensions of micronized drug. Adv. Drug Del. Rev. 59, 419-426.

Hancock, B.C., Parks, M., 2000. What is the true solubility advantage for amorphous pharmaceuticals? Pharm. Res. 17, 397-404.

Healy, A.M., Worku, Z.A., Kumar, D., Madi, A.M., 2017. Pharmaceutical solvates, hydrates and amorphous forms: A special emphasis on cocrystals. Adv. Drug Del. Rev. 117, 25-46.

Honary, S., Zahir, F., 2013. Effect of zeta potential on the properties of nano-drug delivery systems-a review (Part 2). Tropical Journal of Pharmaceutical Research 12, 265-273.

Hong, J.-Y., Kim, J.-K., Song, Y.-K., Park, J.-S., Kim, C.-K., 2006. A new self-emulsifying formulation of itraconazole with improved dissolution and oral absorption. J. Control. Release 110, 332-338.

Huang, Y., Li, J.-M., Lai, Z.-H., Wu, J., Lu, T.-B., Chen, J.-M., 2017. Phenazopyridine-phthalimide nano-cocrystal: Release rate and oral bioavailability enhancement. Eur. J. Pharm. Sci. 109, 581-586.

Ilevbare, G.A., Liu, H., Edgar, K.J., Taylor, L.S., 2013. Impact of polymers on crystal growth rate of structurally diverse compounds from aqueous solution. Mol. Pharm. 10, 2381-2393.

Ilevbare, G.A., Taylor, L.S., 2013. Liquid–liquid phase separation in highly supersaturated aqueous solutions of poorly water-soluble drugs: implications for solubility enhancing formulations. Crystal growth & design 13, 1497-1509.

Jayasankar, A., Somwangthanaroj, A., Shao, Z.J., Rodríguez-Hornedo, N., 2006. Cocrystal formation during cogrinding and storage is mediated by amorphous phase. Pharm. Res. 23, 2381-2392.

Jermain, S.V., Brough, C., Williams III, R.O., 2018. Amorphous solid dispersions and nanocrystal technologies for poorly water-soluble drug delivery–an update. Int. J. Pharm. 535, 379-392.

Jinno, J.-i., Kamada, N., Miyake, M., Yamada, K., Mukai, T., Odomi, M., Toguchi, H., Liversidge, G.G., Higaki, K., Kimura, T., 2006. Effect of particle size reduction on dissolution and oral absorption of a poorly water-soluble drug, cilostazol, in beagle dogs. J. Control. Release 111, 56-64.

Jog, R., Kumar, S., Shen, J., Jugade, N., Tan, D.C.T., Gokhale, R., Burgess, D.J., 2016. Formulation design and evaluation of amorphous ABT-102 nanoparticles. Int. J. Pharm. 498, 153-169.

Juhnke, M., Märtin, D., John, E., 2012. Generation of wear during the production of drug nanosuspensions by wet media milling. Eur. J. Pharm. Biopharm. 81, 214-222.

Jung, M.-S., Kim, J.-S., Kim, M.-S., Alhalaweh, A., Cho, W., Hwang, S.-J., Velaga, S.P., 2010. Bioavailability of indomethacin-saccharin cocrystals. J. Pharm. Pharmacol. 62, 1560-1568.

Junghanns, J.-U.A., Müller, R.H., 2008. Nanocrystal technology, drug delivery and clinical applications. International journal of nanomedicine 3, 295.

Kapsi, S.G., Ayres, J.W., 2001. Processing factors in development of solid solution formulation of itraconazole for enhancement of drug dissolution and bioavailability. Int. J. Pharm. 229, 193-203.

Karagianni, A., Malamatari, M., Kachrimanis, K., 2018. Pharmaceutical cocrystals: new solid phase modification approaches for the formulation of APIs. Pharmaceutics 10, 18.

Karashima, M., Kimoto, K., Yamamoto, K., Kojima, T., Ikeda, Y., 2016. A novel solubilization technique for poorly soluble drugs through the integration of nanocrystal and cocrystal technologies. Eur. J. Pharm. Biopharm. 107, 142-150.

Kayaert, P., Anné, M., Van den Mooter, G., 2011. Bead layering as a process to stabilize nanosuspensions: influence of drug hydrophobicity on nanocrystal reagglomeration following in-vitro release from sugar beads. J. Pharm. Pharmacol. 63, 1446-1453.

Keck, C.M., Müller, R.H., 2011. SmartCrystals—review of the second generation of drug nanocrystals. Handbook of materials for nanomedicine, 555-580.

Kleinebudde, P., 1994. Shrinking and swelling properties of pellets containing microcrystalline cellulose and low substituted hydroxypropylcellulose: I. Shrinking properties. Int. J. Pharm. 109, 209-219.

Kleinebudde, P., 1997. The crystallite-gel-model for microcrystalline cellulose in wet-granulation, extrusion, and spheronization. Pharm. Res. 14, 804-809.

Kocbek, P., Baumgartner, S., Kristl, J., 2006. Preparation and evaluation of nanosuspensions for enhancing the dissolution of poorly soluble drugs. Int. J. Pharm. 312, 179-186.

Krause, K.P., Kayser, O., Mäder, K., Gust, R., Müller, R., 2000. Heavy metal contamination of nanosuspensions produced by high-pressure homogenisation. Int. J. Pharm. 196, 169-172.

Kuentz, M., 2015. Analytical technologies for real-time drug dissolution and precipitation testing on a small scale. J. Pharm. Pharmacol. 67, 143-159.

Kumar, A., Sahoo, S.K., Padhee, K., Kochar, P.S., Sathapathy, A., Pathak, N., 2011. Review on solubility enhancement techniques for hydrophobic drugs. Pharmacie Globale 3, 001-007.

Kumar, S., Gokhale, R., Burgess, D.J., 2014. Sugars as bulking agents to prevent nano-crystal aggregation during spray or freeze-drying. Int. J. Pharm. 471, 303-311.

Kumar, S., Shen, J., Burgess, D.J., 2014. Nano-amorphous spray dried powder to improve oral bioavailability of itraconazole. J. Control. Release 192, 95-102.

Lahtinen, M., Kolehmainen, E., Haarala, J., Shevchenko, A., 2013. Evidence of weak halogen bonding: New insights on itraconazole and its succinic acid cocrystal. Crystal growth & design 13, 346-351.

Lai, F., Sinico, C., Ennas, G., Marongiu, F., Marongiu, G., Fadda, A.M., 2009. Diclofenac nanosuspensions: influence of preparation procedure and crystal form on drug dissolution behaviour. Int. J. Pharm. 373, 124-132.

Laitinen, R., Löbmann, K., Grohganz, H., Priemel, P., Strachan, C.J., Rades, T., 2017. Supersaturating drug delivery systems: the potential of co-amorphous drug formulations. Int. J. Pharm. 532, 1-12.

Lee, J., 2003. Drug nano-and microparticles processed into solid dosage forms: physical properties. J. Pharm. Sci. 92, 2057-2068.

Lee, J., Lee, S.-J., Choi, J.-Y., Yoo, J.Y., Ahn, C.-H., 2005. Amphiphilic amino acid copolymers as stabilizers for the preparation of nanocrystal dispersion. Eur. J. Pharm. Sci. 24, 441-449.

Li, M., Alvarez, P., Bilgili, E., 2017. A microhydrodynamic rationale for selection of bead size in preparation of drug nanosuspensions via wet stirred media milling. Int. J. Pharm. 524, 178-192.

Li, N., Taylor, L.S., 2018. Tailoring supersaturation from amorphous solid dispersions. J. Control. Release 279, 114-125.

Li, S., Wong, S., Sethia, S., Almoazen, H., Joshi, Y.M., Serajuddin, A.T., 2005. Investigation of solubility and dissolution of a free base and two different salt forms as a function of pH. Pharm. Res. 22, 628-635.

Lindfors, L., Skantze, P., Skantze, U., Rasmusson, M., Zackrisson, A., Olsson, U., 2006. Amorphous drug nanosuspensions. 1. Inhibition of Ostwald ripening. Langmuir 22, 906-910.

Ling, A.R., Baker, J.L., 1893. XCVI.—Halogen derivatives of quinone. Part III. Derivatives of quinhydrone. Journal of the Chemical Society, Transactions 63, 1314-1327.

Lipinski, C., 2002. Poor aqueous solubility—an industry wide problem in drug discovery. Am Pharm Rev 5, 82-85.

Liu, D., Yu, S., Zhu, Z., Lyu, C., Bai, C., Ge, H., Yang, X., Pan, W., 2014. Controlled delivery of carvedilol nanosuspension from osmotic pump capsule: in vitro and in vivo evaluation. Int. J. Pharm. 475, 496-503.

Liu, M., Hong, C., Li, G., Ma, P., Xie, Y., 2016. The generation of myricetin–nicotinamide nanococrystals by top down and bottom up technologies. Nanotechnology 27, 395601.

Liu, T., Müller, R.H., Möschwitzer, J.P., 2015. Effect of drug physico-chemical properties on the efficiency of top-down process and characterization of nanosuspension. Expert opinion on drug delivery 12, 1741-1754.

Liversidge, G.G., Cundy, K.C., 1995. Particle size reduction for improvement of oral bioavailability of hydrophobic drugs: I. Absolute oral bioavailability of nanocrystalline danazol in beagle dogs. Int. J. Pharm. 125, 91-97.

Loftsson, T., 2017. Drug solubilization by complexation. Int. J. Pharm. 531, 276-280.

Lu, E., Rodríguez-Hornedo, N., Suryanarayanan, R., 2008. A rapid thermal method for cocrystal screening. CrystEngComm 10, 665-668.

Lu, J., Rohani, S., 2009. Polymorphism and crystallization of active pharmaceutical ingredients (APIs). Curr. Med. Chem. 16, 884-905.

Ma, Y., Gao, J., Jia, W., Liu, Y., Zhang, L., Yang, Q., Guo, J., Zhao, J., Yan, B., Wang, Y., 2020. A Comparison of Spray-Drying and Freeze-Drying for the Production of Stable Silybin Nanosuspensions. Journal of nanoscience and nanotechnology 20, 3598-3603.

Mah, P.T., Laaksonen, T., Rades, T., Aaltonen, J., Peltonen, L., Strachan, C.J., 2014. Unravelling the relationship between degree of disorder and the dissolution behavior of milled glibenclamide. Mol. Pharm. 11, 234-242.

Malamatari, M., Taylor, K.M., Malamataris, S., Douroumis, D., Kachrimanis, K., 2018. Pharmaceutical nanocrystals: production by wet milling and applications. Drug Discov. Today 23, 534-547.

Mangal, S., Gao, W., Li, T., Zhou, Q.T., 2017. Pulmonary delivery of nanoparticle chemotherapy for the treatment of lung cancers: challenges and opportunities. Acta Pharmacol. Sin. 38, 782-797.

Marcato, P.D., Durán, N., 2008. New aspects of nanopharmaceutical delivery systems. Journal of nanoscience and nanotechnology 8, 2216-2229.

Matteucci, M.E., Paguio, J.C., Miller, M.A., Williams Iii, R.O., Johnston, K.P., 2009. Highly supersaturated solutions from dissolution of amorphous itraconazole microparticles at pH 6.8. Mol. Pharm. 6, 375-385.

Medina, C., Daurio, D., Nagapudi, K., Alvarez‐Nunez, F., 2010. Manufacture of pharmaceutical co‐crystals using twin screw extrusion: A solvent‐less and scalable process. J. Pharm. Sci. 99, 1693-1696.

Merisko-Liversidge, E., Liversidge, G.G., 2011. Nanosizing for oral and parenteral drug delivery: a perspective on formulating poorly-water soluble compounds using wet media milling technology. Adv. Drug Del. Rev. 63, 427-440.

Merisko-Liversidge, E., Liversidge, G.G., Cooper, E.R., 2003. Nanosizing: a formulation approach for poorly-water-soluble compounds. Eur. J. Pharm. Sci. 18, 113-120.

Meruva, S., Thool, P., Gong, Y., Agrawal, A., Karki, S., Bowen, W., Mitra, B., Kumar, S., 2021. A Novel Use of Nanocrystalline Suspensions to Develop Sub-Microgram Dose Micro-Tablets. J. Pharm. Sci.

Meruva, S., Thool, P., Karki, S., Bowen, W., Ghosh, I., Kumar, S., 2019. Downstream processing of irbesartan nanocrystalline suspension and mini-tablet development–Part II. Int. J. Pharm. 568, 118509.

Meruva, S., Thool, P., Shah, S., Karki, S., Bowen, W., Ghosh, I., Kumar, S., 2019. Formulation and performance of Irbesartan nanocrystalline suspension and granulated or bead-layered dried powders–Part I. Int. J. Pharm. 568, 118189.

Miller, D.A., DiNunzio, J.C., Yang, W., McGinity, J.W., Williams, R.O., 2008. Targeted intestinal delivery of supersaturated itraconazole for improved oral absorption. Pharm. Res. 25, 1450-1459.

Miller, D.A., McConville, J.T., Yang, W., Williams III, R.O., McGinity, J.W., 2007. Hot-melt extrusion for enhanced delivery of drug particles. J. Pharm. Sci. 96, 361-376.

Mu, R.H., 2002. DissoCubes—a novel formulation for poorly soluble and poorly bioavailable drugs, Modified-Release Drug Delivery Technology. CRC Press, pp. 159-174.

Müller, R.H., Keck, C.M., 2008. Second generation of drug nanocrystals for delivery of poorly soluble drugs: smartCrystal technology. Eur. J. Pharm. Sci. 1, S20-S21.

Nagarwal, R.C., Kant, S., Singh, P., Maiti, P., Pandit, J., 2009. Polymeric nanoparticulate system: a potential approach for ocular drug delivery. J. Control. Release 136, 2-13.

Nair, R., Gonen, S., Hoag, S.W., 2002. Influence of polyethylene glycol and povidone on the polymorphic transformation and solubility of carbamazepine. Int. J. Pharm. 240, 11-22.

Nekkanti, V., Pillai, R., Venkateshwarlu, V., Harisudhan, T., 2009. Development and characterization of solid oral dosage form incorporating candesartan nanoparticles. Pharm. Dev. Technol. 14, 290-298.

Nishimaru, M., Kudo, S., Takiyama, H., 2016. Cocrystal production method reducing deposition risk of undesired single component crystals in anti-solvent cocrystallization. Journal of Industrial and Engineering Chemistry 36, 40-43.

Noyes, A.A., Whitney, W.R., 1897. The rate of solution of solid substances in their own solutions. J. Am. Chem. Soc. 19, 930-934.

O'Nolan, D., Perry, M.L., Zaworotko, M.J., 2016. Chloral hydrate polymorphs and cocrystal revisited: solving two pharmaceutical cold cases. Crystal Growth & Design 16, 2211-2217.

Oswald, I.D., Allan, D.R., McGregor, P.A., Motherwell, W.S., Parsons, S., Pulham, C.R., 2002. The formation of paracetamol (acetaminophen) adducts with hydrogen-bond acceptors. Acta Crystallogr. Sect. B: Struct. Sci. 58, 1057-1066.

Padrela, L., de Azevedo, E.G., Velaga, S.P., 2012. Powder X-ray diffraction method for the quantification of cocrystals in the crystallization mixture. Drug Dev. Ind. Pharm. 38, 923-929.

Padrela, L., Rodrigues, M.A., Velaga, S.P., Matos, H.A., de Azevedo, E.G., 2009. Formation of indomethacin–saccharin cocrystals using supercritical fluid technology. Eur. J. Pharm. Sci. 38, 9-17.

Palmelund, H., Madsen, C.M., Plum, J., Müllertz, A., Rades, T., 2016. Studying the propensity of compounds to supersaturate: a practical and broadly applicable approach. J. Pharm. Sci. 105, 3021-3029.

Panda, R.C., Zank, J., Martin, H., 2001. Modeling the droplet deposition behavior on a single particle in fluidized bed spray granulation process. Powder Technol. 115, 51-57.

Pandey, S., Devmurari, V., Goyani, M., Ashapuri, H., 2010. Nanosuspension: Formulation, characterization and evaluation. International Journal of Pharma and Bio Sciences 1, 1-10.

Paredes, A.J., McKenna, P.E., Ramöller, I.K., Naser, Y.A., Volpe‑Zanutto, F., Li, M., Abbate, M., Zhao, L., Zhang, C., Abu‑Ershaid, J.M., 2021. Microarray patches: poking a hole in the challenges faced when delivering poorly soluble drugs. Adv. Funct. Mater. 31, 2005792.

Park, K., 2013. Facing the truth about nanotechnology in drug delivery. ACS nano 7, 7442-7447.

Parmentier, J., Tan, E.H., Low, A., Möschwitzer, J.P., 2017. Downstream drug product processing of itraconazole nanosuspension: Factors influencing drug particle size and dissolution from nanosuspension-layered beads. Int. J. Pharm. 524, 443-453.

Patel, D.D., Anderson, B.D., 2014. Effect of precipitation inhibitors on indomethacin supersaturation maintenance: mechanisms and modeling. Mol. Pharm. 11, 1489-1499.

Plum, J., Bavnhøj, C.G., Eliasen, J.N., Rades, T., Müllertz, A., 2020. Comparison of induction methods for supersaturation: Amorphous dissolution versus solvent shift. Eur. J. Pharm. Biopharm. 152, 35-43.

Poelma, F., Breäs, R., Tukker, J., Crommelin, D., 1991. Intestinal absorption of drugs. The influence of mixed micelles on on the disappearance kinetics of drugs from the small intestine of the rat. J. Pharm. Pharmacol. 43, 317-324.

Pouton, C.W., 1997. Formulation of self-emulsifying drug delivery systems. Adv. Drug Del. Rev. 25, 47-58.

Qiao, N., Wang, K., Schlindwein, W., Davies, A., Li, M., 2013. In situ monitoring of carbamazepine–nicotinamide cocrystal intrinsic dissolution behaviour. Eur. J. Pharm. Biopharm. 83, 415-426.

Que, C., Gao, Y., Raina, S.A., Zhang, G.G., Taylor, L.S., 2018. Paclitaxel crystal seeds with different intrinsic properties and their impact on dissolution of paclitaxel-HPMCAS amorphous solid dispersions. Crystal Growth & Design 18, 1548-1559.

Rabinow, B.E., 2004. Nanosuspensions in drug delivery. Nature reviews Drug discovery 3, 785-796.

Ranjita, S., 2013. Nanosuspensions: a new approach for organ and cellular targeting in infectious diseases. Journal of Pharmaceutical Investigation 43, 1-26.

Rao, Y.M., Kumar, M.P., Apte, S., 2008. Formulation of nanosuspensions of albendazole for oral administration. Current Nanoscience 4, 53-58.

Rasenack, N., Müller, B.W., 2004. Micron‑size drug particles: common and novel micronization techniques. Pharm. Dev. Technol. 9, 1-13.

Riis, T., Bauer-Brandl, A., Wagner, T., Kranz, H., 2007. pH-independent drug release of an extremely poorly soluble weakly acidic drug from multiparticulate extended release formulations. Eur. J. Pharm. Biopharm. 65, 78-84.

Rodríguez-Spong, B., Price, C.P., Jayasankar, A., Matzger, A.J., Rodríguez-Hornedo, N.r., 2004. General principles of pharmaceutical solid polymorphism: a supramolecular perspective. Adv. Drug Del. Rev. 56, 241-274.

Romero, G.B., Keck, C.M., Müller, R.H., 2016. Simple low-cost miniaturization approach for pharmaceutical nanocrystals production. Int. J. Pharm. 501, 236-244.

Rosenberger, J., Butler, J., Dressman, J., 2018. A refined developability classification system. J. Pharm. Sci. 107, 2020-2032.

Salazar, J., Ghanem, A., Müller, R.H., Möschwitzer, J.P., 2012. Nanocrystals: comparison of the size reduction effectiveness of a novel combinative method with conventional top-down approaches. Eur. J. Pharm. Biopharm. 81, 82-90.

Salazar, J., Müller, R.H., Möschwitzer, J.P., 2014. Combinative particle size reduction technologies for the production of drug nanocrystals. Journal of pharmaceutics 2014.

Sareen, S., Mathew, G., Joseph, L., 2012. Improvement in solubility of poor water-soluble drugs by solid dispersion. International journal of pharmaceutical investigation 2, 12.

Sarnes, A., Kovalainen, M., Häkkinen, M.R., Laaksonen, T., Laru, J., Kiesvaara, J., Ilkka, J., Oksala, O., Rönkkö, S., Järvinen, K., 2014. Nanocrystal-based per-oral itraconazole delivery: Superior in vitro dissolution enhancement versus Sporanox® is not realized in in vivo drug absorption. J. Control. Release 180, 109-116.

SCHMIDT, J., SNIPES, W., 1967. FREE RADICAL FORMATION IN A PYRIMIDINE-PURINE COCCRYSTAL COMPLEX, Radiat. Res. RADIATION RESEARCH SOC 2021 SPRING RD, STE 600, OAK BROOK, IL 60521, pp. 542-&.

Schram, C.J., Taylor, L.S., Beaudoin, S.P., 2015. Influence of polymers on the crystal growth rate of felodipine: correlating adsorbed polymer surface coverage to solution crystal growth inhibition. Langmuir 31, 11279-11287.

Schultheiss, N., Newman, A., 2009. Pharmaceutical cocrystals and their physicochemical properties. Cryst. Growth Des. 9, 2950-2967.

Serajuddin, A.T., 1999. Solid dispersion of poorly water‑soluble drugs: Early promises, subsequent problems, and recent breakthroughs. J. Pharm. Sci. 88, 1058-1066.

Serajuddin, A.T., 2007. Salt formation to improve drug solubility. Adv. Drug Del. Rev. 59, 603-616.

Shan, N., Toda, F., Jones, W., 2002. Mechanochemistry and co-crystal formation: effect of solvent on reaction kinetics. Chem. Commun., 2372-2373.

Shargel, L., Yu, A., Wu-pong, S., 1999. Bioavailability and bioequivalence. Applied biopharmaceutics and pharmacokinetics, 4th ed. New York: McGraw-Hill Medical Publishing Company.

Sharma, P., Denny, W.A., Garg, S., 2009. Effect of wet milling process on the solid state of indomethacin and simvastatin. Int. J. Pharm. 380, 40-48.

Sharma, P., Garg, S., 2010. Pure drug and polymer based nanotechnologies for the improved solubility, stability, bioavailability and targeting of anti-HIV drugs. Adv. Drug Del. Rev. 62, 491-502.

Shegokar, R., Müller, R.H., 2010. Nanocrystals: industrially feasible multifunctional formulation technology for poorly soluble actives. Int. J. Pharm. 399, 129-139.

Shi, N.-Q., Jin, Y., Zhang, Y., Che, X.-X., Xiao, X., Cui, G.-H., Chen, Y.-Z., Feng, B., Li, Z.-Q., Qi, X.-R., 2019. The influence of cellulosic polymer's variables on dissolution/solubility of amorphous felodipine and crystallization inhibition from a supersaturated state. AAPS PharmSciTech 20, 1-14.

Shiraki, K., Takata, N., Takano, R., Hayashi, Y., Terada, K., 2008. Dissolution improvement and the mechanism of the improvement from cocrystallization of poorly water-soluble compounds. Pharm. Res. 25, 2581-2592.

Siewert, C., Moog, R., Alex, R., Kretzer, P., Rothenhäusler, B., 2018. Process and scaling parameters for wet media milling in early phase drug development: A knowledge based approach. Eur. J. Pharm. Sci. 115, 126-131.

Sinha, B., Müller, R.H., Möschwitzer, J.P., 2013. Bottom-up approaches for preparing drug nanocrystals: formulations and factors affecting particle size. Int. J. Pharm. 453, 126-141.

Six, K., Daems, T., de Hoon, J., Van Hecken, A., Depre, M., Bouche, M.-P., Prinsen, P., Verreck, G., Peeters, J., Brewster, M.E., 2005. Clinical study of solid dispersions of itraconazole prepared by hot-stage extrusion. Eur. J. Pharm. Sci. 24, 179-186.

Soisuwan, S., Teeranachaideekul, V., Wongrakpanich, A., Langguth, P., Junyaprasert, V.B., 2019. Impact of uncharged and charged stabilizers on in vitro drug performances of clarithromycin nanocrystals. Eur. J. Pharm. Biopharm. 137, 68-76.

Sosnik, A., das Neves, J., Sarmento, B., 2014. Mucoadhesive polymers in the design of nano-drug delivery systems for administration by non-parenteral routes: a review. Prog. Polym. Sci. 39, 2030-2075.

Srivalli, K.M.R., Mishra, B., 2016. Drug nanocrystals: a way toward scale-up. Saudi Pharmaceutical Journal 24, 386-404.

Stahly, G.P., 2009. A survey of cocrystals reported prior to 2000. Crystal Growth & Design 9, 4212-4229.

Stella, V.J., Rao, V.M., Zannou, E.A., Zia, V., 1999. Mechanisms of drug release from cyclodextrin complexes. Adv. Drug Del. Rev. 36, 3-16.

Sun, C.C., Hou, H., 2008. Improving mechanical properties of caffeine and methyl gallate crystals by cocrystallization. Cryst. Growth Des. 8, 1575-1579.

Sun, D.D., Lee, P.I., 2013. Evolution of supersaturation of amorphous pharmaceuticals: the effect of rate of supersaturation generation. Mol. Pharm. 10, 4330-4346.

Sun, W., Mao, S., Shi, Y., Li, L.C., Fang, L., 2011. Nanonization of itraconazole by high pressure homogenization: stabilizer optimization and effect of particle size on oral absorption. J. Pharm. Sci. 100, 3365-3373.

Tahara, K., 2020. Pharmaceutical formulation and manufacturing using particle/powder technology for personalized medicines. Adv. Powder Technol. 31, 387-392.

Tan, E.H., Parmentier, J., Low, A., Möschwitzer, J.P., 2017. Downstream drug product processing of itraconazole nanosuspension: Factors influencing tablet material properties and dissolution of compacted nanosuspension-layered sugar beads. Int. J. Pharm. 532, 131-138.

Tan, J., Liu, J., Ran, L., 2021. A Review of Pharmaceutical Nano-Cocrystals: A Novel Strategy to Improve the Chemical and Physical Properties for Poorly Soluble Drugs. Crystals 11, 463.

Taylor, L.S., Zhang, G.G., 2016. Physical chemistry of supersaturated solutions and implications for oral absorption. Adv. Drug Del. Rev. 101, 122-142.

Thakuria, R., Delori, A., Jones, W., Lipert, M.P., Roy, L., Rodríguez-Hornedo, N., 2013. Pharmaceutical cocrystals and poorly soluble drugs. Int. J. Pharm. 453, 101-125.

Thalladi, V.R., Smolka, T., Gehrke, A., Boese, R., Sustmann, R., 2000. Role of weak hydrogen bonds in the crystal structures of phenazine, 5, 10-dihydrophenazine and their 1: 1 and 3: 1 molecular complexes. New J. Chem. 24, 143-147.

Trask, A.V., Jones, W., 2005. Crystal engineering of organic cocrystals by the solid-state grinding approach. Organic solid state reactions, 41-70.

Trask, A.V., Motherwell, W.S., Jones, W., 2004. Solvent-drop grinding: green polymorph control of cocrystallisation. Chem. Commun., 890-891.

Tuomela, A., Laaksonen, T., Laru, J., Antikainen, O., Kiesvaara, J., Ilkka, J., Oksala, O., Rönkkö, S., Järvinen, K., Hirvonen, J., 2015. Solid formulations by a nanocrystal approach: Critical process parameters regarding scale-ability of nanocrystals for tableting applications. Int. J. Pharm. 485, 77-86.

Van Eerdenbrugh, B., Van den Mooter, G., Augustijns, P., 2008. Top-down production of drug nanocrystals: nanosuspension stabilization, miniaturization and transformation into solid products. Int. J. Pharm. 364, 64-75.

Van Eerdenbrugh, B., Vermant, J., Martens, J.A., Froyen, L., Humbeeck, J.V., Van den Mooter, G., Augustijns, P., 2010. Solubility increases associated with crystalline drug nanoparticles: methodologies and significance. Mol. Pharm. 7, 1858-1870.

Van Eerdenbrugh, B., Vermant, J., Martens, J.A., Froyen, L., Van Humbeeck, J., Augustijns, P., Van den Mooter, G., 2009. A screening study of surface stabilization during the production of drug nanocrystals. J. Pharm. Sci. 98, 2091-2103.

Van Speybroeck, M., Mols, R., Mellaerts, R., Do Thi, T., Martens, J.A., Van Humbeeck, J., Annaert, P., Van den Mooter, G., Augustijns, P., 2010. Combined use of ordered mesoporous silica and precipitation inhibitors for improved oral absorption of the poorly soluble weak base itraconazole. Eur. J. Pharm. Biopharm. 75, 354-365.

Verma, S., Huey, B.D., Burgess, D.J., 2009. Scanning probe microscopy method for nanosuspension stabilizer selection. Langmuir 25, 12481-12487.

Vo, C.L.-N., Park, C., Lee, B.-J., 2013. Current trends and future perspectives of solid dispersions containing poorly water-soluble drugs. Eur. J. Pharm. Biopharm. 85, 799-813.

Wahlstrom, J.L., Chiang, P.-C., Ghosh, S., Warren, C.J., Wene, S.P., Albin, L.A., Smith, M.E., Roberds, S.L., 2007. Pharmacokinetic evaluation of a 1, 3-dicyclohexylurea nanosuspension formulation to support early efficacy assessment. Nanoscale Research Letters 2, 291-296.

Walters, R.H., Bhatnagar, B., Tchessalov, S., Izutsu, K.-I., Tsumoto, K., Ohtake, S., 2014. Next generation drying technologies for pharmaceutical applications. J. Pharm. Sci. 103, 2673-2695.

Wang, S., Liu, C., Chen, Y., Zhu, A., Qian, F., 2018. Aggregation of hydroxypropyl methylcellulose acetate succinate under its dissolving pH and the impact on drug supersaturation. Mol. Pharm. 15, 4643-4653.

Wang, Y., Zheng, Y., Zhang, L., Wang, Q., Zhang, D., 2013. Stability of nanosuspensions in drug delivery. J. Control. Release 172, 1126-1141.

Warren, D.B., Benameur, H., Porter, C.J., Pouton, C.W., 2010. Using polymeric precipitation inhibitors to improve the absorption of poorly water-soluble drugs: A mechanistic basis for utility. J. Drug Target. 18, 704-731.

Wei, Y., Zhang, L., Wang, N., Shen, P., Dou, H., Ma, K., Gao, Y., Zhang, J., Qian, S., 2018. Mechanistic study on complexation-induced spring and hover dissolution behavior of ibuprofen-nicotinamide cocrystal. Crystal Growth & Design 18, 7343-7355.

Weissig, V., Pettinger, T.K., Murdock, N., 2014. Nanopharmaceuticals (part 1): products on the market. International journal of nanomedicine 9, 4357.

Wöhler, F., 1844. Untersuchungen über das Chinon.

Wouters, J., Quéré, L., 2011. Pharmaceutical salts and co-crystals. Royal Society of Chemistry.

Xia, D., Gan, Y., Cui, F., 2014. Application of precipitation methods for the production of water-insoluble drug nanocrystals: production techniques and stability of nanocrystals. Curr. Pharm. Des. 20, 408-435.

Yamashita, T., Ozaki, S., Kushida, I., 2011. Solvent shift method for anti-precipitant screening of poorly soluble drugs using biorelevant medium and dimethyl sulfoxide. Int. J. Pharm. 419, 170-174.

Yang, H., Kim, H., Jung, S., Seo, H., Nida, S.K., Yoo, S.-Y., Lee, J., 2018. Pharmaceutical strategies for stabilizing drug nanocrystals. Curr. Pharm. Des. 24, 2362-2374.

Yasuji, T., Takeuchi, H., Kawashima, Y., 2008. Particle design of poorly water-soluble drug substances using supercritical fluid technologies. Adv. Drug Del. Rev. 60, 388-398.

Zu, Y., Sun, W., Zhao, X., Wang, W., Li, Y., Ge, Y., Liu, Y., Wang, K., 2014. Preparation and characterization of amorphous amphotericin B nanoparticles for oral administration through liquid antisolvent precipitation. Eur. J. Pharm. Sci. 53, 109-117.

Zuo, J., de Araujo, G.L.B., Stephano, M.A., Zuo, Z., Bou-Chacra, N.A., Löbenberg, R., 2020. Design space approach in the development of esculetin nanocrystals by a small-scale wet-bead milling process. J. Drug Deliv. Sci. Technol. 55, 101486.

7. PUBLICATIONS & PRESENTATIONS

Research publications:

- **Z. Huang**, S. Staufenbiel, R. Bodmeier. Combination of cocrystal and nanocrystal techniques to improve the solubility and dissolution rate of poorly soluble drugs. (Submitted)

- **Z. Huang**, S. Staufenbiel, R. Bodmeier. Itraconazole-succinic acid nano-cocrystals: Kinetic solubility improvement and influence of polymers on controlled supersaturation. (Submitted)

- **Z. Huang**, S. Staufenbiel, R. Bodmeier. Incorporation of itraconazole nano-cocrystal into granulated or bead-layered solid dosage forms. (In preparation)

Poster presentations:

- **Z. Huang**, S. Staufenbiel, R. Bodmeier, Combination of itraconazole cocrystal and nanocrystal techniques to improve the saturation solubility and dissolution rate, PBP world meeting, May 2021, Vienna, Austria.

8. CURRICULUM VITAE

CURRICULUM VITAE

For reasons of data protection, the curriculum vitae is not published in the electronic version.